

# Incentive-Based Expansion Planning and Reliability Enhancement Models for Smart Distribution Systems

by

Majed Alotaibi

A thesis  
presented to the University of Waterloo  
in fulfillment of the  
thesis requirement for the degree of  
Doctor of Philosophy  
in  
Electrical and Computer Engineering

Waterloo, Ontario, Canada, 2018

© Majed Alotaibi 2018

## **Examining Committee Membership**

The following served on the Examining Committee for this thesis. The decision of the Examining Committee is by majority vote.

External Examiner	Mohamed El-Hawary Professor
Supervisor	Magdy Salama Professor
Internal Member	Catherine Gebotys Professor
Internal Member	Mohamed Ahmed Adjunct Assistant Professor
Internal-external Member	Gordon Savage Professor

## **AUTHOR'S DECLARATION**

I hereby declare that I am the sole author of this thesis. This is a true copy of the thesis, including any required final revisions, as accepted by my examiners.

I understand that my thesis may be made electronically available to the public.

## Abstract

Due to the rapid progress toward the implementation of smart grid technologies, electric power distribution systems are undergoing profound structural and operational changes. Climate concerns, a reduction in dependency on fossil fuel as a primary generation source, and the enhancement of existing networks constitute the key factors in the shift toward smart grid application, a shift that has, in fact, already led power industry stakeholders to promote more efficient network technologies and regulation. The results of these advances are encouraging with regard to the deployment and integration of small-scale power generation units, known as distributed generation units (DGs), within distribution networks. DGs are capable of contributing to the powering of the grid from distribution or even sub-distribution systems, providing both a positive effect on network performance and the least adverse impact on the environment. Smart grid deployment has also facilitated the integration of a variety of investor assets into power distribution systems, with a consequent necessity for positive and active interaction between those investors and local distribution companies (LDCs).

This thesis proposes a novel incentive-based distribution system planning (IDSP) model that enables an LDC and DG investors to work collaboratively for their mutual benefit. Using the proposed model, the LDC would establish a bus-wise incentive program (BWIP) based on long-term contracts, which would encourage DG investors to integrate their projects at the specific system buses that would benefit both parties. The model guarantees that the LDC will incur minimum expansion and operation costs while concurrently ensuring the feasibility of DG investors' projects. The proposed model also provides the LDC with the opportunity to identify the least-cost solution among a combination of the proposed BWIP and traditional expansion options (i.e., upgrading or constructing new substations, upgrading or constructing new lines, and/or reconfiguring the system). In this way, the model facilitates the effective coordination of future LDC expansion projects with DG investors. To derive appropriate incentives for each project, the model enforces a number of economic metrics, including the internal rate of return, the profit-investment ratio, and the discounted payback period. All investment plans committed to by the LDC and the DG investors for the full extent of the planning period are then coordinated accordingly. The intermittent nature of both system demand and wind- and PV-based DG output power is handled probabilistically, and a number of DG technologies are taken into account. Several linearization approaches are applied in order to convert the proposed model into a mixed integer linear programming (MILP) model, which is solved using a CPLEX solver.

Reliability of service in a deregulated power environment is considered a major factor in the evaluation of the performance of service providers by consumers and system regulators. Adhering to imposed obligations related to the enhancement of overall system reliability places a substantial burden on the planning engineer

with respect to investigating multiple alternatives and evaluating each option from both a technical and an economical perspective. This thesis also proposes a value-based reinforcement planning model for improving system reliability while maintaining reliability metrics within allowable limits. The optimal allocation of tie lines and normally open switches is determined by this planning model, along with required capacity upgrades for substations and lines. Two hierarchical levels for system operation under contingencies, namely, the restoration process and islanding-based modes, are applied in the model. A probabilistic analytical model is proposed for computing distribution system reliability indices based on consideration of these two hierarchical operating levels and taking into account variations in system demand, DG output power, and the uncertainty associated with system components. Due to the nature and complexity of these kinds of problems, a metaheuristic technique based on a genetic algorithm (GA) is implemented for solving this model.

This thesis also proposes a new iterative planning model for smart distribution systems in which system reliability is considered a primary component in the setting of incentive prices for DG owners. A new concept, called generation sufficiency for dynamic virtual zones, is introduced in the model as a means of enhancing reliability in areas that are subject to reliability issues. To avoid any contravention of operational security boundaries, DG capacity is represented by two components: normal DG operating capacity and reserve DG capacity. The MILP planning model is constructed in a GAMS environment and solved with the use of a CPLEX solver.

## Acknowledgements

All praises are due to Allah for providing me the guidance, strength, and patience to complete this thesis and meet all of the Ph.D. degree requirements successfully.

I would like to express my sincere gratitude and appreciation to my supervisor Professor Magdy Salama for the expert guidance, endless support and encouragement, which he provided throughout my graduate studies at the University of Waterloo. It was my privilege to complete my graduate studies under his supervision.

I am also grateful to Prof. Catherine Gebotys, Prof. Gordon Savage, and Dr. Mohamed Ahmed for serving as members of my Ph.D. thesis examining committee. Their valuable comments and support are highly appreciated. I am also thankful to Prof. Mohamed Elhawary, from Dalhousie University, for serving as the external thesis examiner and for his encouragement and insightful comments. I would like also to thank Prof. Ken Vetzal for chairing my thesis examination committee.

I would like to extend my heartfelt gratitude to my parents for their continual support, love, patience, and prayers. Many thanks to my brothers and sisters for their endless support and faithful love.

I would like to acknowledge my colleagues in the Power and Energy Systems Group in the University of Waterloo for their friendly discussion and suggestions. Special thanks to all of my friends in Waterloo for their kindness and friendship.

My deepest appreciation to my wife, Maha, for her support, patience, understanding, encouragement during my graduate studies journey. Thanks to my son, Fares, and my daughter, Alanoud, who are the source of my inspiration and strength.

Finally, I gratefully acknowledge King Saud University, Riyadh, Saudi Arabia for sponsoring my studies and providing the funding necessary to carry out this research.

## **Dedication**

To my parents

To my brothers and sisters

To my wife

To my son

(with respect and love)

# Table of Contents

Table of Contents .....	viii
List of Figures .....	xi
List of Tables .....	xiii
Nomenclature .....	xiv
Chapter 1 Introduction .....	1
1.1 Motivation .....	1
1.2 Research Objectives .....	5
1.3 Thesis Outline .....	6
Chapter 2 Background and Literature Survey .....	7
2.1 Introduction .....	7
2.2 Power Distribution Systems .....	8
2.3 Distributed Generation .....	10
2.3.1 Distributed Generation Benefits .....	10
2.3.2 Distributed Generation Technologies .....	11
2.4 Power Distribution System Planning .....	13
2.4.1 Factors Affecting Distribution System Planning .....	14
2.4.2 Distribution System Planning Models .....	15
2.4.3 Traditional Distribution System Planning .....	15
2.4.4 Distribution System Planning in the Smart Grid Paradigm .....	19
2.4.5 The Inclusion of System Reliability in Distribution System Planning .....	20
2.4.6 Planning Models for Smart Distribution Systems .....	21
2.5 Distribution System Reliability Analysis .....	24
2.6 Distribution System Reliability Models in the Presence of DGs .....	27
2.7 Summary .....	30
Chapter 3 An Incentive-Based Multistage Planning Model for Smart Distribution Systems .....	31
3.1 Introduction .....	31
3.2 Modeling of the Uncertainty Associated with Demand and DG Output Power .....	33
3.3 IDSP Model Problem Formulation .....	36
3.3.1 The Objective Function .....	36
3.3.2 Power Conservation Constraints .....	37
3.3.3 Other Constraints .....	38
3.3.4 Linearization of the IDSP Model .....	43
3.4 Case Studies and Numerical Results .....	47
3.4.1 Distribution System Under Study .....	47
3.4.2 Uncertainty Modeling Results .....	48

3.4.3	Case Studies and Results.....	48
3.4.4	Incentive Design Based on the Profitability Index .....	53
3.4.5	Effect of Uncertainty on Planning Results.....	57
3.4.6	Comparing Multistage and Single Stage Models.....	58
3.4.7	Computational Aspects .....	59
3.5	Summary .....	59
Chapter 4	Reinforcement Planning Model for Distribution System Reliability Enhancement .....	60
4.1	Introduction.....	60
4.2	Probabilistic System Operating Scenarios for the Incorporation of Uncertainty .....	61
4.2.1	Load Modeling.....	62
4.2.2	Wind and PV-Based DG Modeling .....	62
4.2.3	Building the Probabilistic Operating Scenarios .....	62
4.3	Proposed Reliability-Based Reinforcement Planning Model.....	62
4.3.1	Problem Formulation .....	63
4.3.2	Distribution System Reliability Evaluation with DGs.....	66
4.4	Case Studies and Numerical Results.....	74
4.4.1	Distribution System Under Study .....	74
4.4.2	Case Studies and Results.....	76
4.4.3	Composite Planning Results .....	89
4.5	Summary .....	89
Chapter 5	Distribution System Planning with Reliability Considering Generation Sufficiency for Virtual Dynamic System Zones .....	91
5.1	Introduction.....	91
5.2	Proposed Distribution System Planning Framework That Includes Consideration of Reliability .....	92
5.3	Mathematical Formulation of Distribution System Planning .....	95
5.3.1	The Objective Function.....	96
5.3.2	Planning Model Constraints.....	96
5.4	Distribution System Reliability Evaluation .....	102
5.4.1	Calculating the Probability of Success in Islanded Operation Mode.....	103
5.4.1	Calculating the Unavailability of Load Points and the Reliability Indices .....	104
5.5	Case Study and Numerical Results .....	105
5.5.1	Distribution System Under Study .....	105
5.5.2	Results and Discussion.....	105
5.6	Summary .....	115
Chapter 6	Concluding Remarks.....	117
6.1	Summary and Conclusions.....	117

6.2	Research Contributions .....	120
6.3	Directions for Future Research .....	121
	Bibliography .....	123

## List of Figures

Figure 2-1 Distribution system feeder [20].....	9
Figure 2-2 Distribution system planning stages [17].....	14
Figure 2-3 Traditional DSP model.....	16
Figure 2-4 DSP in smart grid paradigm.....	20
Figure 2-5 N-1 approach for evaluating load point reliability parameters.....	25
Figure 3-1 Flowchart of the proposed IDSP model.....	32
Figure 3-2 Network topology for case 1 with investments.....	51
Figure 3-3 Network topology for case 2 with investment.....	53
Figure 3-4 Variations in planning costs with different PIs for case 1 (CDGs only).....	55
Figure 3-5 Variations in the average BWIP prices and the DPP with different PIs for case 1 (CDGs only) .....	55
Figure 3-6 Variations in planning costs with different PIs for case 2.....	56
Figure 3-7 Variations in average BWIP prices and DPPs with different PIs for case 2.....	56
Figure 3-8 Avg. system buses voltages and their 95% confidence intervals.....	58
Figure 3-9 Avg. system lines currents and their 95% confidence intervals.....	58
Figure 4-1 Proposed general planning framework for distribution systems.....	61
Figure 4-2 Structure of typical chromosome encoding in a planning problem.....	65
Figure 4-3 Flowchart of the proposed reliability-based reinforcement planning model using a GA.....	65
Figure 4-4 Illustrative 11-bus distribution system.....	67
Figure 4-5 Island created because of a fault in line 4.....	67
Figure 4-6 Flowchart for the proposed distribution system reliability evaluation model.....	71
Figure 4-7 Distribution system configuration with candidate tie lines.....	76
Figure 4-8 System topology following reliability-based reinforcement planning for case 1.....	77
Figure 4-9 Optimal restoration process for two different contingencies in case 1.....	78
Figure 4-10 SAIDIs for each bus prior to reliability planning for case 1.....	79
Figure 4-11 SAIDIs for each bus following reliability planning for case 1.....	79
Figure 4-12 SAIDIs for the main feeders prior to reliability planning for Case 1.....	80
Figure 4-13 SAIDIs for the main feeders following reliability planning for case 1.....	80
Figure 4-14 Expected ENS at each stage before and after reliability planning for case 1.....	81
Figure 4-15 ENS for each bus prior to reliability planning for case 1.....	81
Figure 4-16 ENS for each bus following reliability planning for case 1.....	82
Figure 4-17 System topology after reliability-based reinforcement planning for case 2.....	83
Figure 4-18 Optimal restoration process for three different contingencies in case 2.....	85

Figure 4-19 SAIDIs for each bus prior to reliability planning for case 2 .....	86
Figure 4-20 SAIDIs for each bus following reliability planning for case 2.....	86
Figure 4-21 SAIDIs for the main feeders following reliability planning for case 2 .....	86
Figure 4-22 Expected ENS at each stage before and after reliability planning for case 2.....	87
Figure 4-23 ENS for each bus prior to reliability planning for case 2.....	87
Figure 4-24 ENS for each bus following reliability planning for case 2 .....	88
Figure 5-1 Flowchart of the proposed planning model that incorporates reliability.....	94
Figure 5-2 Illustrative example of a 13-bus system with virtual zones .....	95
Figure 5-3 SAIDI at each bus in the system following the initial planning.....	105
Figure 5-4 Zones formed during stage 1 for buses not adhering to reliability standards.....	106
Figure 5-5 Zones formed during stage 2 for buses not adhering to reliability standards.....	106
Figure 5-6 Zones formed during stage 3 for buses not adhering to reliability standards.....	107
Figure 5-7 Graphical representation of the changes in zone dimensions during different iterations.....	109
Figure 5-8 Total DG capacity including both normal operating and reserve capacities for stage 1 .....	110
Figure 5-9 Total DG capacity including both normal operating and reserve capacities for stage 2 .....	110
Figure 5-10 Total DG capacity including both normal operating and reserve capacities for stage 3 .....	110
Figure 5-11 Total CDG installed capacity at the end each planning stage .....	112
Figure 5-12 SAIDI at each bus following planning that includes consideration of reliability .....	113
Figure 5-13 ENS at each bus following planning that includes consideration of reliability.....	113
Figure 5-14 ENS before and after consideration of reliability.....	114
Figure 5-15 Incentives provided to DG owners before and after consideration of reliability .....	114

## List of Tables

Table 1-1 Contracted Capacity Under the FIT Program [7] .....	2
Table 2-1 Various DG Capacities [21] .....	10
Table 3-1 DG Investment and Operation Costs [65], [119], [120] .....	48
Table 3-2 Best Fitting Probability Distribution Results.....	48
Table 3-3 NPV for Planning Costs to be Incurred by the LDC, in (10 <sup>6</sup> US\$) .....	49
Table 3-4 Optimal DG BWIP Prices and Incomes .....	50
Table 3-5 Investment Plans Committed to by the LDC and DG Investors for Each Stage .....	54
Table 3-6 Comparison Between the Proposed Model and MCS Results.....	57
Table 4-1 Sequence Path and Sequence Path Set for Each Bus.....	68
Table 4-2 Set of Affected Buses and Potential Restoration Set for Each Contingency .....	68
Table 4-3 Reliability Data for the System Components [96], [125] .....	75
Table 4-4 Locations and Sizes of DGs in the System.....	75
Table 4-5 Investment Plans Required for Case Study 1 .....	77
Table 4-6 NPV of the Associated Planning Costs for Case 1 .....	82
Table 4-7 Investment Plans Required for Case Study 2 .....	84
Table 4-8 NPV of the Associated Planning Costs for Case 2 .....	88
Table 4-9 Total Planning Cost for the General Planning Framework.....	89
Table 5-1 Sample Iterations of the Planning Process and the Sets Created for Stage 1 Only .....	108
Table 5-2 Cumulative CDG Capacity at Each Bus and the Corresponding Incentive.....	111
Table 5-3 Installed Capacities of Renewable-Based DGs and the Associated Incentives .....	111
Table 5-4 LDC Investment Upgrade Plans for Each Stage.....	112
Table 5-5 NPV of the Required Plan Investments and Planning Costs .....	115

## Nomenclature

### Indices

$i, j$	Indices for system buses.
$t$	Index for time stages.
$e$	Index for uncertainty scenarios.
$ij$	Index for system branches.
$u, c$	Indices for substation alternatives.
$a$	Index for feeder alternatives.
$dg$	Index for DG types.
$y$	Index for the blocks in piecewise linearization.

### Sets

$\Omega_N$	Set of system buses.
$\Omega_{ES}, \Omega_{CS}$	Sets of existing and candidate substation buses.
$\Omega_{SS}$	Set of all substations where $\Omega_{SS} = \Omega_{ES} \cup \Omega_{CS}$ .
$\Omega_{EL}, \Omega_{CL}$	Sets of existing and candidate feeder branches.
$\Omega_L$	Set of all branches where $\Omega_L = \Omega_{EL} \cup \Omega_{CL}$ .
$\Omega_U$	Set of alternatives for upgrading existing substations.
$\Omega_C$	Set of alternatives for constructing new candidate substations.
$\Omega_{se}$	Set of scenarios.
$\Omega_{DG}$	Set of DG types. $\Omega_{DG} = \{CDG, WDG, PVDG\}$ , where $CDG$ is controllable DG, $WDG$ is wind-based DG, and $PVDG$ is PV-based DG.
T	Set of time stages.

### Parameters

$C_u^{US}, C_c^{NS}$	Costs of upgrading an existing substation and constructing a new candidate substation (US\$).
$C_a^{UF}, C_a^{NF}$	Costs of upgrading an existing feeder and constructing a new candidate feeder (US\$/km).
$L_{ij}$	Length of feeder $ij$ (km).
$\alpha_e$	Probability of scenario $e$ .

$\varphi$	Total hours in one year ( $\varphi = 8760$ ).
$\omega$	Substation operation cost.
$\varepsilon$	Cost of energy losses (US\$/MWh).
$C_{e,t}^E$	Market energy purchasing cost (US\$/MWh).
$OP_{dg,e}$	Representative DG state output power as a per unit of the DG rated capacity for type $dg$ in scenario $e$ .
$\rho_{dg}$	Binary parameter (1 if a DG of type $dg$ is considered; 0 otherwise).
$\tau$	Interest rate.
$K$	Number of years in each stage.
$DL_e$	Representative load state as a percentage of the peak load in scenario $e$ .
$P_{D_{i,t}}$	Nodal active power demand (MW).
$Q_{D_{i,t}}$	Nodal reactive power demand (MVAR).
$G_{ij}, B_{ij}$	Conductance and susceptance of branch $ij$ .
$R_{ij}, X_{ij}$	Resistance and reactance of branch $ij$ .
$\overline{S}_{G_i}^{max}$	Maximum existing substation capacity (MVA).
$S_u^{US}$	Existing substation upgrade capacity for alternative $u$ (MVA).
$S_c^{NS}$	New substation capacity for alternative $c$ (MVA).
$\overline{S}_{ij}^{max}$	Maximum existing feeder capacity (MVA).
$S_a^P$	New feeder capacity for alternative $a$ (MVA).
$\underline{V}^{Min}, \overline{V}^{Max}$	Minimum and maximum voltage magnitude.
$\underline{\Delta V}_i^{Min}, \overline{\Delta V}_i^{Max}$	Minimum and maximum voltage magnitude deviation.
$N_b$	Total number of buses.
$N_{ES}$	Total number of existing substations.
$C_{dg}^{IDG}$	DG investment cost for type $dg$ (US\$/MW).
$C_{dg}^{ODG}$	DG operation cost for type $dg$ (US\$/MWh).
$IRR_{dg,i}$	Internal rate of return for a DG investor.
$\underline{\gamma}, \overline{\gamma}$	Minimum and maximum incentive prices (US\$/MWh).
$\overline{DG}_i$	Maximum DG capacity at bus $i$ (MW).

$\mu$	DG penetration level, as a percentage.
$M$	Disjunctive factor, a large positive number.
$\bar{\Delta}^G$	Upper limit for each linear segment of $\Delta P_{G_{i,e,t,y}}$ and $\Delta Q_{G_{i,e,t,y}}$ .
$\bar{\Delta}^L$	Upper limit for each linear segment of $\Delta P_{ij,e,t,y}$ and $\Delta Q_{ij,e,t,y}$ .
$Y$	Number of blocks in piecewise linearization.
$\Delta P$	Step value for the imposed reserve capacity in the system ( $\Delta P = 0.1$ MW)

## Variables

$\sigma_{i,u,t}$	Binary variable associated with upgrading an existing substation.
$u_{j,c,t}$	Binary variable associated with constructing a new substation.
$\beta_{ij,a,t}$	Binary variable associated with upgrading an existing feeder.
$z_{ij,a,t}$	Binary variable associated with constructing a new feeder.
$x_{ij,t}$	Binary variable associated with a feeder configuration (1 if feeder is ON; 0 otherwise).
$v_{h,dg,i}$	Binary variable associated with the binary expansion used for BWIP.
$S_{G_{i,e,t}}^{sqr}$	Square of the apparent power supplied by a substation.
$P_{G_{i,e,t}}$	Active power supplied by a substation (MW).
$Q_{G_{i,e,t}}$	Reactive power supplied by a substation (MVAR).
$\Delta P_{G_{i,e,t,y}}$	$y$ th linear block of active substation power.
$\Delta Q_{G_{i,e,t,y}}$	$y$ th linear block of reactive substation power.
$S_{ij,e,t}^{sqr}$	Square of the apparent power flow in the feeder.
$P_{ij,e,t}$	Active power flow in the feeder (MW).
$Q_{ij,e,t}$	Reactive power flow in the feeder (MVAR).
$\Delta P_{ij,e,t,y}$	$y$ th linear block of active power flow in the feeder.
$\Delta Q_{ij,e,t,y}$	$y$ th linear block of reactive power flow in the feeder.
$P_{ij,e,t}^+, P_{ij,e,t}^-$	Nonnegative variables used to replace $P_{ij,e,t}$ .
$Q_{ij,e,t}^+, Q_{ij,e,t}^-$	Nonnegative variables used to replace $Q_{ij,e,t}$ .
$Pl_{ij,e,t}$	Loss of active power by the feeder (MW).
$Ql_{ij,e,t}$	Loss of reactive power by the feeder (MVAR).

$P_{DG_{dg,i,t}}$	DG output power (MW) (chapter 3). DG normal operation capacity (MW) (in chapter 5)
$P_{CAP_{dg,i,t}}$	DG rated capacity (MW) (in chapter 3).
$P_{DG_{dg,i,t}}^{RES}$	DG reserve capacity (MW) (in chapter 5).
$ICP_{DG_{dg,i,t}}$	DG installed capacity (MW) (in chapter 5).
$\gamma_{dg,i}$	DG BWIP incentive price (US\$/MWh).
$d_{h,dg,i}$	Positive variable used for incentive price linearization.
$INC_{dg,i,t}$	Incentive cost for the DG (US\$).
$V_{i,e,t}$	Bus voltage magnitude.
$\Delta V_{i,e,t}$	Bus voltage magnitude deviation from the nominal voltage.
$\delta_{i,e,t}$	Bus voltage angle.
$INVC_{dg,i,t}^{DG}$	DG investment cost.
$OPC_{dg,i,e,t}^{DG}$	DG operation cost.
$BEN_{dg,i,e,t}^{DG}$	Benefit from the sale of DG-generated energy.

# Chapter 1

## Introduction

### 1.1 Motivation

Ever-expanding population growth and industrial market competition have been accompanied by a simultaneous increase in power consumption and electrical energy demand. Worldwide electricity needs are expected to increase significantly over the next few decades [1]. From 2011 until the end of 2040, the electric energy required is expected to grow by 28 %, from 3,839 billion kWh in 2011 to 4,930 billion kWh in 2040 [1]. The fundamental purpose of power distribution system planning is to satisfy the forecasted growth in power demand for the planning horizon period in the timeliest, most economical, and most reliable way. Distribution system companies are solely responsible for meeting any anticipated increase in demand, which requires large-scale investments, thus making plans for the expansion of distribution system assets an essential top priority for planning engineers [2]. The bottom line is that the high cost of the vast investments involved in distribution networks dictates very careful planning and operation. These tasks necessitate comprehensive economic planning tools that can facilitate the selection of a feasible solution from a variety of available alternatives and resources in order to ensure reliable, affordable, sustainable power delivery to customers.

The electric power industry is currently also undergoing a profound change driven by numerous requirements and regulations and by the implementation of new technologies. There is an imperative need for greater energy efficiency, enhanced environmental and regulatory compliance, and more constructive customer roles in the energy world. Interest in utilizing renewable energy sources in power system networks has increased dramatically. Recent years (2013 to 2017) have witnessed a continual trend of 8 % to 9 % annual growth in global renewable generation capacity [3]. By the end of 2017, the worldwide renewable energy capacity had reached 2,179 GW, an increase of 167 GW, which represents an almost 8.3 % yearly growth in total renewable generation capacity. At 85 %, wind and solar systems combined represent the largest share of last year's growth in renewable capacity, with total current wind and solar installed global capacities at 514 GW and 397 GW, respectively. The increased interest in installing renewable energy is due to the clean and sustainable nature of these resources, as well as to the ability of these resources to support the existing grid with the help of energy storage and other technologies.

Renewable-based generation sources, including wind and solar systems, have garnered the greatest attention from governments and energy regulators, with the result that numerous programs have been initiated for deploying these technologies throughout the grid. As an example, the promotion and

development of these renewable-based technologies is an important goal in Canada, where many programs have been initiated for facilitating investment in this area by both corporate investors and individuals. In particular, in 2005, the province of Ontario, as represented by the Ontario Power Authority (OPA), submitted recommendations to the Ministry of Energy that would increase the share of renewable sources in Ontario’s supply mix, maintain the share of nuclear generation, and replace coal through increases in the share of gas-fired generation and renewable resources as integral components of the power supply plan. The target of this initiative was to increase the installed capacity of renewable resources to 15,700 MW by the end of 2025: roughly 37 % of Ontario’s installed generation capacity [4]. To achieve the target goal, the Ontario Power Authority and Ontario Energy Board (OEB) developed several incentive programs and agreements to encourage and promote renewable-based technologies. For example, 2009 saw the launch of the Feed-in Tariff (FIT) program, whereby a guaranteed pricing structure for renewable electricity production is applied to projects with capacities of more than 10 kW [5]. In the same year, the micro Feed-in Tariff (microFIT) program was launched as well to serve projects with capacities of 10 kW or less [6]. Contracted capacity under the FIT Program grew from 13 MW in March 2010 to 4,803 MW by the end of the first quarter of 2018 [7]. Table 1-1 shows the total contracted renewable capacity through the Independent Electricity System Operator (IESO) under the FIT program up to the end of March 2018 [7]. At 58.9 % and 37.5 %, respectively, wind and solar systems each represent a significant share of these contracted capacities. Contracts for microFIT projects are offered only after the projects have been built and are ready to be implemented into commercial operation; the majority of projects are related to solar systems. Total contracted capacity under the microFIT program for solar and wind systems are 242.4 MW and 20 kW, respectively. All microFIT contracts are either ground-mounted or rooftop-mounted solar mounted projects.

Table 1-1 Contracted Capacity Under the FIT Program [7]

Categories	Contracted Capacity (MW)				Total Capacity (MW)	Capacity %
	Small FIT <sup>1</sup>		Large FIT <sup>2</sup>			
Fuel Category	UD <sup>a</sup>	CO <sup>b</sup>	UD	CO		
Bio-energy	10.5	11.2	0	35.5	57.2	1.19
Hydroelectricity	4	0.5	42.7	63.5	110.7	2.3
Solar	382.7	504.1	0	917.2	1804	37.55
Wind	0.6	1	693.5	2,136.5	2831.6	58.94
<b>Total</b>	<b>397.8</b>	<b>516.8</b>	<b>736.2</b>	<b>3152.7</b>	<b>4803.5</b>	<b>100</b>

UD<sup>a</sup>: Under development.

Small FIT<sup>1</sup>: Projects less than or equal to 0.5 MW.

CO<sup>b</sup>: Commercial operation.

Large FIT<sup>2</sup>: Projects greater than 0.5 MW.

As a result of the rapid movement toward the implementation of Ontario's strategic supply mix plans and the provision of clean generation resources, on April 15, 2014, the Ontario government announced that the province was officially coal-free, with the last coal-fired power plant, the Thunder Bay Generating Station, having burnt off its final supply of coal. However, after several years of implementation, the FIT and microFIT programs are no longer accepting further applications from distributed generation units (DGs). December 2016 marked the end of the FIT program in Ontario, and the microFIT program finished in December 2017 [8]. These regulatory changes thus necessitate innovative planning models to enable local distribution companies (LDCs) to facilitate the integration of DGs into the grid in the absence of government subsidies. A demand also exists for planning models that can respond to independent private investment in power generation and distribution systems under the deregulation frameworks [9].

Its close proximity to consumers and its lower operating voltages make a power distribution system a favorable place for integrating renewable-based DGs: the costs associated with DG integration at the point of common coupling are therefore reasonable compared with those for a transmission system. Integrating DGs into distribution networks offers a number of advantages: they provide a base load operating in parallel with the distribution network; they provide energy during peak loads; they support the distribution network; they improve power supply quality, thus eliminating fluctuations; they serve as backup to ensure an uninterrupted supply of electricity; and they are self-supplying through the use of renewable energy. Currently, electric energy can be injected by end-customers, electrical industries, or third parties; thus, the required distribution system demand can be partially or totally met by DGs from the customer side of the sub-distribution and distribution nodes. In Ontario, as of June 2018, the total contracted capacity connected to the distribution systems for wind-based systems in commercial operation was 590.5 MW while 19 MW remained under development, for a total capacity of 609.5 MW. On the other hand, the total contracted capacity connected to distribution systems for solar-based systems in commercial operation was 2,057.3 MW, with 424.5 MW remaining under development, for a total capacity of 2,481.9 MW [7].

Distribution system utilities are eager to provide for their own customers' need for energy by utilizing new technologies and suitable options while bearing in mind the goal of capturing the optimal benefit for the business. Indeed, due to the particular characteristics and radial structure of a distribution system, the majority of interruptions experienced by customers take place at that level [2]. Several obligations for utilities have been introduced by regulators as a means of maintaining an acceptable level of reliability [10]. In October 2012, for example, the OEB outlined a Renewed Regulatory Framework for Electricity (RRFE) in which system reliability performance plays a critical role [11]. The Government of Ontario has also directed the IESO to coordinate standards development activities with the North American Electric Corporation (NERC) and the Northeast Power Coordinating Council (NPCC) through the Ontario

Reliability Compliance Program (ORCP). The result of measures is that each utility must report two major reliability indices: a system average interruption frequency index (SAIFI) and a system average interruption duration index (SAIDI). The OEB, as a regulator, assesses the performance of each power distribution utility through a scorecard that includes these system reliability indices [11]. According to the performance and costs of the utility, as described in its rate application, the OEB sets “just and reasonable rates” that utilities may collect from ratepayers for the services provided. Any proposal from utilities that wish to increase their rates and pricing schemes in order to seek a higher rate of return must therefore be justified. This process means that distribution system utilities, which are in fact working hard to survive in the competitive electricity market, must devote substantial effort to finding cost-effective expansion and reinforcement plans for future investments while still adhering to the imposed regulations [12].

In addition to providing numerous technical and environmental advantages, DG units are expected to play a pivotal role in addressing problems associated with distribution system expansion planning (DSEP). DGs have also been proven to enhance overall system reliability by serving loads affected by unplanned outages. However, a look at current distribution utility practices reveals that most LDCs are unwilling to invest in DG technologies because of two primary obstacles. First, distribution utilities, which, as mentioned, are struggling to keep afloat in the competitive electricity market, have been subject to massive cost-cutting measures that have drastically reduced their capital budgets [13]. This shortage of funds plus the high initial costs of DGs deter LDCs from investing in these units [14]. Second, from a regulatory perspective, in many countries, an unbundling rule for electricity market participants requires LDCs to be legally separate from generation facilities, thus in effect preventing LDCs from owning DGs [15], [16]. The result is that, in the majority of cases and as a dominant practice, DGs are owned and operated by private investors. The ultimate goal of these parties is to capture all possible profit from their business, regardless of whether the locations of their projects are beneficial for the grid, for example, with respect to deferring upgrading decisions, enhancing system reliability, or reducing losses. The key question is therefore how distribution utilities can take advantage of such DG projects and direct their integration to specific locations that will benefit the system. This thesis presents innovative planning models that provide answers to these questions and help LDCs overcome the above obstacles.

A further factor is that when distribution networks accommodate non-dispatchable DGs, they must also deal with the high degree of uncertainty associated with this type of generation. The stochastic nature of wind speed and solar irradiance may lead to technical concerns such as frequency deviation, high reverse power flow, and bus voltage violation. These issues could also extend to affecting the economic side of the investments as well with respect to determining costs and revenue. For this reason, distribution system utilities require probabilistic models that can handle the uncertainty that arises from the intermittent nature

of system demand, wind speed, and solar radiation.

## 1.2 Research Objectives

The following were the main objectives of the research presented in this thesis:

- Develop a new expansion planning model that will enable smart distribution systems to identify in the timeliest and most economical manner the optimal investments required in order to satisfy the forecasted growth in demand for the period of the planning horizon. The developed model needed to include consideration of the following:
  - Because DGs are investor-owned, LDCs must determine the optimal DG capacity and location, and the appropriate incentive prices to be offered in order to ensure the profitability of the investors' projects.
  - The developed model must include provision for the LDC to have the opportunity to identify the least costly solution from a variety of planning alternatives (e.g., installing DGs, upgrading or constructing new substations, upgrading or constructing new lines, and/or reconfiguring the system).
  - The intermittent nature of wind speed, solar irradiance, and system demand must be treated probabilistically and incorporated into the model so that uncertainty can be taken into account.
- Develop an analytical model for evaluating the reliability of power distribution systems in the presence of controllable and renewable-based DGs. The model must take into account restoration analysis and the possibility of islanded mode of operation. It should also include consideration of the uncertainty caused by variations in the demand and in wind and PV output power.
- Develop a reinforcement planning model for enhancing overall distribution system reliability and maintaining reliability measures within applicable regulatory standards in the presence of DGs. The developed planning model should be able to identify the optimal allocation of tie lines and normally open (NO) switches as well as the required upgrade capacities of feeders and substations. The model also includes two proposed hierarchical levels for system operation under contingencies.
- Develop a generic distribution planning model for minimizing the total planning cost while achieving an acceptable level of system reliability. The concept of generation sufficiency for dynamic virtual zones is introduced as a means of tackling system reliability issues. The model should include consideration of the fact that DGs are owned by private investors, and that the

incentive prices offered to those investors should therefore be distributed based on their contributions to reliability enhancement and the deferment of upgrade decisions.

### **1.3 Thesis Outline**

The remainder of this thesis is organized as follows:

**Chapter 2** reviews basic background information about power distribution systems, including the definition of DG and explanations of wind- and PV-based technologies. Traditional and modern distribution system planning fundamentals and associated literature surveys are also presented in this chapter, which concludes by addressing the evaluation of power distribution system reliability.

**Chapter 3** introduces the proposed incentive-based multistage expansion planning model for smart distribution systems. The chapter begins with a description of the modeling of the uncertainty associated with the load and with DG components. The problem formulation for the proposed model is then explained, following which, the linearization methods used in the model are highlighted. The numerical results obtained for the case studies conducted are reported, and the last section summarizes the research, presents conclusions, and reiterates the primary contributions of the research.

**Chapter 4** presents the distribution system reinforcement planning model for improving system reliability. The probabilistic operating scenarios for the system are first described, followed by an outline of the methodology for evaluating distribution system reliability in the presence of renewable-based DGs. The problem formulation for the reinforcement planning model is introduced, along with the proposed reliability evaluation approach. Case studies and numerical results are then reported, and the final section offers concluding remarks.

**Chapter 5** details the proposed incentive-based distribution system planning that incorporates reliability and includes consideration of generation sufficiency for dynamic virtual system zones. Descriptions are provided for the proposed general planning framework, the planning problem formulation, and the reliability evaluation approach. The case study and its results are then reported, and the chapter ends with concluding remarks.

**Chapter 6** summarizes the research presented in this thesis and provides conclusions, primary contributions, and possible directions for future work.

## Chapter 2

### Background and Literature Survey

#### 2.1 Introduction

There is no doubt that electric energy has become an imperative need in our daily life. In fact, electric energy is considered the main foundation of present day civilization and the development of countries. Electric energy has been given pride of place among other energy types with the most auspicious innovations in technology aiming to transform electric energy into a desired form. This high importance of electric energy has led the stakeholders and policymakers in power system sectors to unbundle the regulated monopoly structure of the power system into a deregulated competitive market in order to maximize the overall system efficiency. One of the essential components in power system structure is the distribution system.

The structure of power system includes three major components of generation, transmission, and distribution. Of these components, the distribution system has been characterized as the second most expansive part in the grid [17]. Its related costs constitute a significant percentage of the total investment costs following the costs associated with generation. Over the past two decades, investments by investor-owned utility in the distribution level in the United States have increased to reach almost \$19 billion by 2013, which is more than the investments of the late 1990s and early 2000s by nearly 46.2% [18]. Moreover, it is estimated that the investments in the electricity grids in European countries will require €600 billion by 2020, and 75% of these investments will be spent in distribution levels [19]. In essence, the vast investments involved in distribution networks are costly, and thereby dictate very careful planning and operation.

The primary function of distribution system planning is to assure that the forecasted growth in a system's demand can be met adequately and economically. In the past, planning in the power distribution level has not been given much consideration as generation and transmission systems [17]. However, with the rapid growth of system demand, the deregulated competitive market, and the new era of smart grid notion, the task of distribution system planner has become increasingly complex. Indeed, this task necessitates comprehensive economic planning tools that provide a feasible solution among a variety of available alternatives and resources in order to deliver the power to the ultimate customers in a reliable, affordable, and sustainable way. Distribution system in general should be addressed with much care due to its close proximity to the customers, its responsibility for most of the system's losses, its high degree of faults interruptions, and its high investment cost.

This thesis explores a new aspect of distribution system planning in the context of smart grid. A brief summary of distribution system's definition, configuration, and main components are presented in section 2.2. Section 2.3 provides a general idea of distributed generations (DGs) definition, types, and benefits to the grid. A comprehensive description and survey for traditional and modern distribution planning are presented in section 2.4. Section 2.5 and section 2.6 outline the distribution system's reliability analysis and the models proposed in the literature to evaluate the system reliability in the presence of DGs. Section 2.7 summarizes this chapter.

## **2.2 Power Distribution Systems**

The bulk of electric power is traditionally generated from power plants located far away from the load centers and delivered to the customers through transmission lines. Due to technical and economic considerations, the bulk power is transmitted at high voltage levels typically 230kV or higher at transmission systems and ranging between 69kV and 138kV at sub-transmission systems. Power distribution systems classically begin from the substations that are served from transmission or sub-transmission lines. Distribution systems primarily consist of two main parts, namely distribution substations and feeders.

The primary role of distribution substation is to step-down the voltage of transmitted power to lower levels. The most common standard voltage ratings in distribution systems are 34.5 kV, 23.9 kV, 14.4 kV, 13.2 kV, 12.47 kV, and 4.16 kV for old systems [20]. Each substation contains protective switch systems for both high and low voltage sides, voltage transformers, voltage regulation system, and metering systems. Power transformers should be protected against the occurrence of short circuits, and this protection is attained by using a variety of protection devices and schemes. Voltage transformers are solely responsible for step-down voltage transformation, and each substation may typically have two or more three-phase transformers. Voltage regulation system is utilized to maintain the voltage at the lower side of the transformer with the variation of the load within an acceptable limit. Load tap changing transformer usually performs this function by adjusting the taps on the low-voltage windings of the transformer. Moreover, most transformers are also equipped with fixed taps at the primary side to respond to any voltage variation from the source. In addition, distribution substations have metering systems comprised of either digital or analog devices to measure, record, and monitor different quantities including voltages, currents, active and reactive power, and substation power factor.

Primary distribution system feeders convey the power from the substation to each load point in the primary distribution system such as industrial loads or to the secondary distribution systems through distributed transformers and laterals. Each substation may have one or multiple outgoing primary feeders. Figure 2-1

shows a simple distribution system feeder with all major components. The main components in distribution feeders may include the following [20]:

- 1- Three-phase primary main feeders and secondary systems.
- 2- Three-phase, two-phase, and single-phase laterals.
- 3- Voltage regulators and shunt capacitor banks.
- 4- In-line and distributed transformers.
- 5- Three-phase, two-phase, and single-phase loads.

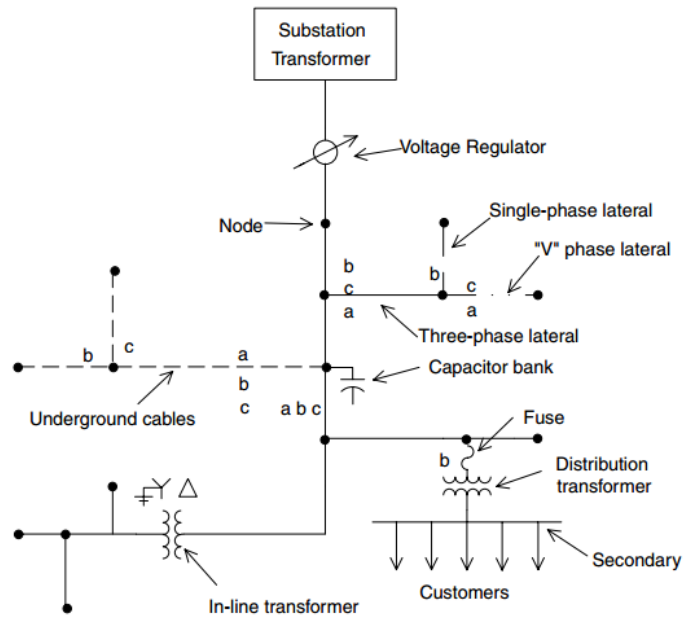


Figure 2-1 Distribution system feeder [20]

Popular distribution system circuits' configurations include radial, loop, network, and a combination of these. Radial configuration (as shown in Figure 2-1), where the power flows from substation towards the loads in one path, is the most used design in practice due to its simplicity, lower associated costs, and ease in operating and maintaining the system. However, this configuration suffers from low system reliability and service continuity. In contrast, loop configuration provides higher service reliability than the radial system. Its associated costs are relatively higher than the costs of the radial systems since loop configuration requires a considerable increase in system equipment capacities and more additional components. Network configuration yields the highest service reliability because in this configuration, each loop is supplied from different bulk sources. The cost of this design is definitely highest among all system configurations since it requires costly power flow control and complicated protection schemes. The research presented in this thesis is concerned with the primary distribution system with radial configuration.

## 2.3 Distributed Generation

In a centralized power system, electrical power essentially flows in one direction from the central power plants, throughout the transmission systems, and ending up at the distribution control centers to reach the end users. However, with deregulation, small scale generating units - called distributed generators (DGs) - can be located in the distribution levels and even at the customer sides to feed their own demand or their neighboring loads. DGs are defined as “*the installation and operation of electric power generation units connected directly to the distribution network or connected to the network on the customer site of the meter*” [21]. However, the types of DGs as well as the owners of these DGs are disregarded in the aforementioned definition. Nevertheless, many researchers suggest that each utility should have its own definition which depends on the conditions of the network. Table 2-1 illustrates a suggested classification for different capacities of DGs [21].

Table 2-1 Various DG Capacities [21]

Class	Capacity
Micro DGs	1 W < 5 kW
Small DGs	5 kW < 5 MW
Medium DGs	5 MW < 50 MW
Large DGs	50 MW < 300 MW

### 2.3.1 Distributed Generation Benefits

Distributed generation is able to provide numerous benefits to the system [22]. Indeed, these benefits could be clustered into three categories of technical, economic, and environmental advantages. When the distributed generation units are properly located and sized in the distribution systems according to adequacy and security regulations, these devices are expected to provide a positive credit to the overall network. These technical advantages involve reducing power losses, improving system reliability, improving voltage levels, enhancing network security, alleviation of congestion at substations and conductors, and improving the system's overall efficiency and quality. Economic benefits gained from installing DGs play a crucial role in reducing power system expenses for either long term or short term planning horizons. Thus, power system utilities are attempting to provide electricity to all consumers at low cost. The economic benefits of DGs include deferring the investments for system upgrades or expansions, reducing operating costs, minimizing the consumption of fossil fuel that leads to decreases in energy prices, and minimizing the cost of maintenance and spinning reserve requirements. Another strong motivation behind employing DGs in power networks lies in their environmental benefits. According to a report illustrated in [22], carbon dioxide emissions have dramatically decreased by 30% in only a three-year period in the Danish power system due

to the wide spread use of renewable-based DGs in the country. Furthermore, wind turbines, PV modules, and hydro turbines are non-polluting and have a high degree of sustainability.

### 2.3.2 Distributed Generation Technologies

Depending on the type of primary fuel source for the distributed generation, these technologies are classified into four categories [23]. The first category is called conventional technologies. Diesel generators, an excellent example of conventional technologies, are usually located in remote areas. Advanced fossil technologies form the second category of these technologies. Advanced fossils contain fuel cells which are mainly fueled by hydrogen in electrochemical power conversion. In addition to fuel cells, micro-turbines, which are fed by natural gas, are another form of advanced fossil technologies that is based on cyclic gas processing. Renewable technologies play a key role among these technologies since they are natural, sustainable, and conservative for the environment. These technologies include wind turbines, hydro turbines, photovoltaic modules, tidal systems, geothermal technologies, and solar thermal systems. The degree of uncertainty in these forms of energy is relatively high. Some technologies that are able to increase the system's overall efficiency such as energy storage and combined heat and power systems could be considered efficient technologies. Since the research in this thesis is concerned with renewable-based DGs, a brief introduction of wind and photovoltaic-based solar energy is presented.

#### 2.3.2.1 Wind Power

Wind, which is generated by heat differences between different areas of the earth's surface, has been used as a source of energy for many years. The availability and usage of wind energy differs from location to location throughout the world. Recently, the kinetic energy of the wind has drawn global attention as a natural source to generate electricity. For this use, wind farms are scattered throughout the world to convert the wind that drives turbine blades into mechanical energy. The movement in the blades results in shaft rotation which drives a generator, and this generator converts the mechanical energy into electrical energy through an electromechanical conversion process.

Weibull probability distribution function (PDF) is one of the probability distributions that are able to model the complicated continuously varying variables. It is commonly and extensively used to model many events including wind speeds. Weibull PDF is driven by two parameters which are shape index  $k$  and scale index  $sc$ . The mathematical model for Weibull PDF is defined by (2.1), as in [24], [25].

$$F(v) = \left(\frac{k}{sc}\right) \times \left(\frac{v}{sc}\right)^{k-1} \exp\left[-\left(\frac{v}{sc}\right)^k\right] \quad (2.1)$$

The parameters of Weibull PDF are calculated using the mean  $v_m$  and standard deviation  $v_\sigma$  of wind speed data. The shape index  $k$  and scale index  $sc$  of Weibull distribution can be obtained using (2.2) and (2.3).

$$k = \left( \frac{v_\sigma}{v_m} \right)^{-1.086} \quad (2.2)$$

$$sc = \frac{v_m}{\Gamma \left( 1 + \frac{1}{k} \right)} \quad (2.3)$$

The cumulative distribution function (CDF) for Weibull distribution is given in (2.4):

$$CDF(v) = 1 - e^{-\left(\frac{v}{sc}\right)^k} \quad (2.4)$$

The active power generated from wind turbines  $P_w(v)$  as a function of wind speed  $v$  can be obtained using (2.5), as in [24], [25].

$$P_w(v) = \begin{cases} 0 & 0 \leq v \leq v_{ci}, v \geq v_{co} \\ P_{rated} \times \frac{v - v_{ci}}{v_r - v_{ci}} & v_{ci} \leq v \leq v_r \\ P_{rated} & v_r \leq v \leq v_{co} \end{cases} \quad (2.5)$$

where  $v_{ci}$ ,  $v_r$ ,  $v_{co}$  are the cut-in speed, rated speed, and cut-off speed of the wind turbine, respectively.

### 2.3.2.2 Photovoltaic Power

Photovoltaic (PV) power conversion is a process whereby sunlight (solar irradiance) is captured by semiconductor material and converted into electrical charges (current) via solar cells. More than 80% of photovoltaic cells in the world are made from silicon as a reliable and long term provider of services [26]. The production is still ongoing to produce efficient cells at low production cost. Generating power from photovoltaic modules has many advantages such as low operation and maintenance costs, zero noise due to stationary and static parts, light weight, high reliability, long lifetime operation, and short lead times for installation. Technically, PV modules are composite solar cells which are connected in series to increase the voltage, or in parallel to increase the current and therefore the output power. PV modules are the basic units of photovoltaic systems. A photovoltaic panel is composed of multiple wired modules, and it is the basic unit of a photovoltaic array. These arrays are then connected to power conditioning units to convert the DC output into AC output in order to match these units with the grid system.

Beta PDF is utilized in a wide range of applications. It has been used in the literature to model the randomness of solar irradiance. Beta PDF is driven by two parameters as well. The mathematical model for

Beta PDF is defined by (2.6), as in [25]:

$$F(s) = \frac{\Gamma(\alpha + \beta)}{\Gamma(\alpha)\Gamma(\beta)} \times s^{\alpha-1} \times (1-s)^{\beta-1} \quad (2.6)$$

$$\beta = (1 - s_m) \left[ \frac{s_m(1 + s_m)}{s_\sigma^2} - 1 \right] \quad (2.7)$$

$$\alpha = \frac{\beta \times s_m}{1 - s_m} \quad (2.8)$$

where  $F(s)$  is the Beta PDF of solar irradiance  $s$ ,  $s$  represents solar irradiance in  $\text{kW/m}^2$ , and  $\alpha, \beta$  are parameters of the Beta PDF.  $s_m, s_\sigma$  are the mean and standard deviation of solar irradiance, respectively.

The active power generated from PV modules  $P_{PV}(s)$  as a function of solar irradiance  $s$  is given in (2.9)-(2.13), as in [24], [25].

$$T_c(s) = T_A + s \left( \frac{N_{OT} - 20}{0.8} \right) \quad (2.9)$$

$$I(s) = s[I_{sc} + K_i(T_c(s) - 25)] \quad (2.10)$$

$$V(s) = V_{oc} - K_v T_c(s) \quad (2.11)$$

$$FF = \frac{V_{MMP} \times I_{MMP}}{V_{oc} \times I_{sc}} \quad (2.12)$$

$$P_{PV}(s) = N_m \times FF \times I(s) \times V(s) \quad (2.13)$$

where  $T_c(s)$  is the cell temperature, in  $^\circ\text{C}$ , at solar irradiance  $s$ ;  $T_A$  is the ambient temperature, in  $^\circ\text{C}$ ;  $K_v$  is the voltage temperature coefficient  $\text{V/C}$ ;  $K_i$  is the current temperature coefficient  $\text{A/C}$ ;  $N_{OT}$  is the nominal operating temperature of the cell, in  $^\circ\text{C}$ ;  $FF$  is the fill factor;  $N_m$  is the number of modules;  $I_{sc}$  is the short circuit current, in  $\text{A}$ ;  $V_{oc}$  is the open circuit voltage, in  $\text{V}$ ;  $I_{MMP}$  is the current at maximum power point, in  $\text{A}$ ;  $V_{MMP}$  is the voltage at maximum power point, in  $\text{V}$ .

## 2.4 Power Distribution System Planning

With ever growing population rates and industrial market competition, power consumption and demand for the electric energy has simultaneously increased. This has placed considerable pressure on system designers to evaluate and address a suitable number of expansion planning alternatives in detail to cope with these changes. Thus, the prime key function of distribution system planning is to ensure that the expected growth

in power demand can be met in a timely manner by adopting certain additions to the grid in adequate, reliable, and economical ways. Once system planners forecast the demand for their location of interest for a specified period of time (typically 5-20 years), then they perform load flow and short circuit analyses to ensure that all system's components will operate within their thermal capacity and capability limits as well as to ensure satisfaction of system operating standards such as voltage operating ranges. If the operating standards have not been met, then the planners dictate when and where the expansion and reinforcement plans should be placed. The planners usually select from a variety of available alternatives based on least-cost criterion using different mathematical formulation and solution techniques. The optimal alternative selection is achieved after constructing a cost function that includes the present-worth value of investment costs for the proposed alternatives and their operation and maintenance cost as well as the operation cost of the system which may involve system losses and reliability associated costs. So, distribution planning process mainly comprises five main stages [17]. After determining the nature of the problem in stage 1, the planner should clearly identify the primary and secondary goals of the planning. Primary goals are mainly concerning the economic side while the secondary goals are targeting the technical constraints. Stage 3 and stage 4 involve the determination of the available and suitable planning alternatives and evaluating these options technically and economically. The best alternatives are selected in the last stage such that the least-cost solution is achieved. Figure 2-2 illustrates the process of distribution system planning and all stages involved. More importantly, planners must adhere to the company's policies and its obligations to the customers in the planning process.

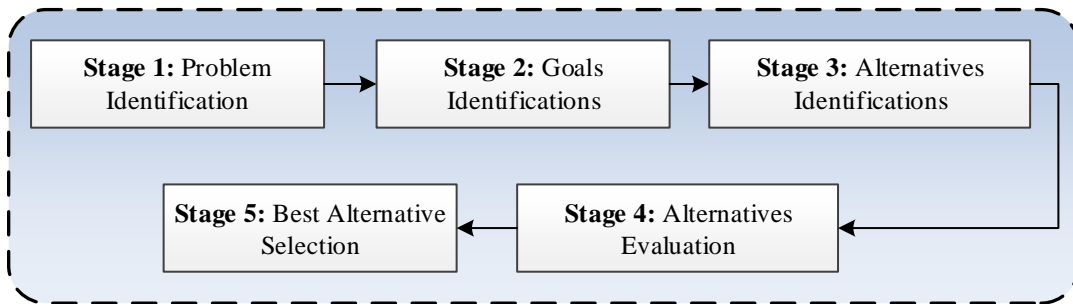


Figure 2-2 Distribution system planning stages [17]

### 2.4.1 Factors Affecting Distribution System Planning

Distribution system planning is affected by many factors, both direct and indirect [17], [27]. Direct factors are those factors that the planners have influence over; conversely, the factors which the planners cannot control are defined as indirect factors. Direct factors include but are not limited to load forecasting, planning horizon, available alternatives, system configuration, substation expansion, substation site selection, size of available equipment, and types of feeders required along with their routes and total cost. Indirect factors

are either difficult to predict or out of control; nevertheless, responsible planning engineers must take these into account. These factors involve equipment and labor costs, frequency and duration of interruptions, fluctuations in fuel markets, environmental and economic issues, weather variations, and social behaviors. Indeed, this wide range of explicit and implicit factors which the designer must consider makes the problem of planning somewhat complex.

#### **2.4.2 Distribution System Planning Models**

Several techniques and mathematical models have been introduced in the literature to handle the problem of distribution system planning. These methodologies and models vary in simplicity, accuracy, applicability to large systems, and computational burden. Linear and non-linear modeling for objective functions, which are mainly comprised of fixed and variable costs for such facilities, and system constraints are introduced and solved using linear, non-linear, mixed integer, and mixed integer nonlinear programming techniques [28]. To deal with discretization in the model, models such as branch-and-bound as well as branch-exchange have been introduced [29], [30]. Metaheuristic approaches like genetic algorithm [31], simulated annealing [32], tabu search [33], ant colony [34], and some evaluative algorithms are utilized in DSP. Most of these approaches depend upon tuning parameters and generating a large population which may lead to a huge number of unfeasible solutions, thereby increasing the execution. Heuristic techniques have also been introduced to expedite the process of solution and handling of a large system as well as ensuring system radial topology. The problem of DSP can be static, where the planning is obtained for a single period of time; or dynamic where a series of planning horizons are considered.

#### **2.4.3 Traditional Distribution System Planning**

Traditional distribution system planning is characterized by identifying the proper placement and sizing of substations and feeders. The distribution system planner somewhat has a limited number of alternatives in this category to meet the expected demand growth. Substation upgrade capacity, feeder upgrade capacity, and system reconfiguration are comprising the main planning decisions of the traditional planning. Figure 2-3 presents the general planning framework for traditional DSP. Exploring the planning models and methodologies that have been addressed in the literature is essential step for the planner. Therefore, this section discusses the previous work that has been devoted for solving the traditional distribution system planning problem.

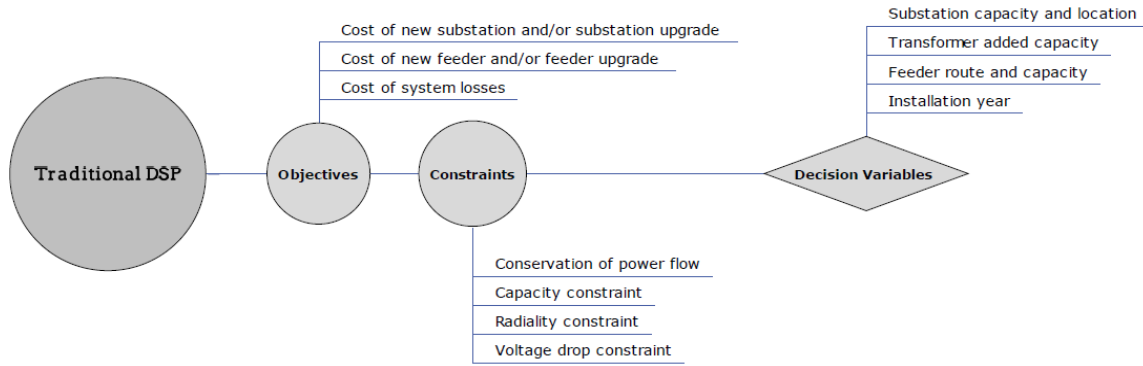


Figure 2-3 Traditional DSP model

The authors in [35] proposed a mixed integer linear programming model in order to optimally design the sub-transmission systems (substations capacities) and select the best conductor sizes and layout for low voltage networks. Branch-and-bound technique with fixed cost transportation model has been utilized to solve the problem while incorporating both security constraints and a linearized cost function for system losses. Moreover, the best timing for such investment is determined. The problem of distribution system planning is solved in two stages in [36]. In the first stage, by using mixed integer programming, the decision of optimal capacity and timing of expanding a substation are obtained. Load transfer is optimized in the second stage using a transportation model to manage the excess substation capacity obtained from stage one. Total substation expansion cost and load transfer cost yield the least cost expansion plan. In [37], the authors used the concept of minimum feasible distance (MFD) between each substation and potential load at each sector as an input for a transportation model. The model was used to minimize the total construction cost by defining the optimal location and capacity for substations as well as their operating boundaries. The work presented in [38] optimized the substations' sites and feeders' routes inspired by capacitated transportation model. The transportation model was solved at each node of branch and bound tree. To handle the complexity of such a large problem, a post-optimization analysis was carried out to ensure radiality and the inclusion of all fixed routes. A large number of associated costs were incorporated in the model as well.

Substation size, feeder size, and loading limits are determined in [39] using a compromised model for different cost factors. The authors extended their work in [40] to optimize the position, capacity, and timing of distribution substation as well as determine the optimal layout of the feeders using a quadratic mixed integer programming. The problem is solved through two phases, where the first phase fixed the substation size, and the second phase determined the best feeder elements and routes. The research presented in [29] used branch-and-bound and fixed charge linear transshipment model (FCNP) to find the optimal capacity, location, and configuration for substations. Shortest path method has been utilized to obtain the lower bound

of the results, and the minimal incremental cost for power flow has been the used to determine the upper bound. The authors in [41] used an iteration-based method to solve the time-phased planning problem incorporating a concave fixed cost model for substation and large feeders and linear cost model for the rest of the elements. The suggested algorithm was solved utilizing branch-and-bound technique as well as a transshipment model. An improved branch-exchange algorithm is used in [30] to optimally design the configuration of a green-field low voltage system. A heuristic Euclidean Steiner trees algorithm has been adopted in the methodology to minimize the total cost of investment, losses, and supply quality.

Owing to advances in computer technologies and storage capabilities, the authors in [42] modeled the problem of distribution planning using mixed-integer programming and solved the problem using MPSX package. The design variables include substation locations, transformer sizes for each substation, incremental capacity of existing transformers, load transfer among substations and load centers, and feeder routes. By using cost linearization models and some logical constraints, the present worth of the total costs involved is minimized. The authors then extended the proposed model to become a multi-stage model in [43], [44] which includes the timing for such investments while assuming that the network will be expanded from the results of base year through the terminal planning year. The work presented in [45] used an advanced sparsity-based mixed integer linear programming model and a heuristic partitioning method for optimal substations and primary feeders planning including year of commissioning after studying the planning period as a single stage. The model gave more detail for limited sized problem and approximated analysis for large systems. The model explicitly includes time-dependent fixed and variable costs as well as a step-wise approximation for feeder losses costs.

The problem of large scale distribution system expansion is solved in [46] through two phases using the concept of long range horizon planning and intermediate year expansion pattern. In the first phase, the planning problem is solved for the terminal year in order to encounter all of the components required during the planning period. This is entitled “horizon year static optimal system”. In the second phase, the load growth is explicitly considered, and the required systems in each of the intermediate years are exclusively selected from phase one result of “successive concatenated single year expansions”. FCNP model and branch-and-bound are incorporated to solve the problem with fixed and variable cost modeling of components. This method was extended in [47], where the voltage drop constraints are considered; and in [48] where accurate representation for non-linear planning costs are incorporated. The authors in [49] applied a heuristic method comprised of five phases to solve the dynamic planning problem. Backward and Forward methods, inspired by horizon year static optimal system proposed in [46], are used in phase one and two, respectively in order to find the optimal set of required projects and the optimal timing for each project. Phase three is applied to reduce the costs resulting from stage two by postponing different projects.

Dealing with radiality and taking the exact loss function are used in phases four and five, respectively.

The integration of geographic information system (GIS) with a stochastic load forecasting module is introduced in [50] to facilitate these technologies in distribution system's long and short range planning. Moreover, the effect of secondary systems on overall system primary planning is addressed in [51], and an integral primary-secondary distribution system planning is introduced. The work presented in [52] proposed an optimal single-period horizon-year design encompassing all distribution design requirements for primary and secondary systems for the objective of minimization total cost per customer. The model considered a substation serving a circular sector of a round area through tree-link feeders and laterals. The authors in [53] approximately solved the distribution system planning problem using branch-exchange method and pivot operation after introducing simplex tableau. Mixed Integer Programming (MIP) model is converted to a set of linear equations at each branch exchange operation, followed by pivot operation to determine the most sensitive branch to optimize the objective function. A heuristic forward/backward algorithm alongside the branch-exchange method is proposed in [54] for the sake of solving multi-year distribution system expansion problem. Although the proposed method provides an approximate result as well as trapping the algorithm in a local minimum, the outcomes of the method are obtained quickly. In order to enhance the efficiency of the algorithm, the authors also proposed in [55] a multi-stage branch-exchange, where more accurate solution is obtained.

A power distribution system is designed in [56] through a two-stage process. The first stage dealt with load growth forecasting where the decomposition method is applied after clustering the service area into small zones to investigate different load patterns. Next, a multi-year expansion was carried out in stage two utilizing the method proposed in [46]. The work presented in [57] proposed a generalized framework for large distribution system planning using an improved genetic algorithm. The problem is split into two phases. Phase one optimizes the capacity and location of MV substations based on loss characteristic matrix while in phase two, the HV substation and feeder routes are attained. A constructive heuristic technique is used in [58] to design the configuration of the distribution system. A concept of relaxed binary variables to convert the MBNLP model into NLP as well as substations and feeders' sensitivity indices are utilized to form the heuristic method. A branching technique and also a local improvement technique are utilized to enhance the algorithm.

Based on directed graph theory and the concept of principle of optimality, the authors in [59] found the optimal feeder routing from substations to load centers. The authors first determined the locations and capacities of substations and all possible paths that energize such a load center, and then the optimal path for each node was attained based on minimum cost criterion. The downsides of this method include the

high computational burden for a large system which requires determining terminal nodes that may not lead to a global optimum solution.

#### **2.4.4 Distribution System Planning in the Smart Grid Paradigm**

The notion of modern distribution system actually arose following the advent of deregulation and privatization in power system sectors. In vertically integrated traditional power systems, there was one entity that planned for the entire system including generation, transmission, and distribution systems. However, these plans are no longer acceptable with deregulation employment where each entity is responsible for planning its territory or area of control to maximize its profit. Therefore, local distribution companies engaged in bilateral contracts with other participants in the market so as to efficiently meet their local demand while the uncertainty in the electricity market could affect the planning outcomes. LDCs in deregulation environment would also buy excess power from their neighboring LDCs.

Recently, power distribution systems are hosting and accommodating high penetration level of renewable-based distributed generations. The active integration of renewable energy sources, storage systems, electrical vehicles, customer participation in demand response programs and willingness to pay based on system performance, smart meters, and communication and automation systems has shifted the traditional and modern distribution systems towards what is called *smart grid*. Figure 2-4 presents the general planning framework for DSP in smart grid paradigm. Deregulation and smart grid transition complicate the planning process and put much effort on system planners to address the various arising issues, and therefore achieving reliable and economic plans. Distributed generations are characterized as one of the main components of smart grid, and system planning in the presence of DGs necessitates innovative planning models and powerful tools. The fact that there are several key players in distribution systems including DGs investors should be taken into consideration. Besides, the bidirectional of power flow and the uncertainty of DGs output power and system demand may lead to inappropriate solutions; therefore, robust planning models have become more essential and mandatory for such plans to be implemented. The imposed regulations towards reducing greenhouse emissions and enhancing system reliability should be adhered and taken into account throughout the planning process in smart grid era.

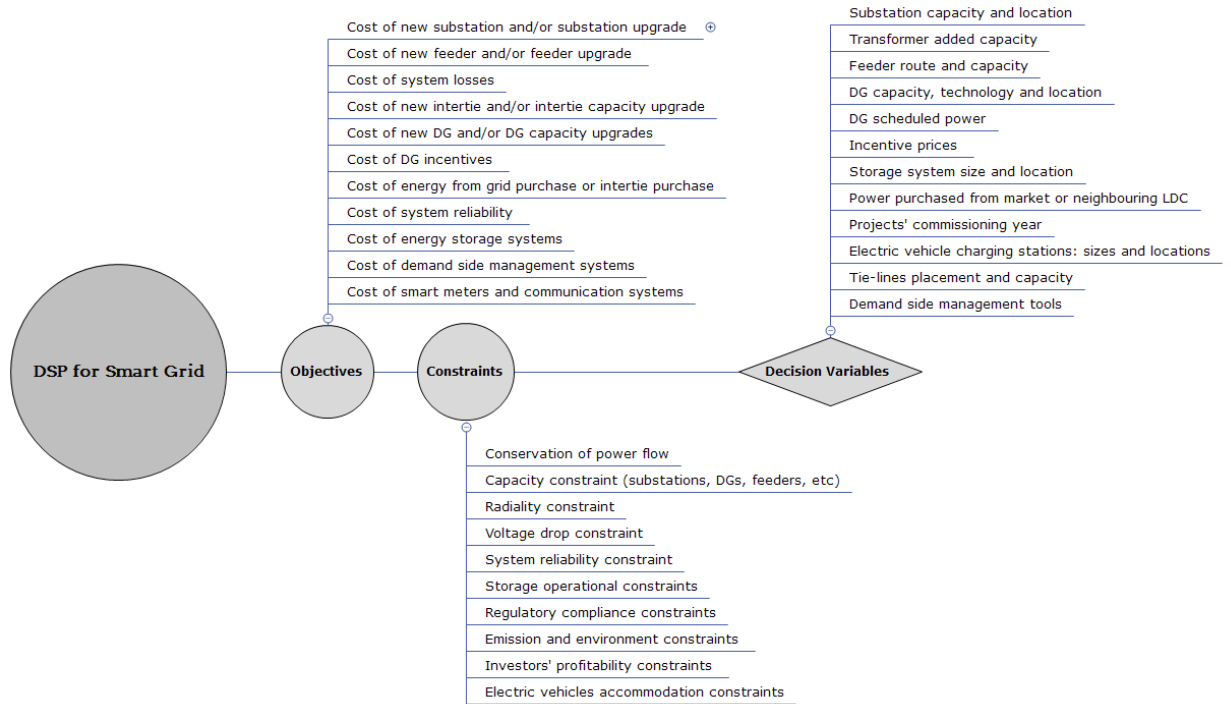


Figure 2-4 DSP in smart grid paradigm

### 2.4.5 The Inclusion of System Reliability in Distribution System Planning

System reliability, in simple words, means continuity of service to the utility's customers or "*the ability of power delivery system to make continuously available sufficient voltage, of satisfactory quality, to meet the customer's needs*" [60]. In the late 18<sup>th</sup> century and early 19<sup>th</sup> century, the interruption in power service was viewed as a loss of revenue where the cost of energy sold was reduced. However, this viewpoint has changed starting in the 20<sup>th</sup> century and onward. With the advent of system automation and installing SCADA components, it became easy to gather and maintain detailed records on system performance including system interruption data, and this led to explicit numerical tracking for system reliability indices. Distribution system reliability came to be seen as a key obligation and priority of utility to its own customers, and the regulatory agencies issued a set of standard metrics to be fulfilled by utilities. The main four reasons for deploying reliability standards in distribution system planning are as follows [60]:

- 1- The increasing sensitivity of customer loads to poor reliability
- 2- The importance of distribution system to customer reliability as the final link to the customer
- 3- The large costs associated with distribution systems
- 4- Regulatory implementation of performance-based rates

For the aforementioned reasons together with the awareness of customers, regulators, and utilities to

the service interruption, the power industry moved toward setting reliability targets, planning for the fulfillment of these targets, monitoring the progress, and taking corrective actions. Distribution system reliability is a competitive advantage for utilities in the deregulation environments, and the system performance indices are frequently reported to the system regulators. Thus, it is very crucial to plan and design the distribution system reliably and economically, with regard to cost.

#### **2.4.6 Planning Models for Smart Distribution Systems**

As reported in the literature, the joint DSP problem, in which DGs are incorporated as key alternatives in addition to conventional options, has been addressed through the introduction of a number of techniques and mathematical models. Most of the research conducted in this regard has assigned the ownership of DGs to LDCs. For example, in the work described in [61], the distribution system was expanded by means of DG integration, system reconfiguration, switch installation, and rewiring. The possibility of performing dynamic planning based on a pseudo-dynamic procedure that included consideration of DGs as an alternative for LDCs was assessed in [34]. The authors of [12] and [62] explored several reinforcement techniques, such as dispatchable DGs, cross-connection feeders, and line and substation upgrades. Based on the assumed LDC ownership of the DGs, the objective was to minimize investment, operation, and reliability costs. The dynamic problem was solved using modified discrete particle swarm optimization: a significant reduction in transformer investment costs was observed. Similar work employing a genetic algorithm was reported in [63], with DGs, lines, and transformers considered as possible alternatives.

The same assumption underlies the study presented in [64], which involved the introduction of a heuristic method for distribution system expansion that utilizes dispatchable DGs, lines, and transformers. The required upgrade components and commissioning year were determined based on a benefit-to-cost ratio concept. Other researchers in [65] achieved two-level hierarchical distribution system planning that takes into account specific factors in a deregulated environment including regulatory policies, market prices, environmental considerations, and taxes. A joint expansion plan for distribution system networks and DG units was investigated in [66], and the planning model has been extended in [67] to incorporate system reliability and DG uncertainty. The authors in [68] proposed a multistage expansion planning model for smart distribution systems taking into account the reliability of the system. Algebraic expressions are utilized instead of using the simulation-based models to calculate the expected energy not served. Multistage long-term planning utilizing multiple alternatives such as voltage regulators, capacitor banks, and DGs was reported in [69].

In reference [70], the authors proposed a distribution system planning model in which all of the planning decisions in the primary and secondary distribution networks are coordinated. The use of low voltage

feeders/substations, medium voltage feeders/substations, and medium voltage DGs represent planning alternatives for the green-field network. The authors in [71] expanded the distribution networks by means of DGs' integration and feeders' reinforcement. The multiyear planning aimed to minimize the investment, operation, and emission costs over the planning period. The deployment of renewable-based DGs was investigated in [72] as an option to reinforce the grid considering the reactive power capability for these DGs. A risk-based optimization method was proposed in [73] to implement DGs as flexible real options for the purpose of large network investments' deferment. A multiobjective distribution planning model was proposed in [74] to minimize the investment, operation, and emission costs incurred by LDCs. A heuristic-based technique was used to obtain the DG planning decisions and evaluate all system savings due to deferment of investments. Pareto front solutions are constructed and the decision making is left for LDC preference.

The authors in [75] introduced a heuristic method to redesign the distribution network for the sake of maximal DG insertion. The proposed method is basically dependent on balancing the multiplication of feeder length and feeder flow for a set of feeders that connects each substation. Manual and automatic switches are installed to define the balanced boundaries. The method is applicable for meshed networks. The authors in [76] used a method called seeker optimization algorithm to optimize distribution system feeder routes with simultaneous placement of automatic reclosers considering weighted aggregation of total system economic cost, overall system reliability, system power losses and voltage deviation as an objective function. Static and dynamic distribution system planning with a multi-objective function comprised of total investment costs and total reliability cost is introduced in [77]. The problem is solved using genetic algorithm and Pareto-front optimal solution sets. The authors in [78] examined the effect of individual quality standards, maximum frequency, and duration of individual interruption on distribution system planning. Obeying individual reliability standards rather than using only system-based indices leads to lowering optimum system reliability. Maximal tradeoff effectiveness solution between customers' quality indices and system reliability is required.

The problem of installing sectionalizing switches simultaneously with network expansion is solved using Multi-Objective Reactive Tabu Search and Pareto optimal solutions in [33] to reach a tradeoff solution for investment costs and reliability costs. The authors in [31] solved the problem of distribution system planning considering short circuit capacity and short circuit ratio in the analysis. The authors in [79] intended to maximize the integration of distributed generators by enabling system reconfiguration, demand response, generation curtailment, and active reactive control. The effect of active DG integration on system upgrade, losses, and interruption costs are then studied. The authors in [80] developed an integrated

planning model considering the energy hub operation and installation of automation resources alongside system alternatives to minimize investment costs and maximize system reliability.

Besides the lack of a proper inclusion of the relevant planning aspects (i.e. absence of uncertainty inclusion, static planning, heuristic-based solution, and deficiency of diverse planning options), all previous researches reviewed so far were in common based on the assumption that LDC is solely responsible for purchasing and operating the DGs which is impractical as it is stated earlier.

Some researchers have addressed the problem of DSP by assuming that DG units belong to private investors. However, these models have been based on the assumptions that DG capacities, geographical locations, and capacity factors are known a priori (i.e. DGs are sized and allocated by investors initially), that the LDC has no control over such decisions which may lead to non-economical upgrade projects incurred by the LDC. Moreover, the bi-lateral financial agreements between DG investors as energy sellers and LDC as energy buyer are not considered, and that LDC and DG investor interaction is therefore nonexistent. For example, the authors in [81] determined the optimal sizes, quantities, and locations of distributed transformers and lines considering a three-phase power loss cost model in the objective function. However, the static model, which is solved heuristically, assumes DG locations and sizes exist initially in the grid and there is no financial interaction between LDC and DG investors.

The same assumptions and shortcomings underlie the research implemented in [82] which solves the distribution planning problem by combining modified load flow with graph theory based on a minimum spanning tree. Investment, losses, and operation costs are minimized. The concept of weighted edges obtained from multiplying edge investment, interruption, and losses costs and power flow is employed. The authors of [32] used an MILP model solved by simulated annealing in order to design a distribution system through a decomposition process. A Planning model for active distribution systems is presented in [83] and solved using a hybrid genetic algorithm–nonlinear programming approach. DGs are assumed to be private investments, and it can provide ancillary services for the grid. Total installation and operation expenditures are minimized while the satisfaction of system constraints is encompassed.

Another example in which LDC has no control over DG planning decisions, is the work presented in [84], which involved the coordination of multiple alternatives, including line/substation upgrades and capacitor bank/voltage regulator allocation. To carry out optimum multistage distribution system planning with DGs owned by investors, the authors of [85] extended the formal application of a linear disjunctive approach in their mathematical programming; however, the interaction between LDC and DG investors has not been considered. Based on the same previous assumptions and with a heuristic-based solution technique, the

impact of microgrids (a group of renewable and non-renewable DGs as well as energy storages) on the planning of primary distribution networks is assessed in [86].

The optimal time for feeder upgrades in addition to the optimal site, size, and time for renewable and dispatchable DG investments are obtained in [87]. A tri-level decomposition approach comprising primal and dual cuts is proposed to solve the problem. Polyhedral uncertainty sets are used to model the uncertainty, and K-means clustering-based method is utilized to obtain the statistical correlation of the uncertain parameters. A multistage expansion planning model for distribution systems is presented in [88] in which optimal substation, feeder, and DG investments are determined. A Distributionally robust chance constrained model is proposed to handle system uncertainty. A bi-objective planning model for system expansion is proposed in [89] in which microgrid aggregators and components' failure uncertainty have been taken into consideration. A hybrid solution method gravitational search algorithm and primal-dual interior point is used to solve the problem.

A multi-stage distribution system expansion planning-based reliability is employed in [2]. The problem is converted to a MILP problem utilizing piecewise linearization method to obtain the optimal planning configuration as well as feeder and substation capacities. In [90], a two-stage stochastic mixed integer second-order conic programming model is utilized to solve the problem of distribution system expansion in which the optimal sizes of substations, feeders, and capacitors are determined. The model incorporates chance-constrained based models to handle the stochastic nature of the system, and it used the bender decomposition method to address the computational challenge associated with the problem.

## **2.5 Distribution System Reliability Analysis**

Distribution system reliability is of keen interest for distribution system planners, operators, and regulators since it measures the level of service quality provided to the customers. The most popular approach for evaluating the reliability of any system is the failure mode and the effect analysis (FMEA). FMEA is defined as “an inductive approach that systematically details, on a component-by-component basis, all possible failure modes and identifies their resulting effects on the system” [91]. N-1 contingency analysis is a popular form of FMEA, and it stipulates that the system should be able to operate and fully meet the required demand and service quality when at least one component in the system goes out of service (i.e., down state).

In this section, N-1 contingency-based analytical methodology for evaluating distribution system reliability is presented [92]. Most power distribution systems are radially configured by a set of series components. These components include lines, busbars, switches, cables, and more. To ensure supply continuity at each load point in the system, all of the components in the path between the supply and the load point must be

functioning (i.e., in up-state). As a result of radial typology, the failure rate of each load point is equal to the summation of failure rate of each component in the series path between the source and the load point as well as the failure rate of each component which is in the protection zone of the corresponding load point. The main three basic reliability parameters that have been utilized to evaluate system reliability indices are average failure rate  $\lambda_s$ , average outage time or repair time  $r_s$ , and average annual outage or unavailability time  $U_s$ . The relationships between these parameters are demonstrated in equations (2.14)-(2.16).

$$\lambda_s = \sum_i \lambda_i \quad (2.14)$$

$$U_s = \sum_i \lambda_i r_i \quad (2.15)$$

$$r_s = \frac{U_s}{\lambda_s} = \frac{\sum_i \lambda_i r_i}{\sum_i \lambda_i} \quad (2.16)$$

Where  $\lambda_i$  and  $r_i$  represent the failure rate and repair time of component  $i$  which is located in the series path between the source and load point  $s$  or which is located in the protection zone of load  $s$ , respectively.

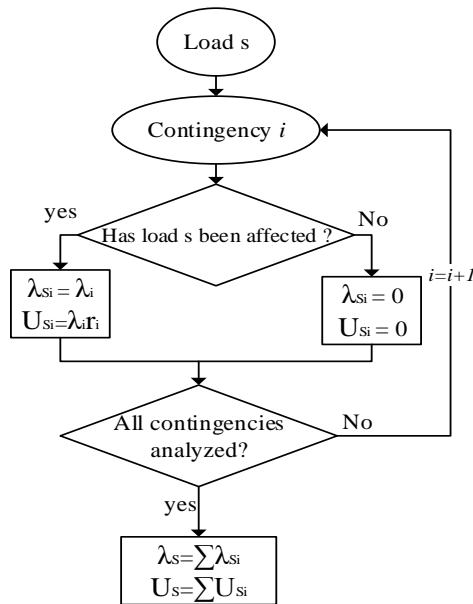


Figure 2-5 N-1 approach for evaluating load point reliability parameters

Figure 2-5 presents the flowchart that illustrates the basic concept of N-1 approach for evaluating load point reliability parameters. The flowchart shows that any possible failure or malfunction of such component in

the system is recognized and, in the meanwhile, analyzed so as to identify its impact on each load point in the network. This results in a list of contingencies corresponding to each load point. Next, these failure events are formed to assess the three basic load point reliability parameters, namely average failure rate, repair time, and annual unavailability time.

Even though the three basic load point reliability parameters are fundamentally important, they do not provide a system-wise reliability behavioral representation in which an outage could affect the system overall. Therefore, additional indices, which basically rely on the three primary parameters, are identified. These indices are divided into two categories: customer-oriented indices and energy-oriented indices [92].

### Customer-oriented indices

- (i) System average interruption frequency index, SAIFI

$$SAIFI = \frac{\text{total number of customer interruptions}}{\text{total number of customer served}} = \frac{\sum_i \lambda_i N_i}{\sum_i N_i} \quad (2.17)$$

where  $\lambda_i$  is the failure rate and  $N_i$  is the number of customers at load point  $i$ .

- (ii) System average interruption duration index, SAIDI

$$SAIDI = \frac{\text{sum of customer interruption durations}}{\text{total number of customers}} = \frac{\sum_i U_i N_i}{\sum_i N_i} \quad (2.18)$$

Where  $U_i$  is the annual outage time and  $N_i$  is the number of customers at load point  $i$ .

- (iii) Customer average interruption duration index, CAIDI

$$CAIDI = \frac{\text{sum of customer interruption durations}}{\text{total number of customer interruptions}} = \frac{\sum_i U_i N_i}{\sum_i N_i \lambda_i} \quad (2.19)$$

where  $\lambda_i$  is the failure rate,  $U_i$  is the annual outage time, and  $N_i$  is the number of customers at load point  $i$ .

- (iv) Average service availability (unavailability) index, ASAI (ASUI)

$$ASAI = \frac{\text{customer hours of available service}}{\text{customer hours demanded}} = \frac{\sum_i N_i \times 8760 - \sum_i U_i N_i}{\sum_i N_i \times 8760} \quad (2.20)$$

$$ASUI = 1 - ASAI \quad (2.21)$$

where  $\lambda_i$  is the failure rate,  $U_i$  is the annual outage time,  $N_i$  is the number of customers at load point  $i$ , and 8760 is the number of hours in a calendar year.

### Energy-oriented indices

- (i) Energy not supplied index, ENS

$$ENS = \text{total energy not supplied bt the system} = \sum_i L_{a(i)} U_i \quad (2.22)$$

where  $L_{a(i)}$  is the average load connected to load point  $i$ .

- (ii) Average energy not supplied index, AENS

$$AENS = \frac{\text{total energy not supplied}}{\text{total number of customer served}} = \frac{\sum_i L_{a(i)} U_i}{\sum_i N_i} \quad (2.23)$$

Both customer-oriented and energy-oriented reliability indices are very useful for assessing overall system reliability and thereby play a pivotal role in distribution system planning. These indices actually provide insight into how the system has been well-established to respond to such a failure. Thus, wiser investments will result in lowering these indices.

## 2.6 Distribution System Reliability Models in the Presence of DGs

DGs contribute to the enhancement of system reliability mainly through their ability to feed all or part of the loads in the islands formed (i.e., islanding operation) or through their ability to mitigate the violation of the system operational security constraints when the restoration process takes place. Until now, islanding operation during an outage is still not permitted by distribution utilities, and this is mainly attributed to the fact that the control and protection systems in the grid are designed to accommodate only a unidirectional power flow from the substations to the load centers. DG interconnection requirements are basically set by utilities to mitigate the negative impact of these DGs on the existing equipments. However, motivated by the emerging of smart grid paradigm and the advancements in the communication, control, and protection technologies, most of the recent research work focuses on facilitating the islanded operation during contingencies. This strategy provides a promising solution for enhancing system reliability and reducing the outage duration for the customers.

When a fault occurs in a section in the distribution system, the affected area is isolated and configured for the islanded mode of operation. What follows is the determination of the ability of the DG units to continuously match the demand in the created island during the outage period. This is called the generation adequacy assessment, and one of the main factors affecting supply adequacy evaluation is the intermittent behavior of the system demand and DG output power. Analytical and simulation-based models have been presented in the literature to evaluate the generation adequacy under the islanded mode of operation.

Monte Carlo simulation (MCS) has been recognized as an effective method to capture the variability of the power generated from renewable-based DGs and the system demand and to simulate the components' failure events. It is more flexible and accurate compared to other analytical approaches and provides probability distributions for the reliability indices; however, MCS approach has high computational burden so that its incorporation in the planning models became more difficult. The authors in [93] investigated the benefits of adding wind turbine generators (WTGs) in the distribution system for enhancing system reliability. A time sequential- based MCS simulation approach is presented, and the WTGs are modeled using a three-state model (i.e., up, down, and de-rated). Wind speed is represented using auto-regressive and moving average (ARMA) time series model, and the variation of the load is disregarded and represented by the average value. The system adequacy is evaluated, and the model proved the effectiveness of WTGs in improving the reliability indices. Random and sequential-based MCS approaches are deployed in [94] to assess distribution system reliability in smart grids considering the intentional islanded operation mode. Using the probability outage table (POT), probabilistic analytical models for system reliability assessment with conventional and renewable-based DGs have been implemented in [95], [96]. These models consider the fluctuation of system demand and DGs output power and incorporate them in the POT to calculate the reliability indices. The work presented in [95] considers load shedding (user load disconnection) and curtailment (user load reduction) policies during the contingency. However, the policy presented in [96] states that if the generation sources inside the island did not match the island demand and losses, then all the generation units must be disconnected from the grid, and this is for safety and protection considerations.

Some of the research work has investigated the variability of the generated power from DGs and the load during the repair time. However, the complexity of the analytical formulation increases when time-dependent fluctuations of load and generation are incorporated. To overcome this problem in the analytical formulation, the hourly load profiles over the year are represented as a set of representative clusters. Generation adequacy of an island and the probability of hourly successful islanding process are evaluated and calculated analytically using hourly-based representative periods for generation and load in [97], [98]. Although the use of clusters of representative hourly periods made the calculation of reliability indices analytically possible, this way of treatment does not capture the whole spectrum of the hourly load and

generation over the year. In [99], the hourly load and generation profiles are incorporated in the sequential MCS to assess the overall system reliability and include the load and generation variation during the outage. To evaluate the generation adequacy during the islanded mode of operation, the authors in [100] modeled the fluctuations of load and DGs by means of Markov chains and incorporate them in the reliability assessment. As long as the number of transitions and the levels of system demand and DGs output increase, the complexity of the model increases. Some of the research work as in [101], [102] has implemented reduction-based techniques to reduce the number of demand and DG power levels in order to evaluate the system reliability analytically.

Even though most of the research work that evaluates distribution system reliability in the presence of DGs has been devoted to the islanded mode of operation, there are few research papers that address the system reliability while DGs are in grid-connected mode during a contingency. In grid-connected mode or restoration process mode, DGs also contribute to the enhancement of system reliability by reducing and alleviating the equipment thermal loading created when the affected loads of the feeder experiencing an outage are transferred to another feeder. Power transfer restrictions should be applied in the grid-connected mode to avoid the violation of network constraints during the restoration process [103]. The authors in [104] presented a reliability evaluation model for radial distribution systems considering restoration sequence and network constraints; however, DGs are not considered in the proposed analytical model. A Sequential Monte Carlo Simulation (SMCS) model is introduced in [105] to evaluate the distribution system reliability and enable chronological modeling of system demand and the output power from wind-based DG. The model utilized ARMA-based time series model to mimic the fluctuations of wind speeds, and dynamic system reconfiguration for the sake of maximizing the back-feeding capacity margin during the contingency was applied. With the help of power flow calculations, the impact of dispatchable DGs on the restoration capability of the distribution system and hence improving system reliability was assessed in [106], taking into account that DGs can be operated in islanded and interconnected mode. However, the stochastic nature of the DG output power and the system demand was not included in the assessment. To reduce the computational time when power flow calculations are incorporated in simulation-based models, the authors [107] proposed a method based on a combination of analytical techniques (cut-sets) and chronological MCS. Using a set of load levels, the allowable amount of power capacity that can be transferred to adjacent feeder during the contingency is determined, and these capacities are incorporated in MCS to calculate the reliability indices.

Based on the above discussion, it can be observed that most of the studies explored the distribution system reliability in the presence of DGs considering only the islanded mode of operation, and few studies have been targeted the inclusion of DGs in grid-connected mode. There is a need for developing analytical

distribution system reliability models that can address the dual operation modes of DGs during the contingency. Moreover, the intermittent nature of DGs output power and load profiles should be modeled properly and incorporated in the models.

## **2.7 Summary**

The fundamentals of power distribution systems have been reviewed in this chapter including definitions, voltage standards, major components, and system configurations. The definitions of distributed generation and their power scales have been addressed. Furthermore, an overview of wind and PV power has been presented. In this chapter, the purpose of power distribution planning and the factors affecting the planning results have been examined, followed by a comparison between the traditional and modern distribution system planning. This chapter also reviewed the models and techniques of the distribution planning problem that have been addressed in the literature. Finally, the chapter is concluded by describing the N-1 approach for evaluating system reliability and the proposed models in the literature for distribution system reliability with DGs. In the next chapter, the first objective of the research proposed in this thesis is presented to develop a new expansion planning model for distribution system.

## Chapter 3

# An Incentive-Based Multistage Planning Model for Smart Distribution Systems

### 3.1 Introduction

The implementation of smart grids has facilitated the integration of a variety of investor assets into power distribution systems, giving rise to the consequent necessity for positive and active interaction between those investors and LDCs. In line with the smart grid trend and inspired by its philosophy of different key players collaborating to achieve win-win solutions, this chapter presents a novel long-term multistage IDSP model of the DSP problem that enables the LDC to establish bus-wise incentive prices for DG investors and to determine upgrade decisions for some of the distribution system assets. The new model invites and encourages DG investors to participate effectively and play a key role in reinforcement and expansion plans. The proposed active interaction between the LDC and DG investors is represented through long or mid-term contracts in which the DG investors are committed to install and operate their DG projects at specific locations and capacities determined by the LDC, whereas the LDC is committed to buy all of the energy generated by these projects at guaranteed prices (incentives) for the full periods of the contracts. Therefore, both parties benefit from this practice with the LDC experiencing substantial savings due to reduced operating and running costs as well as the elimination or deferment of massive infrastructure upgrade plans, and the DG investors investing in such projects wherein their profitability and returns are guaranteed. In other words, the total savings the LDC will realize through the implementation of DG projects will be managed wisely since a portion will be used for incentivizing DG owners and the rest will go into LDC coffers. The major player in this strategy is the LDC, while the DG investors are considered active followers. The proposed model also allows the LDC to identify the least cost solution obtainable from a combination of traditional upgrade alternatives and the proposed BWIP undertaken with the DGs. An additional feature is comprehensive uncertainty modeling that addresses the stochastic nature of system demand and of the output power produced by renewable-based DGs. Figure 3-1 illustrates the flowchart of the proposed IDSP model.

The primary contributions of the work presented in this chapter are fourfold:

1) The proposed incentive-based DSP (IDSP) model will help an LDC define necessary expenditures while also implementing a BWIP to encourage the integration of DG projects at specific buses that will benefit the system. The following are the key features of the proposed IDSP model:

- a) It determines the time, location, capacity, technology, and incentive price for each DG investment.

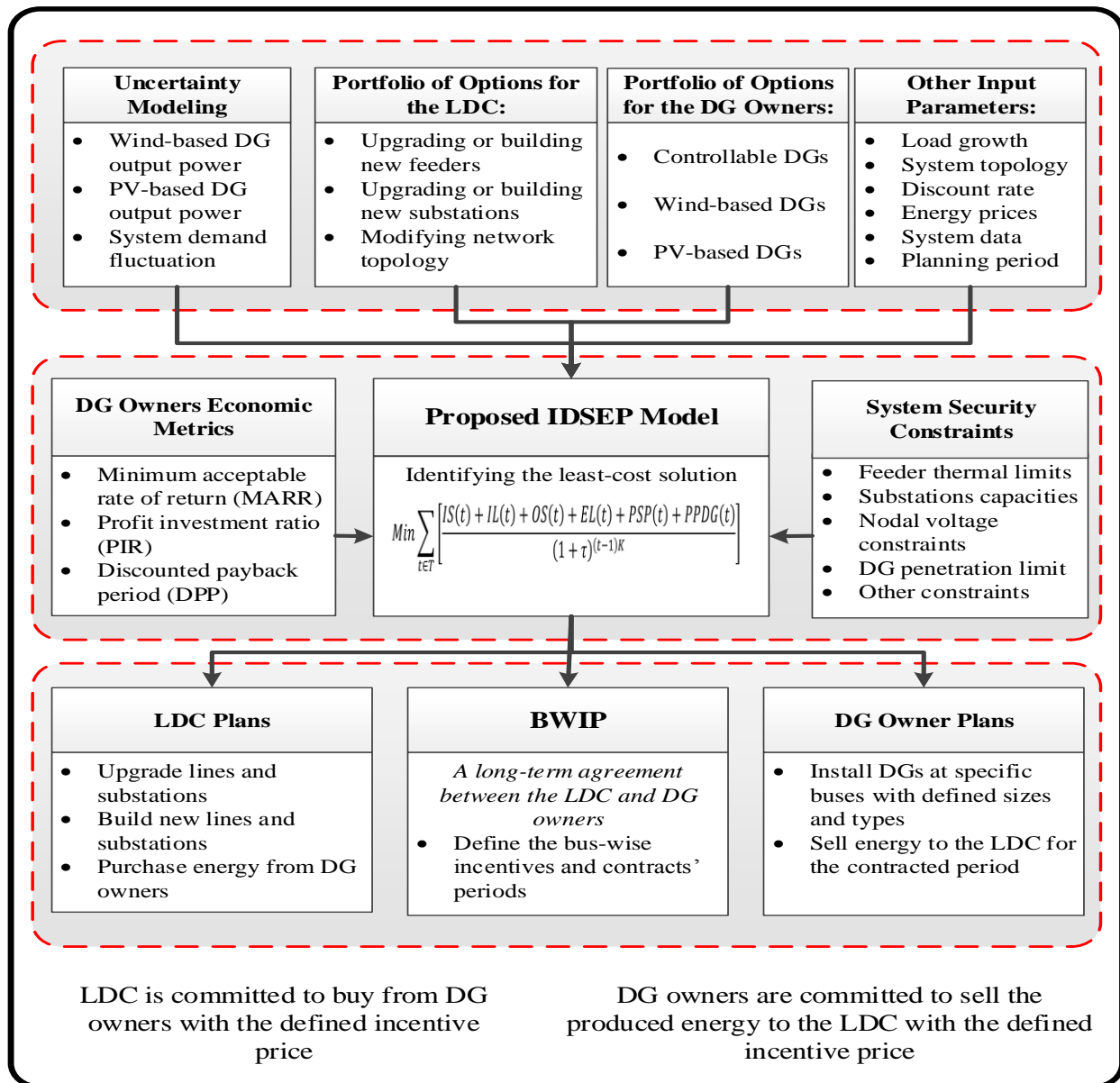


Figure 3-1 Flowchart of the proposed IDSP model

- b) It determines the commissioning year and capacity for the required distribution component upgrade plans to be undertaken by the LDC. This may include upgrading existing substations, constructing new substations, upgrading existing lines, building new lines, or modifying the network topology.
- c) The bus-wise incentive program is more efficient than most regulations whose provisions apply identical incentive prices for all buses.
- d) As a FIT program is phased out, as in Ontario, this model can function as a replacement that allows LDCs to determine incentive prices and appropriate DG locations based on their requirements and system needs.

- 2) A comprehensive methodology is presented for modeling the intermittent behavior of both fluctuating demand and the power generated from wind and PV-based DGs.
- 3) Profitability for DG investors is ensured through the assessment and consideration of a variety of economic indices. The model incorporates the most popular financial-based indicators for DG investors including internal rate of return, profit investment ratio, and discounted payback period.
- 4) Several linearization techniques are presented to transform the proposed IDSP model from MINLP into MILP model in which the convergence to optimality is guaranteed. These linearization methods can be applied to any planning and operation problems.

The remainder of the chapter is organized as follows: Section 3.2 describes the modeling of the uncertainty associated with the load and with DG components. The proposed problem formulation for the IDSP model is introduced in Section 3.3. Subsection 3.3.4 presents the linearization methods used in the thesis. Section 3.4 reports the numerical results for the case studies conducted, and Section 3.5 summarizes the study, presents conclusions, and reiterates the primary contributions.

### **3.2 Modeling of the Uncertainty Associated with Demand and DG Output Power**

The intermittent nature of wind and photovoltaic PV generation introduces several obstacles for both the operation and planning of distribution systems, and these challenges must be managed. Thus, constructing a suitable model that can capture the intermittent behavior resulting from the stochastic nature of wind- and PV-based DG output power and of fluctuations in the demand has become imperative. This factor was a primary consideration in the development of the proposed probabilistic IDSP model. The study presented in this chapter involved the generation of a multi-scenario-based model in which renewable DG output power and power demand are treated probabilistically. The uncertainty modeling entailed the following steps:

- 1) Five successive years of historical wind speed, solar irradiance, and system demand data are collected.
- 2) For each data type, several probability distribution functions are examined in order to determine the best distribution that fits each data type. Based on the methods commonly reported in the literature for modeling the uncertainty of wind speed, solar irradiance, and power demand, five distribution functions are tested: Weibull, Normal, Rayleigh, Gamma, and Lognormal [102]. Kolmogorov-Smirnov algorithm (K-S) is applied to find the best fit for each data type [102], [108]. The methodology of this method consists of the following steps:
  - a) The parameters of the probability density functions are defined using the mean  $v_m$  and standard deviation  $v_\sigma$  of the data. For example, the shape index  $k$  and scale index  $sc$  of the Weibull distribution can be obtained using (3.1) and (3.2), as in [24], [25]:

$$k = \left(\frac{v_\sigma}{v_m}\right)^{-1.086} \quad (3.1)$$

$$sc = \frac{v_m}{\Gamma\left(1 + \frac{1}{k}\right)} \quad (3.2)$$

b) The cumulative distribution function (CDF) for each distribution is constructed using the parameters obtained in step a. For example, the Weibull distribution CDF is given in (3.3):

$$CDF(v) = 1 - e^{-\left(\frac{v}{sc}\right)^k} \quad (3.3)$$

The empirical cumulative distribution function (ECDF) of the data is then constructed.

c) The mean absolute error (MAE) is next computed for each probability distribution. The value of each MAE is equal to the summation of the differences between the data points on the ECDF and on the CDF over the total number of data points  $TP$ , as defined in (3.4):

$$MAE = \frac{\sum_{v=0}^{TP} |CDF(v) - ECDF(v)|}{TP} \quad (3.4)$$

The distribution function that has the minimum MAE for each data type is ultimately chosen as representing that type. Three distribution functions are thus selected for modeling wind and PV output power plus system demand.

3) Once the probability distribution functions for wind speed, solar radiation, and system demand are defined, these PDFs must be divided into many states for incorporation into the calculations. The selection of these states is very crucial since it is a tradeoff between the accuracy of the results and the complexity in the analysis. Depending on the maximum value and how many intervals are required, the PDFs are divided into multiple equal intervals. The size of each state is dependent on the number of intervals required  $N_b$ , the mean  $m$ , and the standard deviation  $S$ . The value of each state is represented by the midpoint of each interval  $MB_{int}(r)$ , as indicated in equation (3.5) where  $r$  is an index for the intervals [102]:

$$MB_{int}(r) = \begin{cases} m + \left(\frac{10S}{N_b}\right)(r - 0.5N_b); & \text{even } N_b \\ m + \left(\frac{10S}{N_b}\right)(r - 0.5(N_b + 1)); & \text{odd } N_b \end{cases} \quad (3.5)$$

For example, for 5 states model, the mid points are  $m - 3S, m - S, m, m + S$ , and  $m + 3S$ .

It is worthwhile to state that wind speeds with values lower than the cut-in speed of wind turbine and higher than the cut-out speed are treated as one single state with a value equaling zero. Moreover, wind speeds with values higher than the rated speed of wind turbine and lower than the cut-out speed are treated as one state with a value equal to rated power.

The probability for each state can be obtained using the integral equation (3.6):

$$P(y_a \leq y \leq y_b) = \int_{y_a}^{y_b} f(y) \cdot dy \quad (3.6)$$

where  $y_a$  and  $y_b$  are the starting and ending variables for state  $y$ , respectively, and  $f(y)$  is the probability density function of the selected distribution.

4) The per unit values of the output power produced from wind- and PV-based DGs are then computed using the applicable equations from (3.7)-(3.12). In the case of wind power, per unit output power for each state is calculated using the following equation [24], [25]:

$$OP_w(v_{ay}) = \begin{cases} 0 & 0 \leq v_{ay} \leq v_{ci}, v_{ay} \geq v_{co} \\ P_{rated} \times \frac{v_{ay} - v_{ci}}{v_r - v_{ci}} & v_{ci} \leq v_{ay} \leq v_r \\ P_{rated} & v_r \leq v_{ay} \leq v_{co} \end{cases} \quad (3.7)$$

where  $v_{ci}$ ,  $v_r$ ,  $v_{co}$  are the cut-in speed, rated speed, and cut-off speed of the wind turbine, respectively;  $OP_w(v_{ay})$  is the output power during state  $y$ ; and  $v_{ay}$  is the average speed of state  $y$ .

The PV per unit output power for each state is calculated using the following equations [25], [102]:

$$T_{C_y} = T_A + s_{ay} \left( \frac{N_{OT} - 20}{0.8} \right) \quad (3.8)$$

$$I_y = s_{ay} [I_{sc} + K_i(T_c - 25)] \quad (3.9)$$

$$V_y = V_{oc} - K_v T_{C_y} \quad (3.10)$$

$$FF = \frac{V_{MMP} \times I_{MMP}}{V_{oc} \times I_{sc}} \quad (3.11)$$

$$OP_{PV}(s_{ay}) = N_m \times FF \times I_y \times V_y \quad (3.12)$$

where  $T_{C_y}$  is the cell temperature, in °C, during state  $y$ ;  $T_A$  is the ambient temperature, in °C;  $K_v$  is the voltage

temperature coefficient  $V/C$ ;  $K_i$  is the current temperature coefficient  $A/C$ ;  $N_{OT}$  is the nominal operating temperature of the cell, in  $^{\circ}C$ ;  $FF$  is the fill factor;  $N_m$  is the number of modules;  $I_{sc}$  is the short circuit current, in A;  $V_{oc}$  is the open circuit voltage, in V;  $I_{MMP}$  is the current at maximum power point, in A;  $V_{MMP}$  is the voltage at maximum power point, in V;  $OP_{PV}(s_{ay})$  is the per unit output power during state  $y$ ; and  $s_{ay}$  is the average irradiance of state  $y$ .

5) After all states for wind power, solar power, and system load are defined, a three-column matrix that includes all possible combinations (scenarios) of the states is created, in which column 1 represents the wind-based DG output power states (p.u.), column 2 represents the solar DG output power states (p.u.), and column 3 represents the different load states or levels (p.u.). This multi-scenario matrix has rows equal to the total number of overall scenarios, which is equal to the multiplication of wind, solar, and load states. The probability of each scenario is equal to the product of the wind state probability, solar state probability, and load state probability for that corresponding scenario, wherein wind speed, solar irradiance, and load are assumed to be independent events.

### 3.3 IDSP Model Problem Formulation

This section presents the proposed multistage IDSP model, which includes consideration of the payments made by the LDC to encourage DG connection at the specific buses that will ensure the financial justification of the DG projects. Also considered are all investment and operation costs for new and existing alternatives. The overall objective is thus to identify the minimum overall planning costs by taking into account all of the above components; establishing the BWIP prices for different types of DGs; and determining the optimal sites, sizes, times, and technologies for any additions, both new generation and upgrades to existing assets. The scope of the work presented in this thesis is concerning the primary distribution systems with high/medium substations and medium voltage feeders.

#### 3.3.1 The Objective Function

The objective function is comprised of all investment and operation costs incurred by the LDC. The components of the objective function are the substation investment (IS), the line investment (IL), the substation operation cost (OS), the cost of energy loss (EL), the energy purchased from the market (PSP), and the energy purchased from the DG investors (PPDG). The mathematical formulation of the objective function is as follows:

$$Min \sum_{t \in T} \left[ \frac{IS(t) + IL(t) + OS(t) + EL(t) + PSP(t) + PPDG(t)}{(1 + \tau)^{(t-1)K}} \right] \quad (3.13)$$

The mathematical formulations for the components of the objective function are shown in (3.14)-(3.19).

$$IS(t) = \sum_{i \in \Omega_{ES}} \sum_{u \in \Omega_U} (C_u^{US} \sigma_{i,u,t}) + \sum_{j \in \Omega_{CS}} \sum_{c \in \Omega_C} (C_c^{NS} u_{j,c,t}) \quad (3.14)$$

$$IL(t) = \sum_{ij \in \Omega_{EL}} \sum_{a \in \Omega_a} C_a^{UF} L_{ij} \beta_{ij,a,t} + \sum_{ij \in \Omega_{CL}} \sum_{a \in \Omega_a} C_a^{NF} L_{ij} z_{ij,a,t} \quad (3.15)$$

$$OS(t) = \sum_{i \in \Omega_{ES}} \sum_{e \in \Omega_{se}} (S_{G_{i,e,t}}^{sqr} \alpha_e \varphi \omega) f(\tau, K) + \sum_{j \in \Omega_{CS}} \sum_{e \in \Omega_{se}} (S_{G_{j,e,t}}^{sqr} \alpha_e \varphi \omega) f(\tau, K) \quad (3.16)$$

$$EL(t) = \sum_{ij \in \Omega_{EL}} \sum_{e \in \Omega_{se}} (Pl_{ij,e,t} \alpha_e \varphi \varepsilon) f(\tau, K) + \sum_{ij \in \Omega_{CL}} \sum_{e \in \Omega_{se}} (Pl_{ij,e,t} \alpha_e \varphi \varepsilon) f(\tau, K) \quad (3.17)$$

$$PSP(t) = \sum_{i \in \Omega_{ES}} \sum_{e \in \Omega_{se}} (P_{G_{i,e,t}} \alpha_e \varphi C_{e,t}^E) f(\tau, K) + \sum_{j \in \Omega_{CS}} \sum_{e \in \Omega_{se}} (P_{G_{j,e,t}} \alpha_e \varphi C_{e,t}^E) f(\tau, K) \quad (3.18)$$

$$PPDG(t) = \sum_{dg \in \Omega_{DG}} \sum_{i \in \Omega_N} \sum_{e \in \Omega_{se}} \rho_{dg} (INC_{dg,i,t} OP_{dg,e} \alpha_e \varphi) f(\tau, K) \quad (3.19)$$

The function  $f(\tau, K) = \left( \frac{1-(1+\tau)^{-K}}{\tau} \right)$  is called the present value of annuity function, which calculates the present value of a series of future constant annualized payments at a given time.

### 3.3.2 Power Conservation Constraints

In each node in the distribution system, active and reactive power flow must be balanced as in (3.20) and (3.21). The parameter  $\epsilon_{dg} = \left( \frac{\sin(\arccos(pf_{dg}))}{pf_{dg}} \right)$  in (3.21) is used for calculating the DG reactive power as a function of the DG active power using the DG power factor ( $pf_{dg}$ ). Equations (3.22) and (3.23) represent the active and reactive power flows associated with line  $ij$  as a function of nodal voltages and nodal voltage angles. They are represented as nonlinear functions multiplied by the feeder utilization binary variable so that, if the feeder is on service or needs to be built, the binary variable equals one. Otherwise, this binary value will be zero.

$$P_{G_{i,e,t}} + \sum_{dg \in \Omega_{DG}} \rho_{dg} OP_{dg,e} P_{DG_{dg,i,t}} - DL_e P_{D_{i,t}} - \sum_{ij \in \Omega_L} P_{ij,e,t} + \sum_{ki \in \Omega_L} P_{ki,e,t} - \sum_{ij \in \Omega_L} Pl_{ij,e,t} = 0 \quad \forall i \in \Omega_N, e \in \Omega_{se}, t \in T \quad (3.20)$$

$$\begin{aligned}
Q_{G_{i,e,t}} + \sum_{dg \in \Omega_{DG}} \rho_{dg} O P_{dg,e} \epsilon_{dg} P_{DG_{dg,i,t}} - DL_e Q_{D_{i,t}} - \sum_{ij \in \Omega_L} Q_{ij,e,t} + \sum_{ki \in \Omega_L} Q_{ki,e,t} - \sum_{ij \in \Omega_L} Q_{ij,e,t}^l \\
= 0 \quad \forall i \in \Omega_N, e \in \Omega_{se}, t \in T
\end{aligned} \tag{3.21}$$

$$\begin{aligned}
P_{ij,e,t} = x_{ij,t} (V_{i,e,t}^2 G_{ij} - V_{i,e,t} V_{j,e,t} G_{ij} \cos(\delta_{i,e,t} - \delta_{j,e,t}) - V_{i,e,t} V_{j,e,t} B_{ij} \sin(\delta_{i,e,t} - \delta_{j,e,t})) \\
\forall ij \in \Omega_L, e \in \Omega_{se}, t \in T
\end{aligned} \tag{3.22}$$

$$\begin{aligned}
Q_{ij,e,t} = x_{ij,t} (-V_{i,e,t}^2 B_{ij} - V_{i,e,t} V_{j,e,t} G_{ij} \sin(\delta_{i,e,t} - \delta_{j,e,t}) + V_{i,e,t} V_{j,e,t} B_{ij} \cos(\delta_{i,e,t} - \delta_{j,e,t})) \\
\forall ij \in \Omega_L, e \in \Omega_{se}, t \in T
\end{aligned} \tag{3.23}$$

### 3.3.3 Other Constraints

This section itemizes other planning constraints.

#### 1) Active and Reactive Power Losses:

$$Pl_{ij,e,t} = x_{ij,t} G_{ij} (V_{i,e,t}^2 + V_{j,e,t}^2 - 2V_{i,e,t} V_{j,e,t} \cos(\delta_{j,e,t} - \delta_{i,e,t})) \quad \forall ij \in \Omega_L, e \in \Omega_{se}, t \in T \tag{3.24}$$

$$Ql_{ij,e,t} = -x_{ij,t} B_{ij} (V_{i,e,t}^2 + V_{j,e,t}^2 - 2V_{i,e,t} V_{j,e,t} \cos(\delta_{j,e,t} - \delta_{i,e,t})) \quad \forall ij \in \Omega_L, e \in \Omega_{se}, t \in T \tag{3.25}$$

2) **Substation Capacity Constraints:** Equation (3.26) ensures that the square of the apparent power drawn from the existing substation must be lower than or equal to the square of existing substation capacity plus the substation upgrade decision. If there is no need to upgrade the substation, the second term on the right side of (3.26) must be zero. Equation (3.27) represents the limit on the power drawn from the candidate substation and basically defines the required capacity of the new candidate substation. The square of the apparent power drawn from the substation as a function in the substation's active and reactive power is shown in (3.28).

$$S_{G_{i,e,t}}^{sqr} \leq \left( \overline{S_{G_i}^{max}} \right)^2 + \sum_{u \in \Omega_U} \sum_{t'=1}^t (S_u^{US})^2 \sigma_{i,u,t} \quad \forall i \in \Omega_{ES}, e \in \Omega_{se}, t \in T \tag{3.26}$$

$$P_{G_{j,e,t}}^2 + Q_{G_{j,e,t}}^2 \leq \sum_{c \in \Omega_C} \sum_{t'=1}^t (S_c^{NS})^2 u_{j,c,t} \quad \forall j \in \Omega_{CS}, e \in \Omega_{se}, t \in T \quad (3.27)$$

$$S_{G_{i,e,t}}^{sqr} = P_{G_{i,e,t}}^2 + Q_{G_{i,e,t}}^2 \quad \forall i \in \Omega_{SS}, e \in \Omega_{se}, t \in T \quad (3.28)$$

**3) Feeder Flow and Thermal Capacity Limits:** Equation (3.29) ensures that the current flow in the feeder is within the thermal capacity of the feeder. If upgrading this feeder is essential, the second term on the right side of (3.29) covers that contingency by replacing the old feeder with the new one. Equation (3.30) is responsible for decisions related to the construction of any new candidate feeders. The square of the apparent power flowing in feeder  $ij$  as a function in the feeder's active and reactive power is shown in (3.31).

$$S_{ij,e,t}^{sqr} \leq (\overline{S_{ij}^{max}})^2 \left( 1 - \sum_{a \in \Omega_a} \sum_{t'=1}^t \beta_{ij,a,t} \right) + \sum_{a \in \Omega_a} \sum_{t'=1}^t (S_a^P)^2 \beta_{ij,a,t} \quad \forall ij \in \Omega_{EL}, \\ e \in \Omega_{se}, t \in T \quad (3.29)$$

$$S_{ij,e,t}^{sqr} \leq \sum_{a \in \Omega_a} \sum_{t'=1}^t (S_a^P)^2 z_{ij,a,t} \quad \forall ij \in \Omega_{CL}, e \in \Omega_{se}, t \in T \quad (3.30)$$

$$S_{ij,e,t}^{sqr} = P_{ij,e,t}^2 + Q_{ij,e,t}^2 \quad \forall ij \in \Omega_L, e \in \Omega_{se}, t \in T \quad (3.31)$$

**4) Bus Voltage Constraint:** The voltage magnitude in each system bus must be kept within permissible voltage limits, as set out in (3.32):

$$\underline{V}^{Min} \leq V_{i,e,t} \leq \overline{V}^{Max} \quad \forall i \in \Omega_N, e \in \Omega_{se}, t \in T \quad (3.32)$$

**5) LDC Investment Decision Constraints:** Equations (3.33)-(3.36) ensure that any upgrade decision for a feeder/substation and any construction decision for a feeder/substation must be executed once over the planning horizon.

$$\sum_{u \in \Omega_U} \sum_{t \in T} \sigma_{i,u,t} \leq 1 \quad \forall i \in \Omega_{ES} \quad (3.33)$$

$$\sum_{c \in \Omega_C} \sum_{t \in T} u_{j,c,t} \leq 1 \quad \forall j \in \Omega_{CS} \quad (3.34)$$

$$\sum_{a \in \Omega_a} \sum_{t \in T} \beta_{ij,a,t} \leq 1 \quad \forall ij \in \Omega_{EL} \quad (3.35)$$

$$\sum_{a \in \Omega_a} \sum_{t \in T} z_{ij,a,t} \leq 1 \quad \forall ij \in \Omega_{CL} \quad (3.36)$$

**6) System Radiality Constraint:** Most existing distribution systems have a radial configuration due to the simplicity of operation and the coordination of radial topology protection. Maintaining this topology during planning and operation processes is therefore crucial. Equation (3.37) is used for preventing any loop in the network and for maintaining the radial topology, based on the definition of the graph tree as in [109].

$$\sum_{ij \in \Omega_L} x_{ij,t} = N_b - N_{ES} - \sum_{j \in \Omega_{CS}} \sum_{c \in \Omega_C} u_{j,c,t} \quad \forall t \in T \quad (3.37)$$

**7) DG Investment and Utilization Constraints:** To direct DG investors to integrate their DGs at specific locations, the LDC should provide bus-wise incentives that guarantee profitability for the DG investors. Due to the high investment costs for such DG projects and different economic perspectives for the investors, it is necessary to analyze and address a variety of economic indicators for that kind of investments. For example, if the DG owners are more interested in the amount of value created per unit of investment, they may use the profit investment ratio to quantify that. Some investors are concerned about the money liquidity and when the project pays off its costs to utilize that money for starting other projects. In this case, discounted payback period is the best way to assist DG owners for that matter. Furthermore, if the investors are interested in the percentage rate earned on each dollar spent along the project period, they may use internal rate of return-based indicator. Therefore, a number of economic indices, namely IRR, PIR, and DPP, are considered in order to ensure the feasibility of an investment with respect to investment and operation costs as well as overall benefit for the DG.

For each bus in the system, equations (3.38) and (3.39) determine the total DG investment and operation costs, and equation (3.40) calculates the total benefit accruing to the DG investors when they sell the energy produced at the incentive price. As explained earlier, the function  $f(IRR_{dg,i}, K) = \left( \frac{1 - (1 + IRR_{dg,i})^{-K}}{IRR_{dg,i}} \right)$  in (3.39) and (3.40) is used for determining the present annuity value. The incentive cost is formulated in (3.41) as a multiplication of DG power and bus-wise incentive price (BWIP).

$$INVC_{dg,i,t}^{DG} = \rho_{dg} \left( P_{DG_{dg,i,t}} - P_{DG_{dg,i,t-1}} \right) C_{dg}^{IDG} \quad \forall dg \in \Omega_{DG}, i \in \Omega_N, t \in T \quad (3.38)$$

$$OPC_{dg,i,e,t}^{DG} = \rho_{dg} \left( OP_{dg,e} P_{DG,dg,i,t} C_{dg}^{ODG} \alpha_e \varphi \right) f(IRR_{dg,i}, K) \quad \forall dg \in \Omega_{DG}, i \in \Omega_N, e \in \Omega_{se}, t \in T \quad (3.39)$$

$$BEN_{dg,i,e,t}^{DG} = \rho_{dg} \left( OP_{dg,e} INC_{dg,i,t} \alpha_e \varphi \right) f(IRR_{dg,i}, K) \quad \forall dg \in \Omega_{DG}, i \in \Omega_N, e \in \Omega_{se}, t \in T \quad (3.40)$$

$$INC_{dg,i,t} = P_{DG,dg,i,t} \gamma_{dg,i} \quad \forall dg \in \Omega_{DG}, i \in \Omega_N, t \in T \quad (3.41)$$

Equations (3.42)-(3.44) compute the present values of DG installation and operation costs as well as the DG benefit at each bus in the network. These values will be used to calculate the economic metrics of the DG projects.

$$PVINV_{dg,i}^{DG} = \sum_{t \in T} INVC_{dg,i,t}^{DG} (1 + IRR_{dg,i})^{-(t-1)K} \quad \forall dg \in \Omega_{DG}, i \in \Omega_N \quad (3.42)$$

$$PVOPE_{dg,i}^{DG} = \sum_{t \in T} \sum_{e \in \Omega_{se}} OPC_{dg,i,e,t}^{DG} (1 + IRR_{dg,i})^{-(t-1)K} \quad \forall dg \in \Omega_{DG}, i \in \Omega_N \quad (3.43)$$

$$PVBEN_{dg,i}^{DG} = \sum_{t \in T} \sum_{e \in \Omega_{se}} BEN_{dg,i,e,t}^{DG} (1 + IRR_{dg,i})^{-(t-1)K} \quad \forall dg \in \Omega_{DG}, i \in \Omega_N \quad (3.44)$$

a) *Internal rate of return and minimum acceptable rate of return:* Widely used for assessing the attractiveness of a project, the internal rate of return (IRR) is a metric that basically represents the interest rate at which the net present value (NPV) of all cash flows from a project becomes zero. This metric is usually compared with the hurdle rate, or minimum acceptable rate of return (MARR) initially specified by the investor. If the IRR is greater than or equal to the MARR, then the project is considered profitable, and the investor would therefore accept the project. Equation (3.45) ensures that the NPV of all cash flows equals zero, taking into consideration that the IRR of each project is equal to the MARR of that corresponding project.

$$PVINV_{dg,i}^{DG} + PVOPE_{dg,i}^{DG} - PVBEN_{dg,i}^{DG} = 0 \quad \forall dg \in \Omega_{DG}, i \in \Omega_N \quad (3.45)$$

b) *Profit investment ratio:* The second economic metric used in this work is the profit investment ratio (PIR), or the profitability index (PI). This index measures the ratio between the present value of the gain or benefit to be derived from an investment and the present value of the cost of the investment. If the PI is

greater than one, the NPV of the project is positive, and the project will thus be accepted. A DG investor may also state an acceptable PI, which should be constrained in the planning, as expressed in (3.46).

$$PVBEN_{dg,i}^{DG} \geq PIR \left( PVINV_{dg,i}^{DG} + PVOPE_{dg,i}^{DG} \right) \quad \forall dg \in \Omega_{DG}, i \in \Omega_N \quad (3.46)$$

c) *Discounted payback period*: The payback period defines the length of time (typically in years) at the end of which the project will recoup or recover the cost of the investment. The discounted payback period (DPP) incorporates a discount rate for taking into account the time value of money. The DPP metric is not normally used for evaluating project feasibility since it ignores all incoming cash flows that follow the breakeven point. In the work presented in this thesis, DPP is calculated after the planning outcomes are obtained so that it is not included in the optimization. Equation (3.47) calculates the DPP of the DG projects at each bus:

$$DPP_{dg,i} = Y_{NN} + \frac{|CCF_{Y_{NN}}|}{CCF_{Y_{NN}+1} + |CCF_{Y_{NN}}|} \quad \forall dg \in \Omega_{DG}, i \in \Omega_N \quad (3.47)$$

where  $Y_{NN}$  is the year in which the last negative value of the cumulative discounted cash flow occurs,  $CCF_{Y_{NN}}$  is the last negative value of the cumulative discounted cash flow, and  $CCF_{Y_{NN}+1}$  is the first positive value of the cumulative discounted cash flow.

8) **DG Penetration Constraints**: The maximum DG capacity that can be connected to any bus in the network is constrained as in (3.48), a limit based on technical studies conducted by the LDC. Equation (3.49) ensures that the penetration level of each renewable-based DG in the last stage of planning conforms with environmental regulation requirements.

$$\sum_{dg \in \Omega_{DG}} \rho_{dg} P_{DG_{dg,i,t}} \leq \overline{DG}_i \quad \forall i \in \Omega_N, t \in T \quad (3.48)$$

$$\sum_{dg \in \Omega_{DG} \setminus \{CDG\}} \sum_{i \in \Omega_N} \rho_{dg} P_{DG_{dg,i,t}} \geq \mu \sum_{i \in \Omega_N} P_{D,i,t} \quad \forall t = LT \quad (3.49)$$

9) **DG Dynamic Constraint**: The dynamic constraint denoted in (3.50) governs cumulative DG capacities between planning stages:

$$P_{DG_{dg,i,t}} - P_{DG_{dg,i,t+1}} \leq 0 \quad \forall dg \in \Omega_{DG}, i \in \Omega_N, t \in T \quad (3.50)$$

10) **DG Discretization Constraints**: DGs are typically sized in a discrete way to represent the available capacities in the market. Equation (3.51) ensures that the power generated from the DG is lower than the

DG capacity. Equation (3.52) defines the DG capacity as a multiplication of an integer variable with available DG sizes. It is assumed that the available ratings of the DG units can be found in steps of 0.1 MW.

$$OP_{dg,e} P_{DG_{dg,i,t}} \leq P_{CAP_{dg,i,t}} \quad \forall dg \in \Omega_{DG}, e \in \Omega_{se}, i \in \Omega_N, t \in T \quad (3.51)$$

$$P_{CAP_{dg,i,t}} = n_{dg,i,t} \times 0.1\text{MW} \quad \forall dg \in \Omega_{DG}, i \in \Omega_N, t \in T \quad (3.52)$$

Where  $n_{dg,i,t}$  is an integer variable.

**11) Incentive Prices Constraint:** Incentive prices should be constrained with respect to minimum and maximum values (3.53):

$$\underline{\gamma} \leq \gamma_{dg,i} \leq \bar{\gamma} \quad \forall dg \in \Omega_{DG}, i \in \Omega_N \quad (3.53)$$

**12) Binary Variables Constraints:**

$$\sigma_{i,u,t} \in \{0,1\} \quad \forall i \in \Omega_{ES}, u \in \Omega_U, t \in T \quad (3.54)$$

$$u_{j,c,t} \in \{0,1\} \quad \forall j \in \Omega_{CS}, c \in \Omega_C, t \in T \quad (3.55)$$

$$\beta_{ij,a,t} \in \{0,1\} \quad \forall ij \in \Omega_{EL}, a \in \Omega_a, t \in T \quad (3.56)$$

$$z_{ij,a,t} \in \{0,1\} \quad \forall ij \in \Omega_{CL}, a \in \Omega_a, t \in T \quad (3.57)$$

$$x_{ij,t} \in \{0,1\} \quad \forall ij \in \Omega_L, t \in T \quad (3.58)$$

### 3.3.4 Linearization of the IDSP Model

The mathematical model of the proposed IDSP is described by (3.13)-(3.58). However, this model is MINLP due to the non-linearity of some constraints and expressions (i.e., equations (3.22)-(3.25), (3.28), (3.31), and (3.41)). In order to obtain a robust and efficient model, the non-linear expressions are linearized in this section; thus, the IDSP model is converted from MINLP to MILP.

#### 3.3.4.1 Linearization of Equations (3.22) and (3.23)

The power flow equations explained in (3.22) and (3.23) are approximated by considering two valid practical assumptions. The first assumption is that the voltage magnitude at each bus is very close to 1 p.u.; thus, the bus voltages can be rewritten as a sum of 1 p.u. and small voltage deviation ( $V_{i,e,t} = 1 + \Delta V_{i,e,t}$ ). The second assumption is that the angle difference across a line is very small so that the approximations

$\cos(\delta_{i,e,t} - \delta_{j,e,t}) \approx 1$  and  $\sin(\delta_{i,e,t} - \delta_{j,e,t}) \approx \delta_{i,e,t} - \delta_{j,e,t}$  can be applied. Therefore, equations (3.22) and (3.23) can be approximated as follows:

$$P_{ij,e,t} \cong x_{ij,t} \left( (\Delta V_{i,e,t} - \Delta V_{j,e,t}) G_{ij} - (\delta_{i,e,t} - \delta_{j,e,t}) B_{ij} \right) \quad \forall ij \in \Omega_L, e \in \Omega_{se}, t \in T \quad (3.59)$$

$$Q_{ij,e,t} \cong x_{ij,t} \left( -(\Delta V_{i,e,t} - \Delta V_{j,e,t}) B_{ij} - (\delta_{i,e,t} - \delta_{j,e,t}) G_{ij} \right) \quad \forall ij \in \Omega_L, e \in \Omega_{se}, t \in T \quad (3.60)$$

$$\underline{\Delta V_i}^{Min} \leq \Delta V_{i,e,t} \leq \overline{\Delta V_i}^{Max} \quad \forall i \in \Omega_N, e \in \Omega_{se}, t \in T \quad (3.61)$$

The full approximation steps can be found in [110]. However, equations (3.59) and (3.60) are still non-linear due to the bilinear product of the feeder utilization binary and voltage and angle variables. This non-linearity can be avoided by using the big-M formulation as follows:

$$(x_{ij,t} - 1)M \leq P_{ij,e,t} - \left( (\Delta V_{i,e,t} - \Delta V_{j,e,t}) G_{ij} - (\delta_{i,e,t} - \delta_{j,e,t}) B_{ij} \right) \leq (1 - x_{ij,t})M \quad \forall ij \in \Omega_L, e \in \Omega_{se}, t \in T \quad (3.62)$$

$$(x_{ij,t} - 1)M \leq Q_{ij,e,t} - \left( -(\Delta V_{i,e,t} - \Delta V_{j,e,t}) B_{ij} - (\delta_{i,e,t} - \delta_{j,e,t}) G_{ij} \right) \leq (1 - x_{ij,t})M \quad \forall ij \in \Omega_L, e \in \Omega_{se}, t \in T \quad (3.63)$$

$$-\overline{S_{ij}^{max}} x_{ij,t} \leq P_{ij,e,t} \leq \overline{S_{ij}^{max}} x_{ij,t} \quad \forall ij \in \Omega_L, e \in \Omega_{se}, t \in T \quad (3.64)$$

$$-\overline{S_{ij}^{max}} x_{ij,t} \leq Q_{ij,e,t} \leq \overline{S_{ij}^{max}} x_{ij,t} \quad \forall ij \in \Omega_L, e \in \Omega_{se}, t \in T \quad (3.65)$$

### 3.3.4.2 Linearization of Equations (3.24) and (3.25)

By following the same two assumptions above and neglecting the higher order terms, the active and reactive power losses can be rewritten as follows:

$$Pl_{ij,e,t} = x_{ij,t} R_{ij} S_{ij,e,t}^{sqr} \quad \forall ij \in \Omega_L, e \in \Omega_{se}, t \in T \quad (3.66)$$

$$Ql_{ij,e,t} = x_{ij,t} X_{ij} S_{ij,e,t}^{sqr} \quad \forall ij \in \Omega_L, e \in \Omega_{se}, t \in T \quad (3.67)$$

Researchers are referred to reference [111] for the full derivation of equations (3.66) and (3.67). Equations (3.66) and (3.67) are still non-linear due to the presence of bilinear product. This issue is avoided by using the big-M method as follows:

$$(x_{ij,t} - 1)M \leq Pl_{ij,e,t} - R_{ij} S_{ij,e,t}^{sqr} \leq (1 - x_{ij,t})M \quad \forall ij \in \Omega_L, e \in \Omega_{se}, t \in T \quad (3.68)$$

$$(x_{ij,t} - 1)M \leq Ql_{ij,e,t} - X_{ij}S_{ij,e,t}^{sqr} \leq (1 - x_{ij,t})M \quad \forall ij \in \Omega_L, e \in \Omega_{se}, t \in T \quad (3.69)$$

$$-\overline{S_{ij}^{max}}x_{ij,t} \leq Pl_{ij,e,t} \leq \overline{S_{ij}^{max}}x_{ij,t} \quad \forall ij \in \Omega_L, e \in \Omega_{se}, t \in T \quad (3.70)$$

$$-\overline{S_{ij}^{max}}x_{ij,t} \leq Ql_{ij,e,t} \leq \overline{S_{ij}^{max}}x_{ij,t} \quad \forall ij \in \Omega_L, e \in \Omega_{se}, t \in T \quad (3.71)$$

### 3.3.4.3 Linearization of Equation (3.28)

The quadratic expressions of the right member of equation (3.28) can be linearized by using piecewise linearization with sufficient linear segments or blocks  $Y$  as in [69]. Therefore, equation (3.28) can be rewritten as:

$$S_{G_{i,e,t}}^{sqr} \cong \sum_{y=1}^Y (2y - 1)\overline{\Delta}^G \Delta P_{G_{i,e,t,y}} + \sum_{y=1}^Y (2y - 1)\overline{\Delta}^G \Delta Q_{G_{i,e,t,y}} \quad \forall i \in \Omega_{SS}, e \in \Omega_{se}, t \in T \quad (3.72)$$

The active and reactive powers drawn from the substations are expressed as a sum of a series of linear segments  $\Delta P_{G_{i,e,t,y}}$  and  $\Delta Q_{G_{i,e,t,y}}$ , respectively, as shown in (3.73) and (3.74). The discretization variables for the active and reactive power are constrained, as in (3.75) and (3.76), while equation (3.77) defines the value used for discretization.

$$P_{G_{i,e,t}} = \sum_{y=1}^Y \Delta P_{G_{i,e,t,y}} \quad \forall i \in \Omega_{SS}, e \in \Omega_{se}, t \in T \quad (3.73)$$

$$Q_{G_{i,e,t}} = \sum_{y=1}^Y \Delta Q_{G_{i,e,t,y}} \quad \forall i \in \Omega_{SS}, e \in \Omega_{se}, t \in T \quad (3.74)$$

$$\Delta P_{G_{i,e,t,y}} \leq \overline{\Delta}^G \quad \forall i \in \Omega_{SS}, e \in \Omega_{se}, t \in T, y \in Y \quad (3.75)$$

$$\Delta Q_{G_{i,e,t,y}} \leq \overline{\Delta}^G \quad \forall i \in \Omega_{SS}, e \in \Omega_{se}, t \in T, y \in Y \quad (3.76)$$

$$\overline{\Delta}^G = \frac{\overline{V}^{Max}}{Y} \max\{S_u^{US}, u \in \Omega_U\} \quad (3.77)$$

### 3.3.4.4 Linearization of Equation (3.31)

The linearization process in this section is similar to the method applied previously in *section 3.3.4.3*. By using the piecewise linearization, equation (3.31) can be approximated as follows:

$$S_{ij,e,t}^{sqr} \cong \sum_{y=1}^Y (2y-1)\bar{\Delta}^L \Delta P_{ij,e,t,y} + \sum_{y=1}^Y (2y-1)\bar{\Delta}^L \Delta Q_{ij,e,t,y} \quad \forall ij \in \Omega_L, e \in \Omega_{se}, t \in T \quad (3.78)$$

The active and reactive power flows in the feeder are expressed using non-negative auxiliary variables to obtain their absolute values as in (3.79) and (3.80). Also, the active and reactive power flows in feeder  $ij$  are expressed as a sum of a series of linear segments  $\Delta P_{ij,e,t,y}$  and  $\Delta Q_{ij,e,t,y}$ , respectively, as shown in (3.81) and (3.82). The discretization variables are constrained as in (3.83) and (3.84), while equation (3.85) defines the value used for discretization.

$$P_{ij,e,t} = P_{ij,e,t}^+ - P_{ij,e,t}^- \quad \forall ij \in \Omega_L, e \in \Omega_{se}, t \in T \quad (3.79)$$

$$Q_{ij,e,t} = Q_{ij,e,t}^+ - Q_{ij,e,t}^- \quad \forall ij \in \Omega_L, e \in \Omega_{se}, t \in T \quad (3.80)$$

$$P_{ij,e,t}^+ + P_{ij,e,t}^- = \sum_{y=1}^Y \Delta P_{ij,e,t,y} \quad \forall ij \in \Omega_L, e \in \Omega_{se}, t \in T \quad (3.81)$$

$$Q_{ij,e,t}^+ + Q_{ij,e,t}^- = \sum_{y=1}^Y \Delta Q_{ij,e,t,y} \quad \forall ij \in \Omega_L, e \in \Omega_{se}, t \in T \quad (3.82)$$

$$0 \leq \Delta P_{ij,e,t,y} \leq \bar{\Delta}^L \quad \forall ij \in \Omega_L, e \in \Omega_{se}, t \in T, y \in Y \quad (3.83)$$

$$0 \leq \Delta Q_{ij,e,t,y} \leq \bar{\Delta}^L \quad \forall ij \in \Omega_L, e \in \Omega_{se}, t \in T, y \in Y \quad (3.84)$$

$$\bar{\Delta}^L = \frac{\bar{V}^{Max}}{Y} \max\{S_a^P, a \in \Omega_a\} \quad (3.85)$$

#### 3.3.4.5 Linearization of Equation (3.41)

The nonlinearity in equation (3.41) occurs due to the product of two continuous variables. This can be easily linearized by using the binary expansion approach as in [112]. Since the BWIP ranges between  $\underline{\gamma}$  and  $\bar{\gamma}$  as in (3.53), the BWIP can be approximated discretely as follows:

$$\gamma_{dg,i} = \underline{\gamma} + \Delta\gamma \sum_{h=1}^{H+1} 2^{(h-1)} v_{h,dg,i} \quad \forall dg \in \Omega_{DG}, i \in \Omega_N \quad (3.86)$$

where  $v_{h,dg,i}$  is a binary variable,  $\Delta\gamma = \frac{\bar{\gamma}-\underline{\gamma}}{W}$ , and  $W = 2^H$  for some non-negative integer value  $H$ . By multiplying both sides with  $P_{DG dg,i,t}$ , equation (3.86) can be rewritten as follows:

$$INC_{dg,i,t} = \underline{\gamma} P_{DG_{dg,i,t}} + \Delta\gamma \sum_{h=1}^{H+1} 2^{(h-1)} d_{h,dg,i,t} \quad \forall dg \in \Omega_{DG}, i \in \Omega_N, t \in T \quad (3.87)$$

where  $d_{h,dg,i,t} = v_{h,dg,i} P_{DG_{dg,i,t}}$ . The bilinear product can be transformed into a linear expression using the big-M approach as follows:

$$0 \leq P_{DG_{dg,i,t}} - d_{h,dg,i,t} \leq M(1 - v_{h,dg,i}) \quad \forall dg \in \Omega_{DG}, i \in \Omega_N, t \in T, h = 1, 2, \dots, H + 1 \quad (3.88)$$

$$0 \leq d_{h,dg,i,t} \leq M v_{h,dg,i} \quad \forall dg \in \Omega_{DG}, i \in \Omega_N, t \in T, h = 1, 2, \dots, H + 1 \quad (3.89)$$

### 3.3.4.6 MILP Model for the Proposed IDSP

The MINLP formulation of the proposed IDSP model is transformed to MILP considering the linearization techniques applied in section 3.3.4. Therefore, the full MILP model for the proposed IDSP model is defined as follows

IDSP Model	
Objective:	<i>Min</i> (3.13)
Constraints:	(3.14)-(3.21), (3.26)-(3.27), (3.29)-(3.30), (3.33)-(3.40), (3.42)-(3.46), (3.48)-(3.52), (3.54)-(3.58), (3.61)-(3.65), (3.68)-(3.85), and (3.87)-(3.89)

## 3.4 Case Studies and Numerical Results

### 3.4.1 Distribution System Under Study

The proposed IDSP model was tested using a primary 54-node distribution system, whose full data can be found in [113]. The system operating voltage is 15 kV, and it has 50 existing feeders, 11 new candidate feeders, three existing substations, and one new candidate substation. The expansion of the existing substation was achieved by inserting two alternative transformers with capacities of 13.3 MVA and 16.7 MVA and associated costs of  $8 \times 10^6$  US\$ and  $10 \times 10^6$  US\$, respectively. Constructing a new substation also involved two alternatives, with capacities of 16.7 MVA and 22.2 MVA and associated total costs of  $14 \times 10^6$  US\$ and  $20 \times 10^6$  US\$, respectively [114]. The capacity of the existing substations is 16.7 MVA. The studies entailed three alternative feeders with thermal capacities of 250 A, 450 A, and 900 A and installation costs of  $35 \times 10^4$  US\$/km,  $46 \times 10^4$  US\$/km, and  $92 \times 10^4$  US\$/km [115], respectively. The thermal capacities and lengths of the system feeders can be obtained from [113]. The planning horizon is assumed

to be 15 years with 3 % annual load growth. The planning horizon is divided into three stages, each of which has a five-year period (K). The cost of energy losses is 50 US\$/MWh, and the substation operation cost is 1 (US\$/((MVA)<sup>2</sup> h)) [109]. The interest rate is assumed to be 10 %, and the system power factor is 0.9. After analyzing Hourly Ontario Energy Prices (HOEP), the costs of purchasing power from the market corresponding to the off-peak, mid-peak, and on-peak load states 23.6 US\$/MWh, 28.2 US\$/MWh, and 32.5 US\$/MWh, respectively [116]. Investment and operation costs for each DG type are listed in Table 3-1. The maximum DG capacity at each bus is equal to 10 MW, and the penetration level for renewable-based DGs ( $\mu$ ) at last stage is assumed to be 15%, with 7.5% for each type. Historical wind speed, solar irradiance, and system demand data were obtained from [116]-[118].

Table 3-1 DG Investment and Operation Costs [65], [119], [120]

	CDG	WDG	PVDG
Investment cost (10 <sup>6</sup> US\$/MW)	0.825	1.3	1.5
Operation cost (US\$/MWh)	30	0	0

### 3.4.2 Uncertainty Modeling Results

The historical data used in this study are analyzed based on the procedures described in section 3.2. The results revealed that the Normal distribution was found to be the best distribution for mimicking fluctuations in system demand, while the Weibull distribution was best fit for modeling the wind speed variations. The Beta distribution is the best fit to model the solar irradiances. The parameters of the selected PDFs are listed in Table 3-2.

Table 3-2 Best Fitting Probability Distribution Results

	Best Fitted PDF	Distribution Parameters
System demand (p.u.)	Normal	Mean = 0.69, Stdev. = 0.1
Wind speed (m/s)	Weibull	Shape =1.9, Scale = 6.07
Solar irradiance (kW/m <sup>2</sup> )	Beta	Alpha = 0.27, Beta =1.3

### 3.4.3 Case Studies and Results

To validate the proposed IDSP model, two case studies were conducted: 1) IDSP with controllable DGs (CDG), and 2) IDSP with controllable, wind, and PV-based DGs. For the work described in this case study, the proposed IDSP was designed based on the IRR of the DG investments only, and the MARR for each DG type was assumed to be 10 %. The results of these case studies are summarized in Table 3-3, Table 3-4, and Table 3-5. Table 3-3 presents the net present values (NPV) of the planning costs incurred by the LDC, with a breakdown of costs for each case. Table 3-4 shows the NPV of the DG project benefits and the

optimal BWIP price that guarantees the financial feasibility of each DG investment at each bus. Table 3-5 lists the planning decisions committed to by the LDC and DG investors.

Table 3-3 NPV for Planning Costs to be Incurred by the LDC, in (10<sup>6</sup>US\$)

	Base case	Case 1	Case 2
Substation investment (2)	22.0	0.00	6.17
Substation operation (4)	2.21	0.985	0.892
Feeder investment (3)	7.6	0.552	1.641
Cost of energy losses (5)	1.53	0.39	0.35
Cost of energy purchased from the market (6)	74.7	41.45	39.68
Cost of energy purchased from CDG (7)	0.00	46.05	42.95
Cost of energy purchased from WDG (7)	0.00	0.00	5.992
Cost of energy purchased from PVDG (7)	0.00	0.00	7.064
Total NPV of planning costs	108.03	89.4	104.74
NPV of the net savings for LDC	0.00	18.63	3.29

1) *IDSP with Controllable DGs (CDG)*: In this case, which deals only with controllable DGs, the results revealed that the NPV of the planning costs incurred by the LDC is  $89.4 \times 10^6$  US\$. Almost 46.3 % of these costs represent the cost of purchasing energy from the market, whereas 51.5 % of the costs represent the cost of purchasing energy generated by controllable DGs, as shown in Table 3-3. A comparison of these numbers with the base case results when DGs are not considered reveals that the savings the LDC can gain from inserting DGs is  $64.6 \times 10^6$  US\$. However, the LDC should spend  $46.05 \times 10^6$  US\$ as incentives for DG investors, making the net LDC savings  $18.63 \times 10^6$  US\$. The DG investor plans are indicated in Table 3-5. 15 locations are identified as optimal for integrating the DGs, and the cumulative DG capacity at each location for each planning stage is shown in Table 3-5. Table 3-4 displays the BWIP long-term contract price committed to for each DG and the NPV for the DG benefits. The BWIP prices vary from 42.5 US\$/MWh to 48.7 US\$/MWh, depending on the capacity of each DG at each stage and the required MARR. These prices guarantee that the project is financially feasible at each bus where the IRRs equal 10 %. For this scenario, there was no need for either a substation upgrade or construction plans since the anticipated growth in energy consumption for each stage is met by the contracted DGs. The LDC must upgrade one feeder in stage 1 and two feeders in stage 3, as noted in Table 3-5.

Table 3-4 Optimal DG BWIP Prices and Incomes

	Bus No.	BWIP price (\$/MWh)	NPV of DG income (Benefit) (10 <sup>6</sup> US\$)
<b>Case 1</b>	CDG	6	47.9
		8	45.2
		10	48.7
		16	45.6
		17	46.3
		23	43.7
		25	44.1
		26	42.6
		28	43.1
		34	42.5
		36	44.6
		37	48.3
		38	45.2
		48	42.5
		50	45.6
<b>Case 2</b>	CDG	6	44.5
		8	42.9
		10	43.1
		16	45.6
		17	45.6
		23	44
		25	43.8
		26	42.9
		28	43.6
		34	42.6
		36	42.7
		37	45.9
		38	44.1
		48	43.8
		50	42.9
	WDG	3	67.4
		13	67.4
		19	67.4
		31	67.4
		42	67.4
PVDG	6	87.5	
	22	87.5	
	32	87.5	
	40	87.5	
	44	87.5	

Feeder 30-43 is upgraded in stage 1 utilizing alternative A1, and Feeders 18-19 and 18-21 are upgraded in final stage using alternatives A1 and A2, respectively. An interesting finding is that the average CDG incentive price is equal to 45 \$/MWh, higher than the average price of purchasing energy from the market, which would cost 27 \$/MWh. However, if the LDC decided to purchase all the energy from the market with this price (i.e., 27 \$/MWh), the total planning cost will be 108.03 M\$ as can be seen in the base case results in Table 3-3. This high planning cost is attributed to the need for high number of substation and feeder upgrade plans and high energy losses and system operation costs. Thus, it is more economical for the LDC to purchase some of the energy from the DG owners since the presence of the DGs enables the deferment of most of the feeder upgrade decisions, reduces the cost of energy losses, and eliminates the need for substation upgrade decisions. Figure 3-2 illustrates the network topology for case 1.

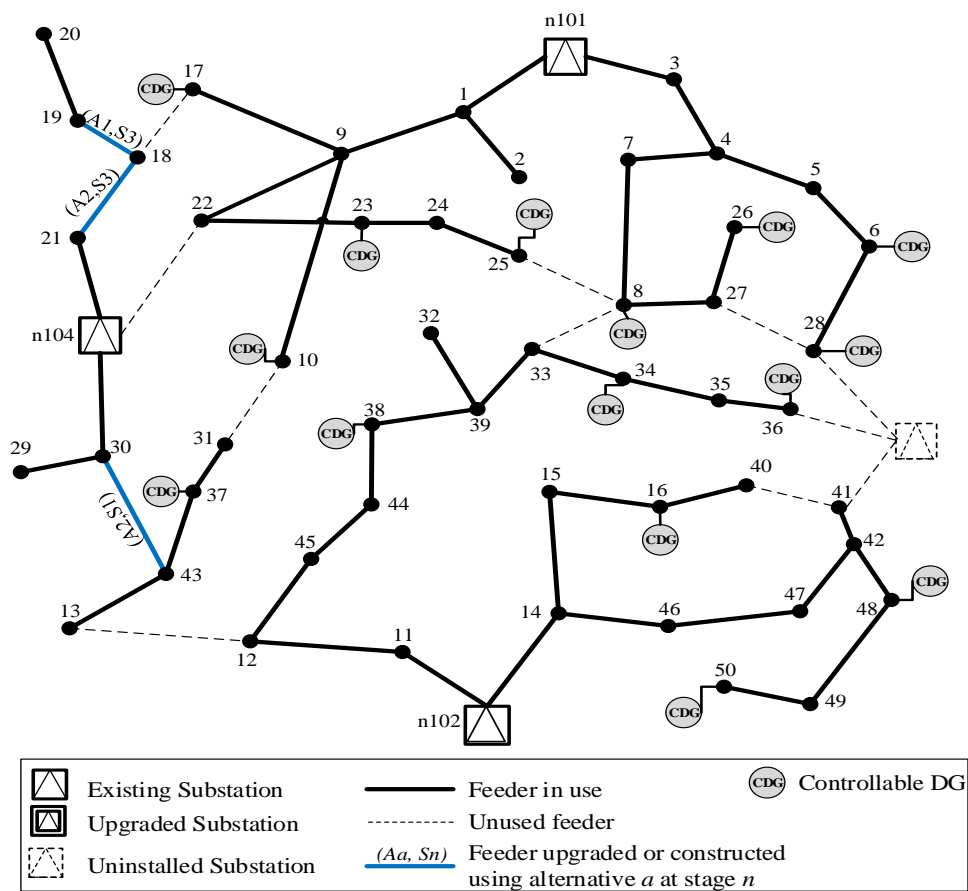


Figure 3-2 Network topology for case 1 with investments

2) *IDSP with CDGs, WDGs, and PVDGs*: The NPV of the total planning costs in the case in which all DG types are included in the model is  $104.74 \times 10^6$  US\$. As can be seen in Table 3-3, the LDC can save almost  $59.3 \times 10^6$  US\$ by introducing these DGs into the grid. However, the LDC must spend  $42.95 \times 10^6$  US\$,  $5.992 \times 10^6$  US\$, and  $7.06 \times 10^6$  US\$ to incentivize CDG, WDG, and PVDG owners, respectively, with the incentives being distributed so as to ensure the feasibility of the DG projects. The total net savings with this scenario are therefore  $3.29 \times 10^6$  US\$. However, this net saving can be considerably increased when the emission costs are incorporated in the model. DG investments are located at a total of 15 system buses, as evident in stage 3. The penetration level of renewable DGs is 15 %, almost 7.5% for each renewable-based DG. Since the IRRs equal the 10 %, as determined by the investors, the contracted BWIP prices shown in Table 3-4 guarantee that the DG projects are financially feasible for all defined buses, for all DG types. The WDG contract price is 67.4 US\$/MWh while the PVDG contract price is 87.5 US\$/MWh. An interesting observation here is that the incentive price for a given bus is different for every DG type. For example, the incentive prices at bus 6 for all DG types are as follows; CDG = 44.5 \$/MWh, WDG = 0, and PVDG = 87.5 \$/MWh as can be seen in Table 3-4. This means that the only DG types that should be connected to bus 6 are CDGs and PVDGs. This shows the selectivity of the DG types at each bus in the proposed model. Figure 3-3 illustrates the network topology for case 2. The planned network topology in this case remains the same as in case 1. It can be observed that most LDC investment plans are deferred and that the feeder-upgrade investment costs in this case are higher than the costs obtained in case 1. The need for more feeder upgrade plans and higher feeder capacities compared to case 1 is attributed to the uncertainty caused by the renewable-based DG output power fluctuation. The possibility that there is no power generated from renewable-based DGs at several hours made the feeder upgrade plans essential to accommodate the high power flowing in the circuits. Substation upgrade decisions were produced for substation n101 and substation n102 at the third stage using the substation upgrade alternative 1 for both of them. Table 3-5 lists the planning decisions committed to by the LDC and DG investors.

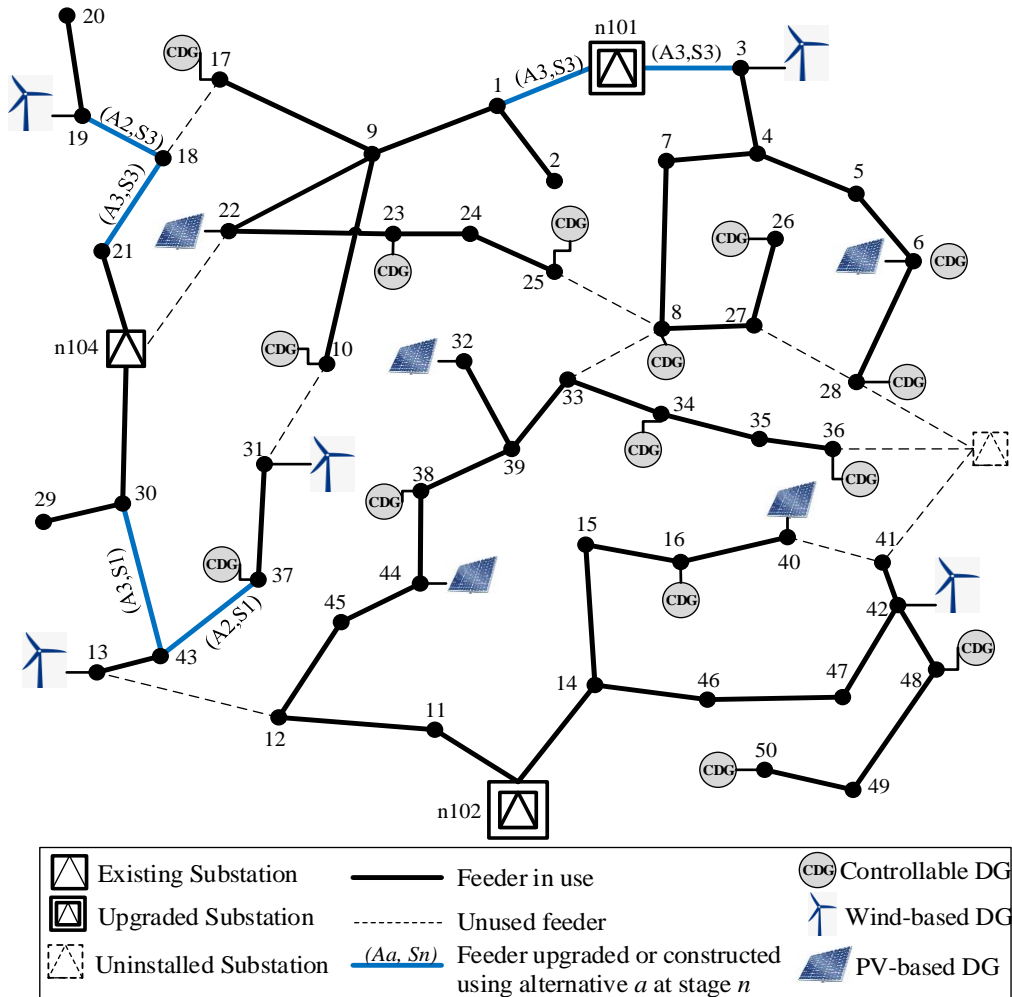


Figure 3-3 Network topology for case 2 with investment

### 3.4.4 Incentive Design Based on the Profitability Index

The previous section (*Section 3.4.3*) dealt with an IDSP design based on the specified MARR of the DG investors. However, it is more appropriate and convenient for DG investors to apply other economic measures to ensure the profitability of their projects. This section discusses an IDSP design based on the PI, addressing the results for both case 1 and case 2. For case 1, in which only CDGs are considered, Figure 3-4 shows the variations in the NPV of the LDC costs and total incentive costs, along with the changes in the PI. As long as the PI increases, the NPV of the LDC costs increases, and the LDC savings decrease. It can also be seen that when the PI reaches 1.5, LDC costs are almost equal to the base case cost for LDC expansion plans with no DGs, and consequently the net savings are equal to zero. The LDC should therefore avoid designing the system with a PI above 1.5. It is important to mention that this number is only valid for the system under study and it may be different for different systems.

Table 3-5 Investment Plans Committed to by the LDC and DG Investors for Each Stage

Stage	Case 1		Case 2			
	LDC Plans	CDG Owner Plans	LDC Plans	CDG Owner Plans	WDG Owner Plans	PVDG Owner Plans
1	30-43 (A2)	8 (0.7), 10 (1.5), 16 (0.4), 17 (0.1), 23 (0.9), 25 (0.7), 26 (1.1), 28 (0.4), 34 (2.6), 36 (0.4), 37 (0.3), 38 (0.9), 48 (1.3), 50 (0.4)	30-43 (A3) 37-43 (A2)	6 (0.1), 8 (0.8), 10 (1.5), 16 (0.4), 17 (0.1), 23 (0.8), 25 (0.7), 26 (1.1), 28 (0.3), 34 (2.4), 36 (0.5), 37 (0.1), 38 (1), 48 (0.9), 50 (0.8)	3 (0.1) 13 (1.3) 19 (1.0) 31 (1.9) 42 (0.3)	6 (2.0) 22 (0.6) 32 (1.2) 40 (0.8) 44 (0.1)
2	NA	6 (0.5), 8 (1.4), 10 (1.8), 16 (1.3), 17 (0.7), 23 (1.4), 25 (0.7), 26 (1.2), 28 (0.5), 34 (2.6), 36 (0.5), 37 (0.6), 38 (2.2), 48 (1.4), 50 (0.7)	NA	6 (0.3), 8 (1), 10 (2.1), 16 (1.1), 17 (0.8), 23 (1.1), 25 (0.9), 26 (1.4), 28 (0.5), 34 (2.5), 36 (0.5), 37 (0.3), 38 (2.2), 48 (1.9), 50 (0.8)	3 (0.1) 13 (1.3) 19 (1.0) 31 (1.9) 42 (0.3)	6 (2.0) 22 (0.6) 32 (1.2) 40 (0.8) 44 (0.1)
3	18-19 (A1) 18-21 (A2)	6 (0.9), 8 (1.9), 10 (2.5), 16 (2), 17 (1.1), 23 (1.7), 25 (0.8), 26 (1.2), 28 (0.5), 34 (2.7), 36 (0.5), 37 (1.2), 38 (3.5), 48 (1.4), 50 (1.3)	n101 (U1) n102 (U1) n101-1 (A3) n101-3 (A3) 18-19 (A2) 18-21 (A3)	6 (0.3), 8 (1), 10 (2.3), 16 (1.7), 17 (1), 23 (1.6), 25 (0.9), 26 (1.4), 28 (0.5), 34 (2.7), 36 (0.5), 37 (1.2), 38 (2.3), 48 (2.1), 50 (0.9)	3 (0.1) 13 (1.3) 19 (1.0) 31 (1.9) 42 (0.3)	6 (2.0) 22 (0.6) 32 (1.2) 40 (0.8) 44 (0.1)

For LDC plans, (U) represents a substation upgrade alternative, (C) represents a substation construction alternative, and (A) represents a feeder alternative. For DG investor plans, the first number represents the bus number and the number in parentheses represents the cumulative DG capacity in MW.

It can be observed that although the incentive prices are higher than the average purchasing price from the market, the proposed model found that it is more economical for the LDC to form contracts with the DG investors since the defined locations and capacities of the DGs will eliminate the upgrade investments of the substations, reduce the line investments, and minimize the losses and operation costs. The average prices for the BWIP and the average DPP for CDG projects can be seen in Figure 3-5.

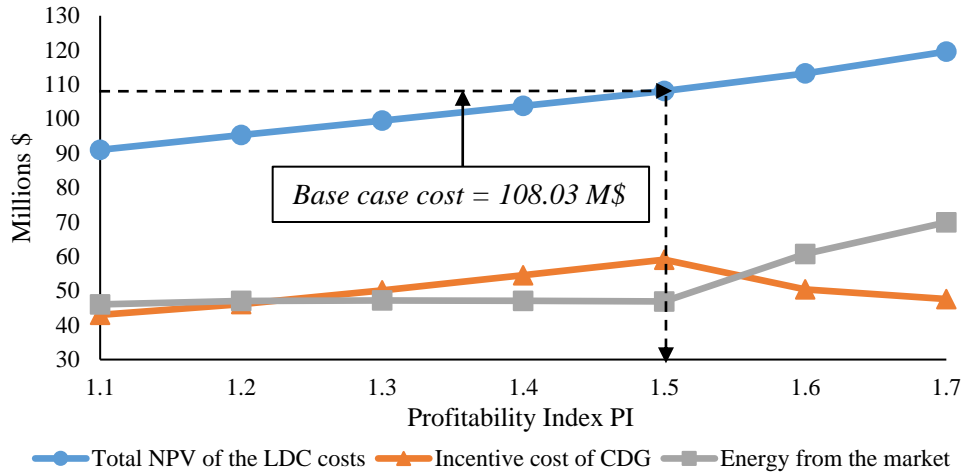


Figure 3-4 Variations in planning costs with different PIs for case 1 (CDGs only)

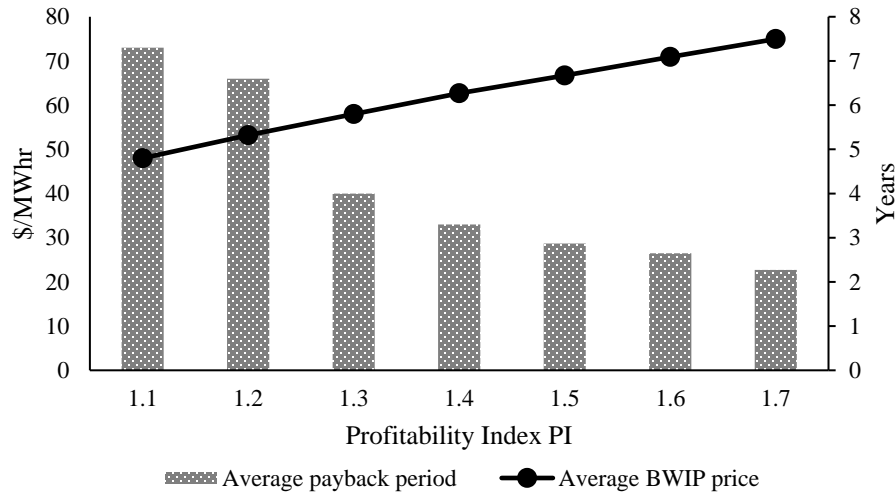


Figure 3-5 Variations in the average BWIP prices and the DPP with different PIs for case 1 (CDGs only)

For case 2, in which all types of DGs are considered, the results also reveal that when the PI increases, the BWIP prices and the total LDC costs increase as well, as shown in Figure 3-6 and Figure 3-7. From another perspective, as long as the PI increases, the net LDC savings decrease until a threshold point is reached, which is almost 1.21, the point at which the LDC cost is equal to the base case cost. The LDC should therefore not design the system with a PI above 1.21. It is important to mention that this number is only valid for the system under study and it may be different for different systems. It should be noted that the incentive costs for WDGs and PVDGs increase along with the rising PI. This increase would be expected

regardless of a BWIP price that is higher than the average market price in order to satisfy the constraint imposed on renewable-based DG penetration. As expected, although the average BWIP price for CDGs is higher than the average market price at the design point (i.e. PI = 1.21), it is still more economical for the LDC to purchase power at that price to avoid or defer substation upgrade costs, as indicated in Figure 3-6. The average BWIP price for each DG type and the average payback period are shown in Figure 3-7.

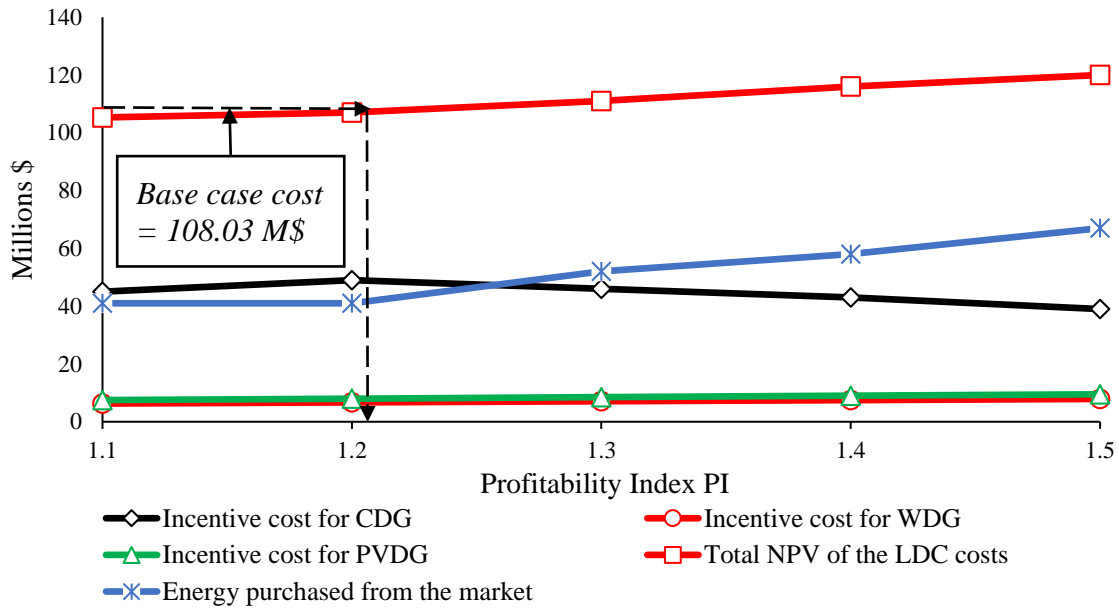


Figure 3-6 Variations in planning costs with different PIs for case 2

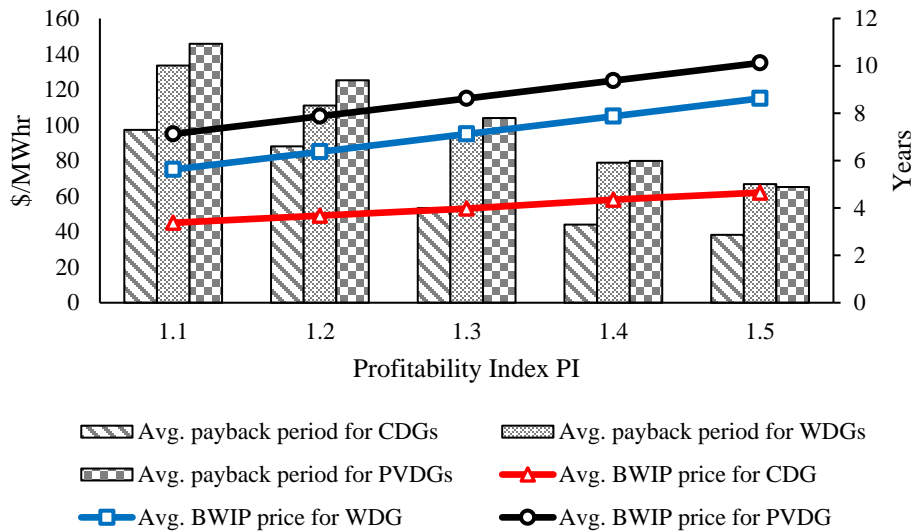


Figure 3-7 Variations in average BWIP prices and DPPs with different PIs for case 2

### 3.4.5 Effect of Uncertainty on Planning Results

To examine the results of the proposed model from the uncertainty perspective (i.e. uncertainty of system demand, wind and PV-based DG output power, and energy prices), a Monte Carlo Simulation (MCS) coupled with power flow analysis [121] has been executed for a large number of iterations (i.e. 10,000 iterations).

#### 1) Planning costs and profitability indices

The effect of uncertainty upon planning costs and profitability indices is studied in this section. It can be observed that, at different profitability indices, the total planning costs obtained from the proposed model are very close to those obtained using MCS. Moreover, the differences between the designed PIs and the evaluated PIs using MCS are very small, as can be seen in Table 3-6. These results provide evidence that the uncertainty model captures the system randomness efficiently.

Table 3-6 Comparison Between the Proposed Model and MCS Results

Proposed Model Results		MCS Results	
PI	Total Cost (M\$)	PI	Total Cost (M\$)
1.1	105.30	1.122	104.91
1.2	107.82	1.194	107.37
1.3	111.52	1.288	110.76
1.4	116.2	1.412	115.96
1.5	120.36	1.508	119.85

#### 2) Planned network topology robustness

The robustness of the network planned topology can be assessed through the use of MCS-based probabilistic power flow. With a 95% confidence level, it can be observed in Figure 3-8 that the voltages at each bus in the system are within the permissible limit (i.e., 0.95-1.05 p.u.). Moreover, with a 95% confidence level, it can be observed in Figure 3-9 that the feeder currents are within the designed thermal capacities of the lines taking into account the new capacities of the upgraded feeders obtained from the model outcomes. These two assessments provide a very good indication that the planned topology is robust with respect to the uncertainty caused by the fluctuations of system demand and renewable-based DGs output power.

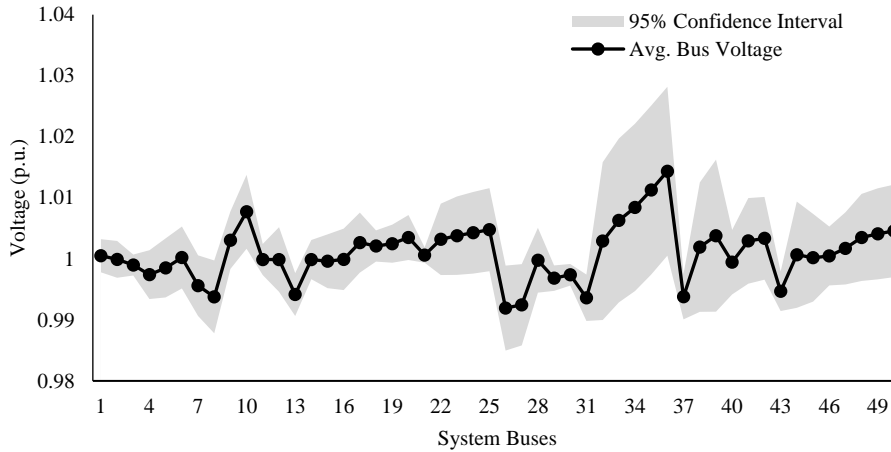


Figure 3-8 Avg. system buses voltages and their 95% confidence intervals

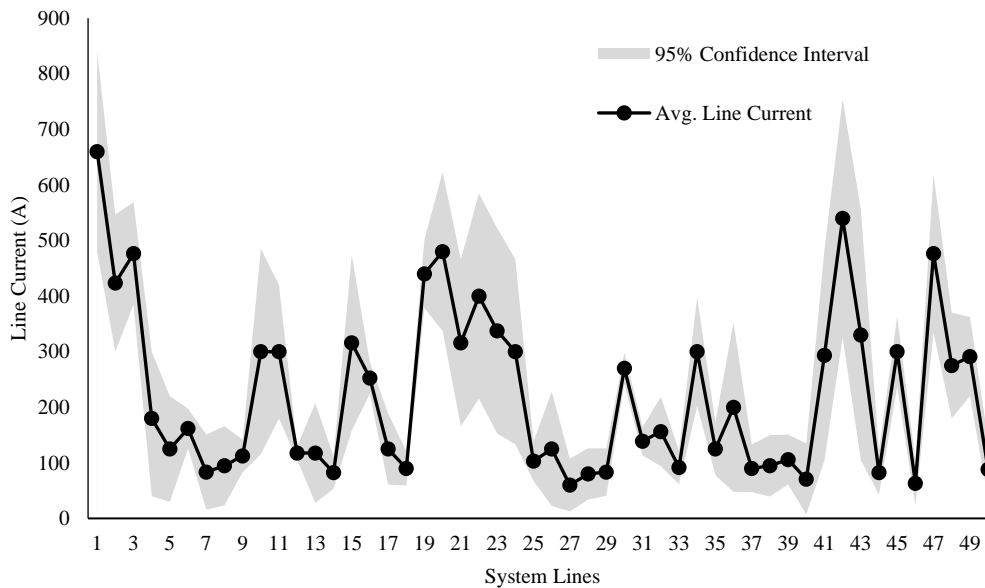


Figure 3-9 Avg. system lines currents and their 95% confidence intervals

### 3.4.6 Comparing Multistage and Single Stage Models

The proposed IDSP model is a dynamic model (i.e. multistage-based model) in which the planning decisions take place at different time stages in the planning horizon based on the system needs, following the load growth at each stage. Thus, to present the advantages of the multistage model over a single stage model, the planning model is solved using a single stage (i.e., a 15-year planning period) where the planning investments occur at the beginning of the planning period (i.e., year 1) considering the demand in the last stage. The single stage results showed that the total planning cost for case 1 and case 2 are 94.87 and 110.4×

10<sup>6</sup> US\$, respectively. These results are higher than the multistage results obtained by the proposed model. The multistage model allows for efficient utilization of the investments over the entire planning period.

### **3.4.7 Computational Aspects**

The mixed integer linear programming (MILP) optimization model was solved by utilizing the CPLEX solver with programming and execution in GAMS environment [122] using a desktop computer with an Intel® Core™ i7 3.60 GHz processor and 16 GB of RAM. CPLEX solver utilizes Branch and Cut-based algorithm to solve the proposed model with an optimality gap set to 1%. For Case 1 with only CDG, the elapsed time is 12.3 minutes, and for Case 2 with all DG types, the solver takes 722 minutes to reach the optimal solution. Considering that the planning studies are basically offline problems, the computational effort is not a primary concern. This, combined with the fact that the equations and the variables of the proposed model can accommodate any increase in the system size without causing model breakdown, the proposed model is applicable for large scale distribution systems.

## **3.5 Summary**

This chapter has presented a novel IDSP model that incorporates the active participation of DG investors in the planning problem. The proposed model establishes a BWIP and determines the incentives that should be offered by the LDC to DG investors. The proposed model enables the LDC to direct the connection of DG projects to specific buses that will benefit the overall system and that will ensure the profitability of the investments of the corresponding investors based on the BWIP prices offered. The IDSP model takes into account DG installation and operation by the investor and analyzes several economic indices: the MARR, PI, and DPP of the DG projects. At the same time, the LDC has the opportunity to identify the least cost solution from a combination of the proposed BWIP and traditional expansion planning options. In this way the model allows the LDC to coordinate its future expansion projects effectively with DG investors. Three types of DGs are considered: controllable, wind-based, and PV-based. The uncertainty associated with the intermittent nature of wind speed, solar irradiance, and system demand is treated probabilistically, and all possible operating scenarios are created. A number of linearization methods are used to convert the MINLP model into a MILP model. The results of the case studies presented demonstrate the effectiveness of the proposed model, which will encourage DG investors to play a crucial role in the distribution planning process, increase LDC savings, guarantee the profitability of DG projects, and consequently minimize total planning costs.

## **Chapter 4**

# **Reinforcement Planning Model for Distribution System Reliability Enhancement**

### **4.1 Introduction**

The previous chapter dealt with expansion planning for distribution systems that would enable them to address load growth economically without taking system reliability into consideration. However, in a deregulated power environment, service reliability is considered a major factor that consumers and system regulators take into account when evaluating the performance of service providers. As stated in chapters 1 and 2, it is therefore crucial that, during the planning process, system planners maintain reliability indices within the permissible limits stipulated by regulators. The obligations imposed with the goal of enhancing overall system reliability require substantial effort on the part of the planning engineer to investigate a number of alternatives and assess them from both a technical and economic perspective [10]. Achieving a high level of system reliability results in costly expenditures by the utilities, and aiming for such a goal might lead to unnecessary plans and overestimated costs. The notion of value-based reliability planning has thus emerged as a means of exploring the most cost-effective solutions for improving system reliability.

Indeed, from a reliability perspective, distribution system reinforcement planning can be performed through two main approaches. The first is to allocate normally closed and normally open (NO) switches and tie lines in the distribution system in order to enhance overall system reliability under contingency conditions. This approach can also require upgrading some of the system assets, such as substations and feeders, thus allowing this equipment to accommodate any transferred load without creating conditions that violate thermal capacity limits. The second approach is to increase the capacities of the DGs embedded in the system in order to allow the affected areas to operate adequately in islanded mode under contingency conditions. It is this second approach that was the target of the research investigation discussed in the next chapter.

This chapter presents a proposed value-based reinforcement planning model for enhancing system reliability and maintaining reliability metrics within allowable limits. The research described in this chapter can be viewed as an extension of the work introduced in the previous chapter, thus forming a general planning framework that incorporates consideration of reliability, as illustrated in Figure 4-1. The optimal allocation of tie lines and NO switches is determined based on this planning framework, as are the required capacity upgrades for substations and lines. Two hierarchical levels for system operation under contingencies are adopted in this model: restoration and islanding. These levels are discussed extensively

in the following sections.

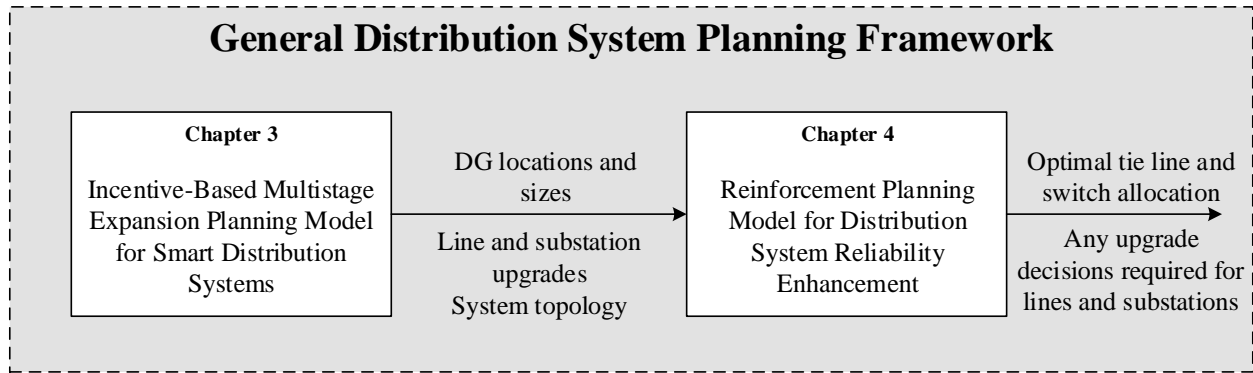


Figure 4-1 Proposed general planning framework for distribution systems

The main contributions of the work presented in this chapter can be summarized as follows:

- A planning methodology is proposed for determining the optimal allocation of tie lines and NO switches so as to improve system reliability and maintain reliability indices within permissible boundaries. The required upgrade capacities of feeders and substations are also obtained.
- Two hierarchical levels for system operation under contingencies are proposed in order to allow the load points affected by the fault to be restored from either restoration paths in the system or islanded operation mode.
- A probabilistic analytical model is proposed for computing distribution system reliability indices based on consideration of the two hierarchical operation levels under contingencies and taking into account variations in system demand, DG output power, and the uncertainty associated with system components.

In the next sections, the probabilistic system operating scenarios, the problem formulation with the proposed reliability evaluation approach, and a case study and its results are discussed. The chapter then ends with concluding remarks.

## 4.2 Probabilistic System Operating Scenarios for the Incorporation of Uncertainty

The intermittent nature of system demand and the primary sources of wind- and PV-based DG power (i.e., wind speed and solar irradiance) are considered the primary factors that affect planning and reliability analysis. Since reliability planning is characterized as a long-term application, probabilistic models that rely on probability density functions (PDFs) are employed because of their suitability for that kind of application. The modeling of the power output from DGs and the system demand as well as the building of

system operating scenarios are discussed extensively in chapter 3. This section provides a brief summary with references to section 3.2 for more details.

#### **4.2.1 Load Modeling**

With respect to determining the best representative PDF for modeling system demand, the following process has been followed. Historical demand data are analyzed and investigated against several PDFs. The K-S test is applied, with a normal distribution being selected as the best fit for mimicking the historical data. The normal distribution is next divided into several states, and the probability of each state is then calculated.

#### **4.2.2 Wind and PV-Based DG Modeling**

Historical wind speeds and solar radiation in the system under study are collected and then analyzed in order to identify the best distribution density functions to be fitted to those random data. As established using the K-S test, the Weibull distribution and the beta distribution are the best choices for modeling the randomness of wind speed and solar irradiance, respectively. Each distribution is then divided into several states, and the probability of each state is calculated. The multistate output power from wind-based DGs is then calculated using a wind turbine power curve, as described in detail in section 3.2. The multistate power output from the PV modules is calculated using the PV power equations and the I-V characteristics of the PV modules.

#### **4.2.3 Building the Probabilistic Operating Scenarios**

After all states for wind power, solar power, and system load are defined, a matrix is created that consists of three columns that include all possible operating scenarios for the wind and solar output power states as well as the load states (i.e., column 1 represents the wind-based DG output power, column 2 represents the solar DG output power, and column 3 represents the different load levels). The matrix created has rows equal to the multiplication of wind, solar, and load states, and the probability of each state is equal to the product of wind probability, solar probability, and load probability at that corresponding state. These calculations are based on the assumption that wind speed, solar irradiance, and load are independent events.

### **4.3 Proposed Reliability-Based Reinforcement Planning Model**

Distribution system reliability planning models are never aimed at achieving the highest level of service reliability but instead have the goal of maintaining satisfactory service quality through the setting of several reliability targets and attempts to achieve those targets at the lowest possible cost. The following sections provide a thorough discussion of the problem formulation and the methodology for evaluating system reliability.

### 4.3.1 Problem Formulation

This section presents the formulation of the distribution system reinforcement reliability optimization problem. The objective function of the planning problem is to minimize the cost of the energy not served (CENS), the cost of tie lines (CTL), the cost of NO switches (CNOS), and the costs of existing substation and feeder upgrades (CUPG), expressed as follows:

$$\text{Min } Z = \sum_{t \in T} \left[ \frac{\text{CENS}(t) + \text{CTL}(t) + \text{CNOS}(t) + \text{CUPG}(t)}{(1 + \tau)^{(t-1)K}} \right] + Pf \sum_c^{nc} x_c \quad (4.1)$$

where  $x_c$  is a binary variable corresponding to reliability constraint  $c$ ,  $nc$  is the total number of reliability constraints, and  $Pf$  is the penalty factor (a very large number if a reliability constraint is not satisfied, and equal to zero otherwise). The mathematical formulations for the components of the objective function are presented in the following equations:

$$\text{CENS}(t) = \sum_{i \in N} \text{ENS}_{i,t} IC \quad (4.2)$$

$$\text{CTL}(t) = \sum_{f \in Tf} \text{ITC}_{f,t} \times N_{f,t} \quad (4.3)$$

$$\text{CNOS}(t) = \sum_{NO \in NOS} \text{INOC}_{NO,t} \times N_{NO,t} \quad (4.4)$$

$$\text{CUPG}(t) = \sum_{i \in \Omega_{ES}} \sum_{u \in \Omega_U} (C_u^{US} \sigma_{i,u,t}) + \sum_{ij \in \Omega_{EL}} \sum_{a \in \Omega_a} C_a^{UF} L_{ij} \beta_{ij,a,t} \quad (4.5)$$

where

- $\text{ENS}_{i,t}$ : Energy not served at bus  $i$  at stage  $t$ ;
- $IC$ : Interruption cost penalty (\$/MWhr);
- $\text{ITC}_{f,t}$ : Investment cost of tie lines  $f$  at stage  $t$ ;
- $\text{INOC}_{NO,t}$ : Investment cost of normally open switch  $NO$  at stage  $t$ ;
- $N_{f,t}$ : = 1 if tie line  $f$  is chosen in stage  $t$  and zero otherwise;
- $N_{NO}$ : = 1 if normally open switch  $NO$  is chosen in stage  $t$  and zero otherwise;
- $C_u^{US}$  and  $C_a^{UF}$ : Respective costs of upgrading existing substations and feeders that correspond to Alternative  $c$  for substations and alternative  $a$  for feeders;
- $L_{ij}$ : Feeder length (km);
- $\sigma_{i,u,t}$  and  $\beta_{ij,a,t}$ : Binary variables that correspond to substation and feeder upgrades, respectively;
- $N$ : Set of system buses;

$Tf$ :	Set of candidate tie lines;
$NOS$ :	Set of normally opened switches;
$ES$ :	Set of existing substations;
$EL$ :	Set of existing feeders;
$\Omega_U$ :	Set of substation upgrade alternatives;
$\Omega_a$ :	Set of feeder upgrade alternatives.

The CENS for the whole system is equal to the summation of the energy not served ( $ENS$ ) at each bus multiplied by the per megawatt hour interruption cost. The  $ENS$  at each bus can be calculated using equation (4.27).

The optimization constraints are indicated as follows:

$$SAIDI_{i,t} \leq SAIDI_i^{targeted} \quad (4.6)$$

$$ENS_{i,t} \leq ENS_i^{targeted} \quad (4.7)$$

$SAIDI_i^{targeted}$  and  $ENS_i^{targeted}$  are the targeted system average interruption duration and  $ENS$  based-indices set by the regulator. It is worth mentioning that there are other system operational constraints that should be satisfied (i.e., supply demand balance, feeder thermal limits, substation thermal limits, and bus voltage limits) and that these constraints, which are discussed explicitly in the next sections, should be maintained for each contingency analysis.

Since reliability optimization is dependent mainly on the system configuration, a metaheuristic searching algorithm is preferable for this kind of problem. A genetic algorithm (GA) is used for solving the reliability-based reinforcement planning problem. In a GA population, a large number of chromosomes (initial candidate solutions) are generated. Each string or each chromosome is composed of a number of genes. At any generation, the fitness function is evaluated for each string, and these strings are then ranked based on their evolution to the objective function. An exterior penalty function is used as a means of penalizing infeasible solutions, and a penalty function is added to the objective function in order to handle the constraints.

Prior to GA processing, the strings should be prepared so that they are compatible with the GA format. Since a chromosome represents a candidate solution and the problem is to allocate the tie lines and NO switches and to upgrade some of the feeders and substations, the chromosome is composed of multiple genes that represent vector control variable components (binary variables for tie lines and NO switches,

binary variables for upgrade decisions, and integer variables for the investment year). Figure 4-2 illustrates the structure of typical chromosome encoding in a planning problem. Figure 4-3 presents the flowchart outlining the proposed optimization process.

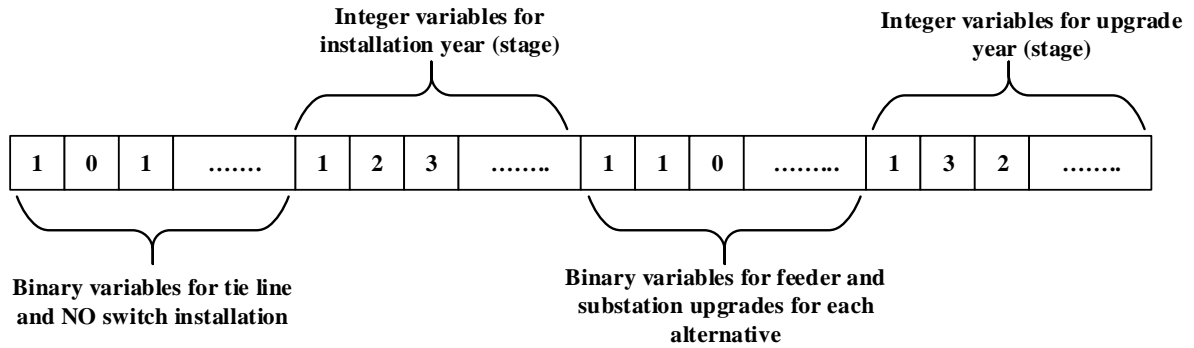


Figure 4-2 Structure of typical chromosome encoding in a planning problem

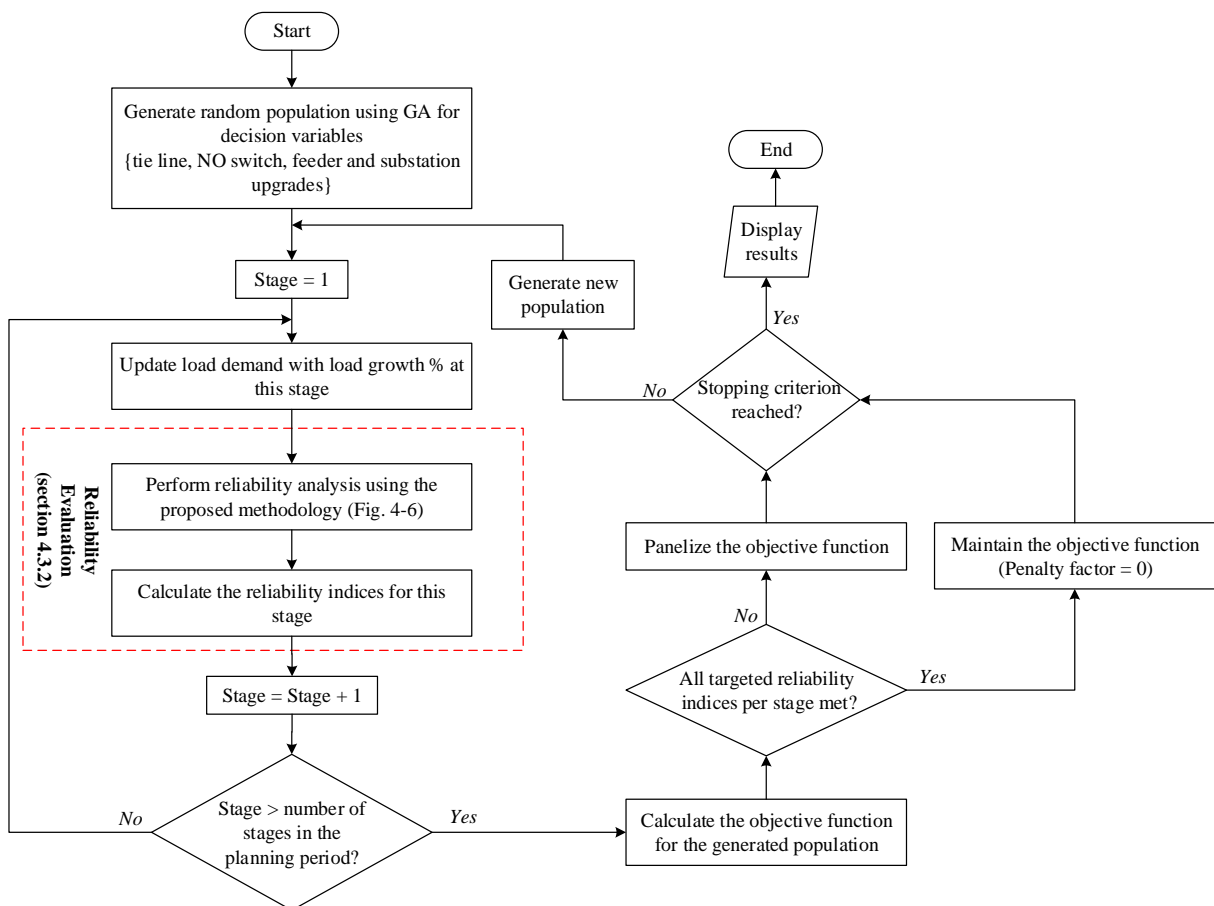


Figure 4-3 Flowchart of the proposed reliability-based reinforcement planning model using a GA

### 4.3.2 Distribution System Reliability Evaluation with DGs

This section explains the N-1 contingency-based analysis performed for evaluating system reliability. The N-1 approach stipulates that the system should be able to operate and fully meet the required demand and service quality when at least one component in the system goes out of service (i.e., down state). The N-1 analysis includes consideration of the outage of every component in the system. For the purposes of the research presented in this thesis, only failures or outages in lines and at substations are taken into account.

The inclusion of dispatchable or renewable-based DGs in distribution systems in fact proves the enormous potential of these generation resources with respect to improving overall system reliability [96]. When a disturbance of this kind occurs in the system, protection devices isolate the faulty parts, thus permitting healthy operation for the rest of the network, and this action results in island formation. DGs contribute to the enhancement of system reliability mainly through their ability to feed all or part of the loads in the islands formed or through their ability to mitigate the violation of the system operational security constraints when the restoration process takes place.

The proposed reliability evaluation method begins with the definition of three important sets:

**1- Sequence path set for each bus ( $SP_i$ ):** The sequence path set for each bus includes all of the components in the series path between the substation and the bus under investigation. The unavailability of each bus is dependent primarily on the outage at any component located between the source and the bus under investigation. This means that any failure of a component in the sequence path between the source and the bus under study will require a waiting time (downtime) for the repair of this component. Such a delay results in a load interruption at that bus.

**2- Set of affected buses for each contingency ( $AB_C$ ):** When a contingency occurs, the protection devices in the network operate to isolate the faulty part, resulting in a sustained power interruption for loads located downstream from the faulty equipment. For this reason, only the group of loads that are affected by such a contingency are considered in this set.

**3- Potential restoration for each contingency ( $PR_C$ ):** When an outage takes place, part of the system is isolated by the protective devices. This action results in island formation, and the island formed requires a waiting time (i.e., repair time) for the problem to be fixed and power from the main source to be restored. However, if any restoration paths are able to reconnect the customers in the formed island with the main source, the down time for those customers will be reduced from the time needed for repair to the time needed for switching, thus enabling faster power restoration.

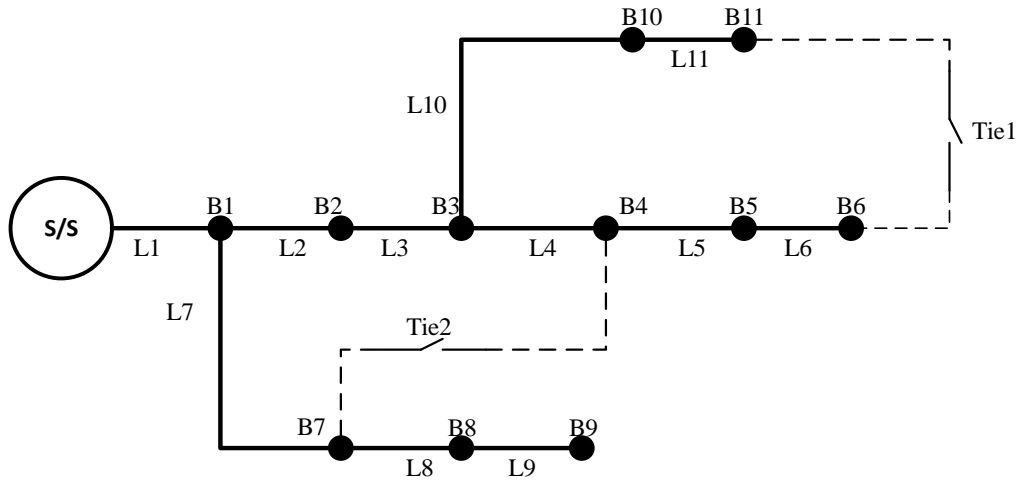


Figure 4-4 Illustrative 11-bus distribution system

For a better understanding of the creation of the above sets, an illustrative example for a small distribution system is presented. Consider the 11-bus system shown in Figure 4-4. If an outage occurs in line 4, then the buses affected are B4, B5, and B6, as can be seen in Figure 4-5. Two restoration paths can be formed in order to restore the affected buses: the paths associated with tie 1 and tie 2. Table 4-1 presents the sequence path set for each bus, and Table 4-2 shows the set of affected buses and the potential restoration set for each contingency.

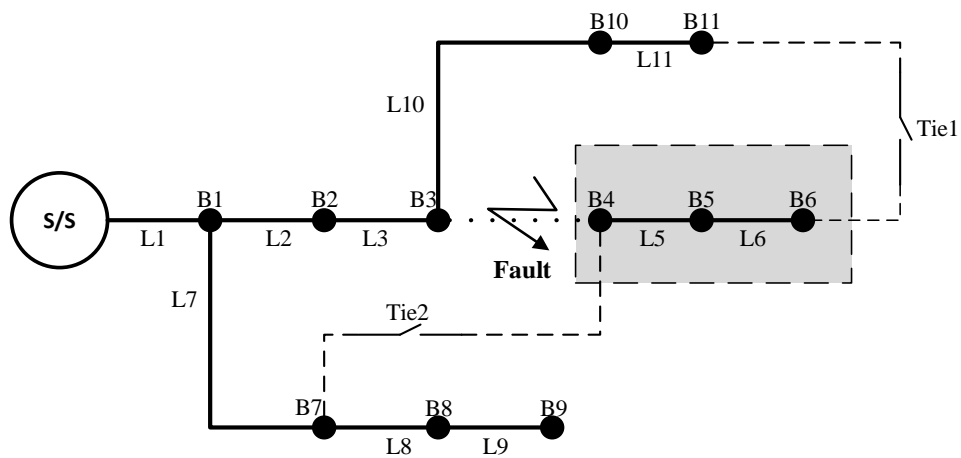


Figure 4-5 Island created because of a fault in line 4

Table 4-1 Sequence Path and Sequence Path Set for Each Bus

Bus (i)	Sequence Path	Sequence Path Set ( $SP_i$ )
B1	S/S→L1	{S/S, L1}
B2	S/S→L1→L2	{S/S, L1, L2}
B3	S/S→L1→L2→L3	{S/S, L1, L2, L3}
B4	S/S→L1→L2→L3→L4	{S/S, L1, L2, L3, L4}
B5	S/S→L1→L2→L3→L4→L5	{S/S, L1, L2, L3, L4, L5}
B6	S/S→L1→L2→L3→L4→L5→L6	{S/S, L1, L2, L3, L4, L5, L6}
B7	S/S→L1→L7	{S/S, L1, L7}
B8	S/S→L1→L7→L8	{S/S, L1, L7, L8}
B9	S/S→L1→L7→L8→L9	{S/S, L1, L7, L8, L9}
B10	S/S→L1→L2→L3→L10	{S/S, L1, L2, L3, L10}
B11	S/S→L1→L2→L3→L10→L11	{S/S, L1, L2, L3, L10, L11}

Table 4-2 Set of Affected Buses and Potential Restoration Set for Each Contingency

Contingency (C)	Affected Buses Set ( $AB_C$ )	Potential Restoration Set ( $PR_C$ )
S/S	{B1,B2,B3,B4,B5,B6,B7,B8,B9,B10,B11}	{ $\phi$ }
L1	{B1,B2,B3,B4,B5,B6,B7,B8,B9,B10,B11}	{ $\phi$ }
L2	{B2,B3,B4,B5,B6, B10,B11}	{Tie2}
L3	{B3,B4,B5,B6, B10,B11}	{Tie2}
L4	{B4,B5,B6}	{Tie1, Tie2}
L5	{B5,B6}	{Tie1}
L6	{B6}	{Tie1}
L7	{B7,B8,B9}	{Tie2}
L8	{B8,B9}	{ $\phi$ }
L9	{B9}	{ $\phi$ }
L10	{B10,B11}	{Tie1}
L11	{B11}	{Tie1}

After all of the sets have been determined for each bus and each contingency, the reliability indices for each bus can be calculated, taking into account the intentional islanding and intentional restoration. When this kind of contingency occurs, some of the system buses (i.e., buses that are affected due to contingency  $AB_C$ )

are isolated by the protection systems, resulting in island formation. Intentional restoration will be successful if and only if at least one restoration path is available for the island that is out of service, the restoration path does not cause an overload or an excessive voltage drop along the feeders, and the restoration path does not create an overload at the substation to which the disconnected loads will be transferred. If these conditions are not fulfilled, the intentional restoration will be considered an unsuccessful restoration. All of the potential restoration paths for the formed island are addressed and evaluated. It is worth noting that the system topology is modified as a result of the investigation of each restoration path. Forward/backward sweep-based load flow analysis [20] is executed for each topology and system operating scenario so as to obtain the operational system conditions (i.e., feeder power flow, bus voltages, and power withdrawn from substations) and also to verify whether these conditions have been met.

- ***Conditions for successful restoration (success mode 1)***

The restoration process will be successful if all five of the following conditions are satisfied:

- 1- At least one restoration path exists that once again connects the formed island with the source.
- 2- The restoration path will not cause an overload for the feeder to which the island's loads will be transferred:

$$I_f \leq I_f^{MAX} \quad (4.8)$$

- 3- The restoration path will not cause an overload for the substation to which the island's loads will be transferred:

$$S_{sub} \leq S_{sub}^{MAX} \quad (4.9)$$

- 4- The restoration process will not create an excessive voltage drop along the feeder that will cause some buses to operate outside the voltage standard limits:

$$V_i^{MIN} \leq V_i \leq V_i^{MAX} \quad (4.10)$$

- 5- The power conservation condition (i.e., the generation-demand balance constraint) must be met: all generation sources in the system must meet the system demand and losses:

$$\sum_{i \in S} P_{G_i} + \sum_{i \in DG} P_{DG_i} - \sum_{i \in N} P_{D_i} - \sum_{f \in TF} P_{loss_f} = 0 \quad (4.11)$$

$$\sum_{i \in S} Q_{G_i} + \sum_{i \in DG} Q_{DG_i} - \sum_{i \in N} Q_{D_i} - \sum_{f \in TF} Q_{loss_f} = 0 \quad (4.12)$$

where

$P_{G_i}$  and  $Q_{G_i}$ : Active and reactive power generated from the substation, respectively;

$P_{DG_i}$  and  $Q_{DG_i}$ : Active and reactive power generated from the DG, respectively;

$P_{D_i}$  and  $Q_{D_i}$ : Active and reactive power demand at bus  $i$ , respectively;

$P_{loss_f}$  and  $Q_{loss_f}$ : Active and reactive power loss of feeder  $f$ , respectively;

$S$ : Set of substation buses;

$DG$ : Set of DG buses;

$N$ : Set of system demand buses;

$TF$ : Set of system feeders.

Once the intentional restoration has failed or no restoration path exists for the buses out of service, then the second evaluation level (i.e., intentional islanding) is investigated. Intentional islanding will be successful if and only if the power generated from the DGs inside the island is greater than or equal to the total demand and losses for the island. If not, then the intentional islanding is considered to be unsuccessful.

- ***Condition for successful islanding (success mode 2)***

The necessary condition for the disconnected loads to be in successful islanded mode is that the total power generated from the DGs in the island must match the total load and losses of the island:

$$P_{DG_I} \geq P_{D_I} + P_{L_I} \quad (4.13)$$

$P_{DG_I}$ : Total power generated by DGs inside the formed island  $I$ ;

$P_{D_I}$ : Total power demand in the formed island  $I$ ;

$P_{L_I}$ : Total power losses in the island  $I$ , assumed to be 5 % from the state island load [96].

The result is two success modes, successful restoration and successful islanding, as well as one failure mode. For each operating scenario and each contingency, the algorithm should select one of these modes. Figure 4-6 demonstrates the flowchart of the proposed general framework for evaluating distribution system reliability when the system includes DGs.

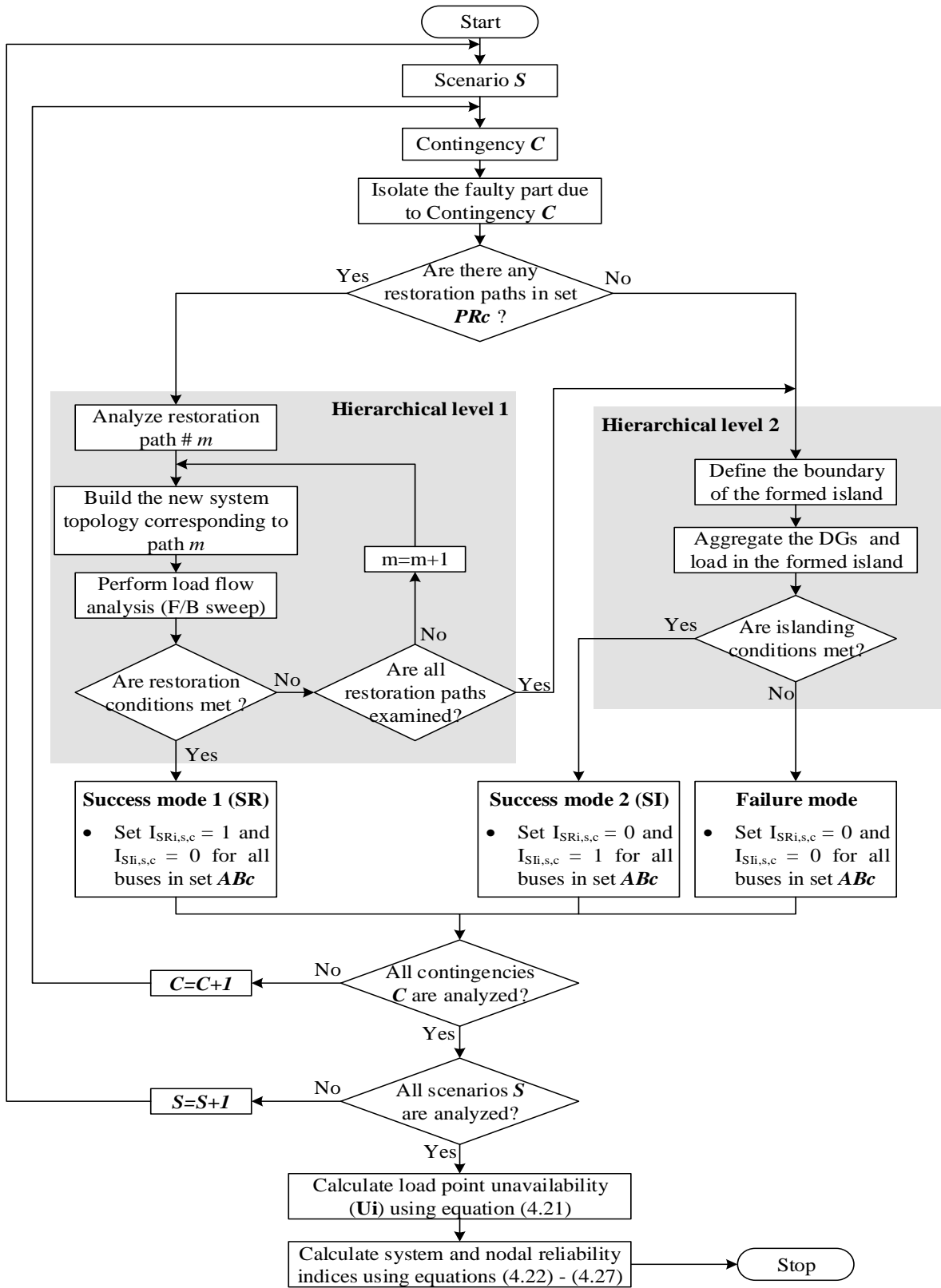


Figure 4-6 Flowchart for the proposed distribution system reliability evaluation model

- **Calculating the reliability indices using the proposed method**

The downtime of any load point in the system is calculated as follows:

$$DT_i = \sum_{C \in SP_i} \lambda_C r_C \quad (4.14)$$

where

$\lambda_C$ : Failure rate of component  $C$  where  $C$  belongs to the set of  $SP_i$ ;

$r_C$ : Repair rate of component  $C$  where  $C$  belongs to the set of  $SP_i$ .

The probability of load point  $i$  to be in isolated mode due to equipment outages in its series path to the main source can therefore be calculated as follows:

$$P_i^{isolated} = \frac{\sum_{C \in SP_i} \lambda_C r_C}{NH} \quad (4.15)$$

where  $NH$  is the number of hours in a calendar year (i.e.,  $NH = 8760$ ).

The probability of load point  $i$  to be in isolated mode due to contingency  $C$  is calculated as follows:

$$P_{i,c}^{isolated} = \begin{cases} \frac{\lambda_C r_C}{NH} & \text{if } c \in SP_i \\ 0 & \text{if } c \notin SP_i \end{cases} \quad (4.16)$$

The probability of load point  $i$  to be working in a success mode of operation after contingency  $C$  has taken place is dependent mainly on the probability of load point  $i$  to be in isolated mode due to contingency  $C$  and the probability of either successful restoration or successful islanding for that contingency. Given that the probability of the load point being in isolated mode and the probability of a success mode of operation are independent, the probability of a success mode of operation for bus  $i$  due to contingency  $C$  can be calculated by multiplying these two probabilities, as shown in the following equation:

$$P_{i,c}^{success} = P_{i,c}^{isolated} \times P_{i,c}^{SRSI} \quad (4.17)$$

where  $P_{i,c}^{SRSI}$  is the probability of either successful restoration or successful islanding.

The probability of either successful restoration or successful islanding  $P_{i,c}^{SRSI}$  is dependent primarily on the probability of the scenario in which renewable-based DG output power and power demand reside.

Therefore,  $P_{i,c}^{SRSI}$  is equal to the summation of the occurrence probabilities for the scenarios that result in the restoration conditions being met or the islanding condition being satisfied; otherwise, the probability is considered to be zero.

$$P_{i,c}^{SRSI} = \sum_{s=1}^{Ts} P_s [I_{SRi,s,c} + I_{SIi,s,c}] \quad (4.18)$$

$$I_{SRi,s,c} = \begin{cases} 1 & \text{if resoration conditions are met} \\ 0 & \text{otherwise;} \end{cases} \quad (4.19)$$

$$I_{SIi,s,c} = \begin{cases} 1 & \text{if islanding condition is met} \\ 0 & \text{otherwise;} \end{cases} \quad (4.20)$$

where  $I_{SRi,s,c}$  and  $I_{SIi,s,c}$  are indices for successful restoration and successful islanding, respectively;  $P_s$  is the probability of occurrence of scenario  $s$ ; and  $Ts$  is the total number of operating scenarios.

It is important to state that, under any contingency and any scenario, if success mode 1 is attainable,  $I_{SRi,s,c}$  is forced to be one and  $I_{SIi,s,c}$  is forced to be zero. Likewise, if success mode 2 is attainable,  $I_{SRi,s,c}$  is forced to be zero and  $I_{SIi,s,c}$  is forced to be one. Otherwise,  $I_{SRi,s,c}$  and  $I_{SIi,s,c}$  are both forced to be zeros for the failure mode. All three modes are considered to be mutually exclusive, as indicated in the flowchart shown in Figure 4-6.

Now, the unavailability of load point  $i$  can be calculated using the following equation:

$$U_i = \sum_{c \in SP_i} (\lambda_c r_c - P_{i,c}^{success} \times NH) \quad (4.21)$$

In the above equation, the second part ( $P_{i,c}^{success} \times NH$ ) represents the improvement in the unavailability of the annual load point  $i$  due to the successful restoration or successful islanding.

The distribution system reliability indices are then calculated from the following equations:

$$SAIDI = \frac{\sum_i U_i N_i}{\sum_i N_i} \quad (4.22)$$

$$ASAI = \frac{\sum_i N_i \times NH - \sum_i U_i N_i}{\sum_i N_i \times NH} \quad (4.23)$$

$$ASUI = 1 - ASAI \quad (4.24)$$

$$ENS = \sum_i L_{a(i)} U_i \quad (4.25)$$

where  $N_i$  is the number of customers at load point  $i$ ;  $L_{a(i)}$  is the average load connected to load point  $i$ ; and  $NH$  is the number of hours in a calendar year ( $NH = 8760$ ).

The total reliability indices for each bus in the system can be calculated using the following equations:

$$SAIDI_i = \sum_{c \in SP_i} (\lambda_c r_c - P_{i,c}^{success} \times NH) \quad (4.26)$$

$$ENS_i = L_{a(i)} \sum_{c \in SP_i} (\lambda_c r_c - P_{i,c}^{success} \times NH) \quad (4.27)$$

## 4.4 Case Studies and Numerical Results

A number of case studies were conducted as a means of verifying the efficacy of the proposed framework. The studies and their results are detailed below.

### 4.4.1 Distribution System Under Study

The proposed reliability-based reinforcement planning model was tested using a primary 54-node distribution system, whose full data can be found in [113]. Figure 4-7 illustrates the configuration of the system. The system operating voltage is 15 kV; it has 50 existing feeders, three existing substations, and eight candidate tie lines. The reliability data for the system components are shown in Table 4-3. The targeted system average interruption duration index (SAIDI) and ENS at each stage and each bus in the system are 2.5 hrs/yr and 5 MWh/yr, respectively [123]. The interruption cost penalty is assumed to be 2000\$/MWhr [2], and the cost of a NO switch is 4700 US\$ [124]. The cost of constructing a new tie line is  $2 \times 10^6$  US\$/km. Two alternative transformers with capacities of 13.3 MVA and 16.7 MVA and associated installation costs of  $8 \times 10^6$  US\$ and  $10 \times 10^6$  US\$, respectively, are considered for upgrading the substations. The capacity of the existing substations is 16.7 MVA. The studies entailed three alternatives for feeder upgrades with thermal capacities of 250 A, 450 A, and 900 A and installation costs of  $35 \times 10^4$  US\$/km,  $46 \times 10^4$  US\$/km, and  $92 \times 10^4$  US\$/km [115], respectively. The thermal capacities and lengths of the system feeders can be obtained from [113]. The planning horizon is assumed to be 15 years with 3 % annual load growth. The planning horizon is divided into three stages, each of which has a five-year period. The interest rate is assumed to be 10 %, and the system power factor is 0.9.

Table 4-4 lists the locations and sizes of the DGs in the system, which were obtained from the results detailed in the previous chapter (Chapter 3).

Table 4-3 Reliability Data for the System Components [96], [125]		
	Failure rate ( $\lambda_C$ )	Repair time ( $r_C$ )
Feeder	0.12/km	8 h
Substation	0.6/100	24 h

Table 4-4 Locations and Sizes of DGs in the System

Case 1	Stage 1	6 (0), 8 (0.7), 10 (1.5), 16 (0.4), 17 (0.1), 23 (0.9), 25 (0.7), 26 (1.1), 28 (0.4), 34 (2.6), 36 (0.4), 37 (0.3), 38 (0.9), 48 (1.3), and 50 (0.4)
	Stage 2	6 (0.5), 8 (1.4), 10 (1.8), 16 (1.3), 17 (0.7), 23 (1.4), 25 (0.7), 26 (1.2), 28 (0.5), 34 (2.6), 36 (0.5), 37 (0.6), 38 (2.2), 48 (1.4), and 50 (0.7)
	Stage 3	6 (0.9), 8 (1.9), 10 (2.5), 16 (2), 17 (1.1), 23 (1.7), 25 (0.8), 26 (1.2), 28 (0.5), 34 (2.7), 36 (0.5), 37 (1.2), 38 (3.5), 48 (1.4), and 50 (1.3)
Case 2	Stage 1	<b>CDG:</b> 6 (0.1), 8 (0.8), 10 (1.5), 16 (0.4), 17 (0.1), 23 (0.8), 25 (0.7), 26 (1.1), 28 (0.3), 34 (2.4), 36 (0.5), 37 (0.0), 38 (1.0), 48 (0.9), and 50 (0.8)
		<b>WDG:</b> 3 (0.1), 13 (1.3), 19 (1.0), 31 (1.9), and 42 (0.3)
		<b>PVDG:</b> 6 (2.0), 22 (0.6), 32 (1.2), 40 (0.8), and 44 (0.1)
	Stage 2	<b>CDG:</b> 6 (0.3), 8 (1.0), 10 (2.1), 16 (1.1), 17 (0.8), 23 (1.1), 25 (0.9), 26 (1.4), 28 (0.5), 34 (2.5), 36 (0.5), 37 (0.3), 38 (2.2), 48 (1.9), and 50 (0.8)
		<b>WDG:</b> 3 (0.1), 13 (1.3), 19 (1.0), 31 (1.9), and 42 (0.3)
		<b>PVDG:</b> 6 (2.0), 22 (0.6), 32 (1.2), 40 (0.8), and 44 (0.1)
Stage 3	<b>CDG:</b> 6 (0.3), 8 (1.0), 10 (2.3), 16 (1.7), 17 (1.0), 23 (1.6), 25 (0.9), 26 (1.4), 28 (0.5), 34 (2.7), 36 (0.5), 37 (1.2), 38 (2.3), 48 (2.1), and 50 (0.9)	
	<b>WDG:</b> 3 (0.1), 13 (1.3), 19 (1.0), 31 (1.9), and 42 (0.3)	
	<b>PVDG:</b> 6 (2.0), 22 (0.6), 32 (1.2), 40 (0.8), and 44 (0.1)	
The first number represents the bus number, and the number in parentheses indicates the cumulative DG capacity in MW.		

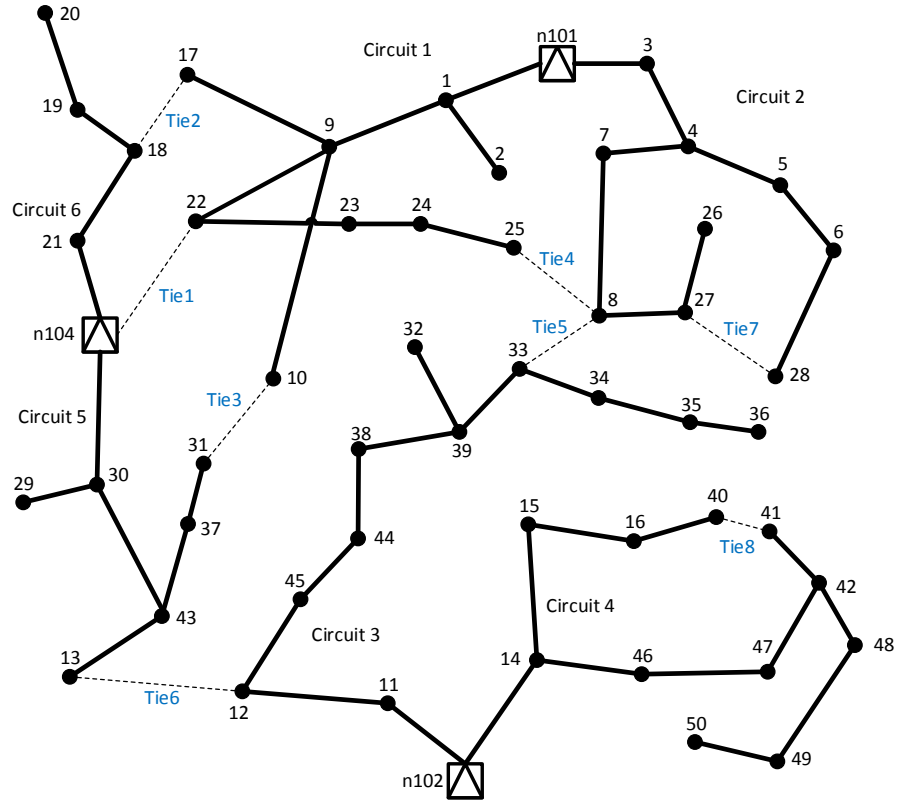


Figure 4-7 Distribution system configuration with candidate tie lines

#### 4.4.2 Case Studies and Results

To validate the proposed reliability-based planning model, two case studies were conducted: 1) reliability reinforcement planning with consideration of only controllable DGs (CDGs), and 2) reliability reinforcement planning with consideration of controllable, wind, and PV-based DGs. Since the studies described in this chapter constitute an extension of the work presented in Chapter 3, the locations and sizes of the DGs presented in Table 4-4 were known a priori.

##### 4.4.2.1 Reliability reinforcement planning considering only controllable DGs (CDG)

In this case study, the uncertainty in the system is caused by variations in system demand and failures sustained in system components. CDGs generate fixed power according to their nameplate rated power. The results show that in order to improve overall system reliability and achieve the targeted SAIDI and ENS at each bus, the installation of five tie lines and NO switches is required. Tie lines 3, 4, 5, 7, and 8 are installed at stage 1, as shown in Figure 4-8. Four feeders at the first stage must also be upgraded in order to enable a successful restoration process during the contingency and to alleviate the feeder congestion created when the affected loads are transferred to another feeder. Feeders 14-15, 15-16, and 33-39 are upgraded

using alternative 2 while feeder 16-40 is upgraded using alternative 1; all of these upgrade plans are required during the first stage. Figure 4-8 shows the system topology after reliability planning is applied for case 1, and Table 4-5 presents all of the installation and upgrade plans required.

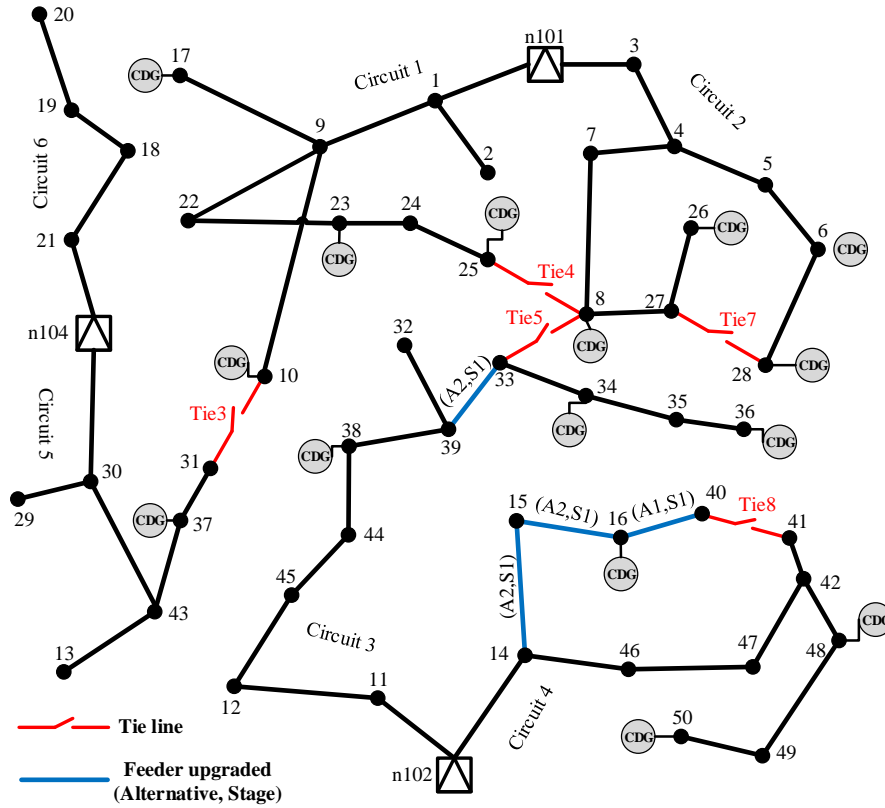


Figure 4-8 System topology following reliability-based reinforcement planning for case 1

Table 4-5 Investment Plans Required for Case Study 1

Tie lines and NO Switches to be Installed	System Assets to be Upgraded
Tie 3	Feeder 14-15 (A2, S1)
Tie 4	Feeder 15-16 (A2, S1)
Tie 5	Feeder 16-40 (A1, S1)
Tie 7	Feeder 16-40 (A1, S1)
Tie 8	Feeder 33-39 (A2, S1)

Figure 4-9 illustrates how the system would react in response to two different contingencies. When a fault takes place in feeder 1-9, the affected demand points (i.e., 9, 10, 17, 22, 23, 24, and 25) can be restored by opening the switches at feeder 1-9 and closing the NO switch at tie feeder 10-31. This restoration process would allow the affected demand point to be reconnected with the main source (i.e., substation n104)

without causing any bus to be under voltage violation and without creating thermal overloading at any feeder or substation. The DGs located in the affected area participate positively in the restoration process by alleviating any thermal congestion that could occur due to the load transfer process. In addition, when an outage occurs in feeder 33-34, the affected demand points (i.e., 34-36) are totally isolated from the grid because no restoration path exists that could reconnect these loads with the main sources. However, the DGs in bus 34 and bus 36 can pick up the load for the affected area, thus permitting successful islanding since the DG capacities can meet both the required demand and the losses for the affected area.

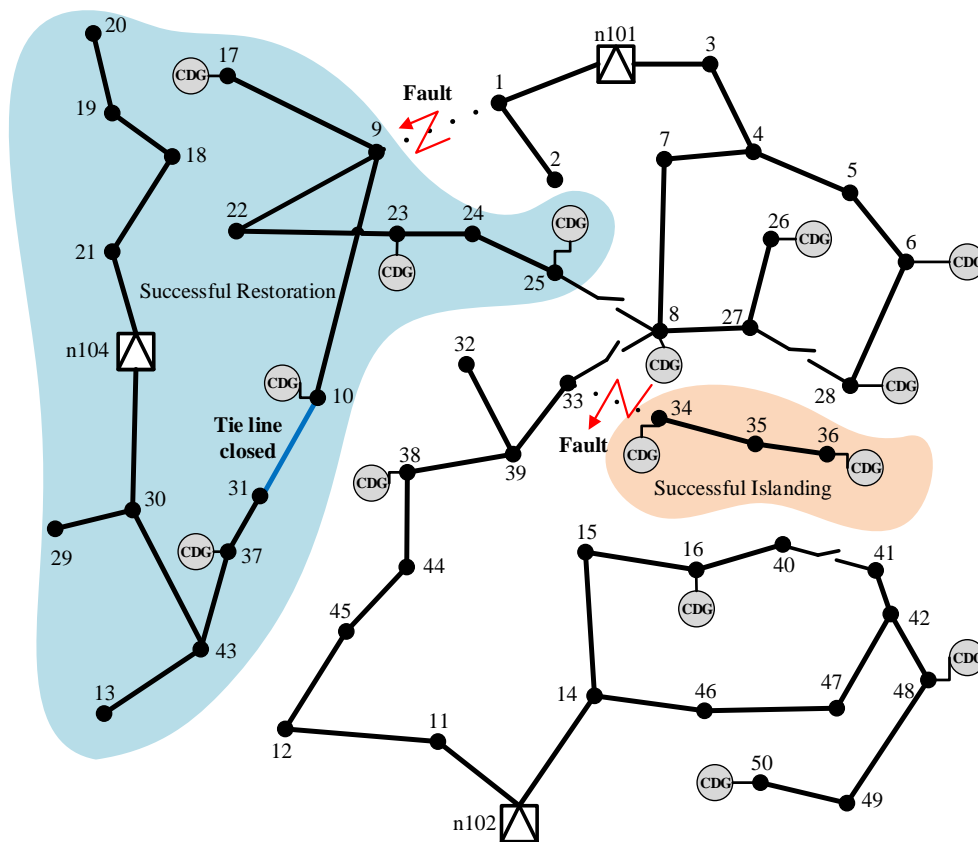


Figure 4-9 Optimal restoration process for two different contingencies in case 1

Figure 4-10 and Figure 4-11 show the SAIDI index for each bus in the network before and after the proposed reliability reinforcement planning, respectively. As can be seen from Figure 4-10, prior to reinforcement planning deployment, 27 buses in the system, which represent 54 % of the total network buses, were in violation of the nodal SAIDI-based reliability constraint. All 27 buses exceeded the nodal SAIDI regulatory threshold (i.e., 2.5 h/yr) at several stages in the planning horizon. However, when the five tie lines are

placed properly and the required feeder upgrade plans are placed as shown in Table 4-5, the SAIDI at each bus in the system and at each planning stage is substantially reduced and maintained below the regulatory standard, as indicated in Figure 4-11. The SAIDIs of the primary feeders are also reduced significantly as a result of the reductions in the SAIDIs at all system buses. Figure 4-12 and Figure 4-13 depicts the main feeder SAIDIs before and after implementation of the reinforcement planning, respectively.

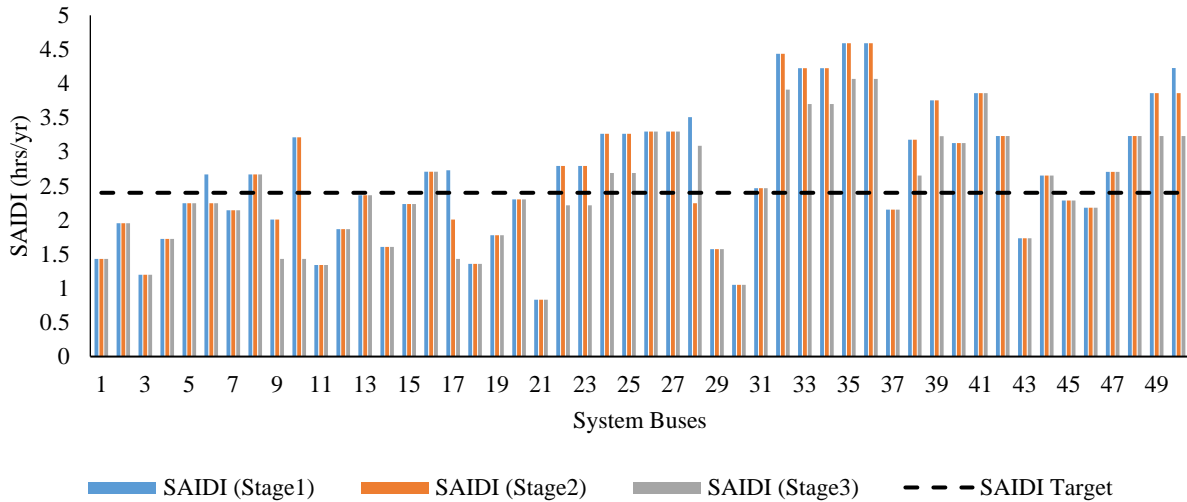


Figure 4-10 SAIDIs for each bus prior to reliability planning for case 1

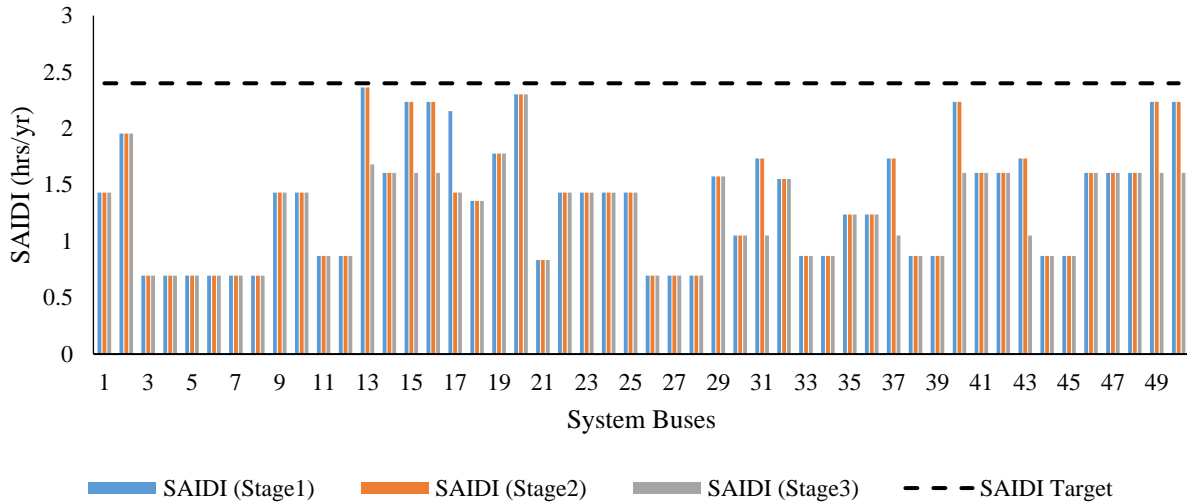


Figure 4-11 SAIDIs for each bus following reliability planning for case 1

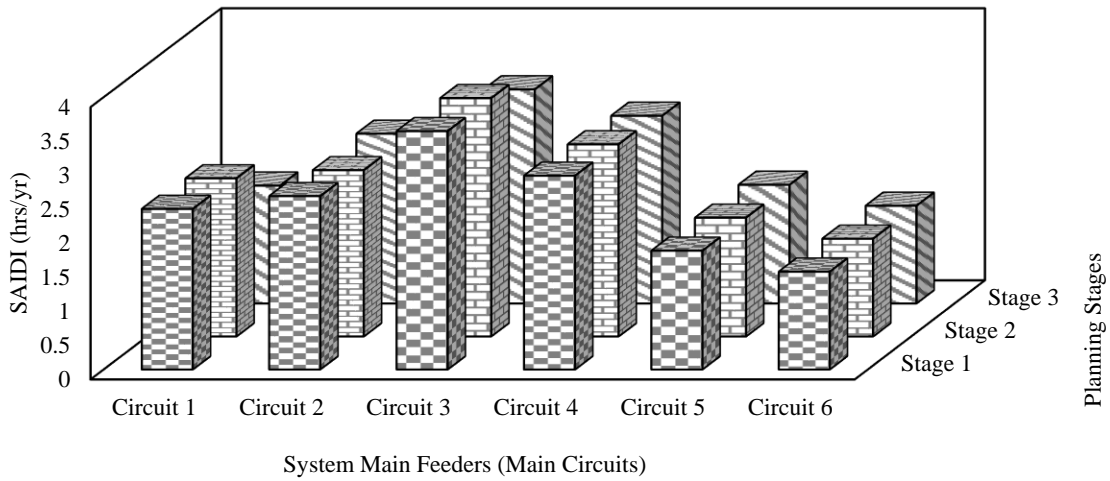


Figure 4-12 SAIDIs for the main feeders prior to reliability planning for Case 1

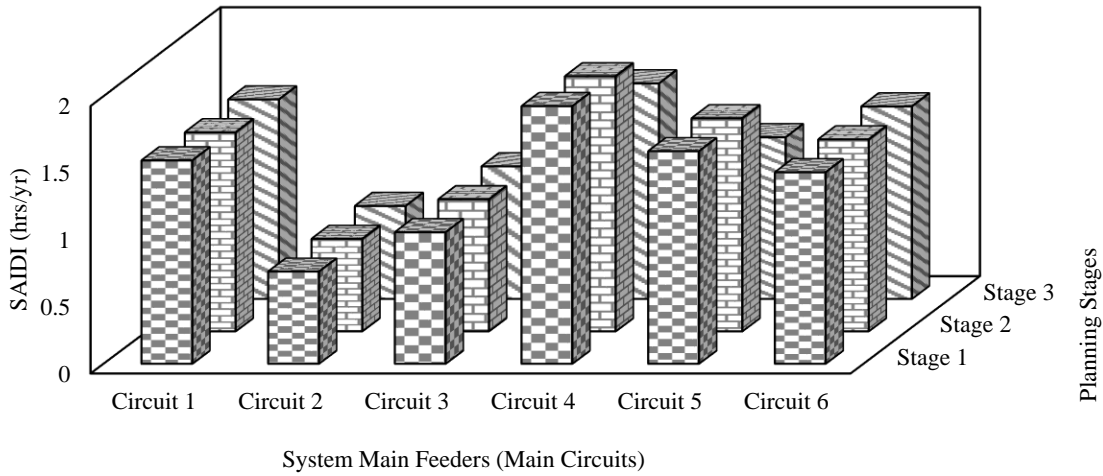


Figure 4-13 SAIDIs for the main feeders following reliability planning for case 1

The expected ENS is considerably reduced following the implementation of the proposed planning model. Figure 4-14 indicates the expected ENS at each stage both before and after the planning. It can be clearly observed that the ENS is reduced from 92.5 MWh/yr to 48.9 MWh/yr at stage 1. For stage 2, the ENS is reduced from 103.4 MWh/yr to 54.8 MWh/yr. The ENS is also reduced for stage 3: from 106 MWh/yr to 56 MWh/yr. The planning model achieved almost a 47 % reduction in the total ENS at each stage of the

planning period. The cost of the ENS dropped as well: from  $1.5 \times 10^6$  US\$ to  $0.739 \times 10^6$  US\$. Figure 4-15 and Figure 4-16 show the ENS for each bus at each stage before and after the planning, respectively. Prior to the determination of the planning decisions, three buses were in violation of the constraint that specifies the maximum ENS allowed at a bus; however, following the planning implementation, these violations are resolved and most of the ENS values of most of the buses are minimized.

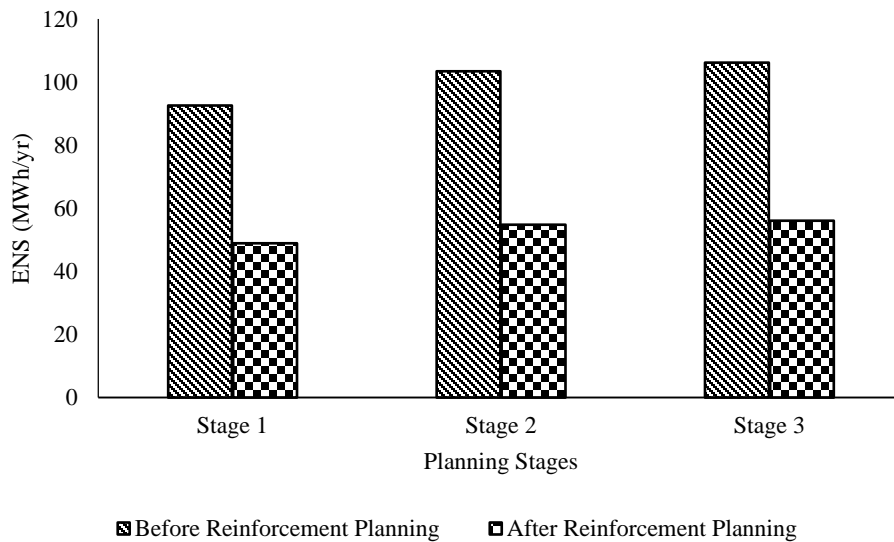


Figure 4-14 Expected ENS at each stage before and after reliability planning for case 1

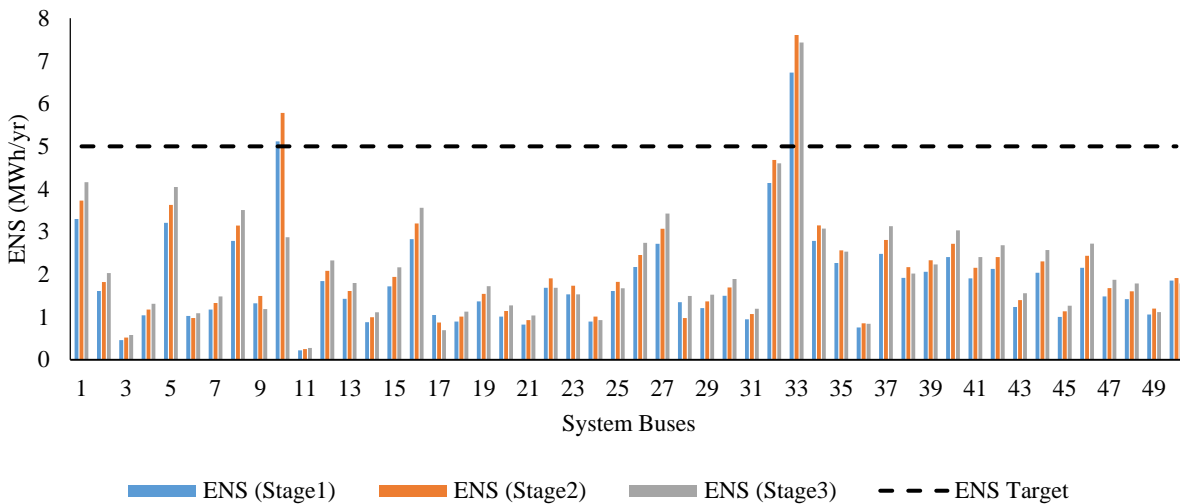


Figure 4-15 ENS for each bus prior to reliability planning for case 1

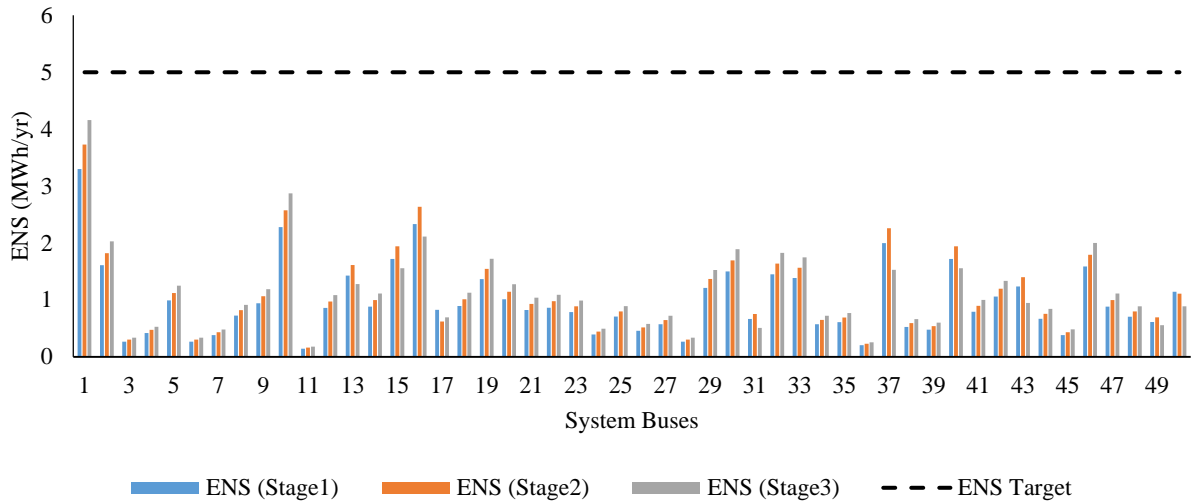


Figure 4-16 ENS for each bus following reliability planning for case 1

The results also reveal that the net present value (NPV) of the total reinforcement-based reliability investment cost incurred by the LDC is equal to  $8.84522 \times 10^6$  US\$. Almost 79 % of the total cost is for the installation of the tie lines that represent the largest share of the total expenditure. Of the total cost, 11.7 % goes toward upgrading some of the system feeders. The NPV of the total CENS for the planning horizon represents roughly 9 % of the total cost. The cost of NO switches is equal to  $23.5 \times 10^3$  US\$. Table 4-6 presents the NPV of the total planning cost and of all of the costs associated with the reinforcement process.

Table 4-6 NPV of the Associated Planning Costs for Case 1

<b>Reinforcement Planning Costs Breakdown</b>	<b>Cost in dollars (\$)</b>
Cost of energy not served (CENS)	792,680
Cost of tie lines (CTL)	6,992,000
Cost of normally open switches (CNOS)	23,500
Cost of feeder and substation upgrades (CUPG)	1,037,040
<b>NPV of total reinforcement planning cost</b>	<b>8,845,220</b>

#### 4.4.2.2 Reliability reinforcement planning considering controllable, wind, and PV-based DGs

This case study deals with reinforcement planning, taking into account the randomness of the power output from generation sources, fluctuations in system loads, and failures sustained in system equipment. The results of this study reveal that it is essential to install four tie lines and four NO switches, and to upgrade six feeders so as to enhance system reliability and maintain the reliability indices within the regulator-

imposed permissible limits. Tie lines 3, 5, 7, and 8 as well as the NO switches must be installed during the first stage of the planning, as shown in Figure 4-17. As well, feeders 9-10, 31-37, and 37-43 must be upgraded using alternative 2 during the first stage while feeder 16-40 is to be upgraded during the second stage using the same alternative. Feeders 30-43 and n104-30 require an upgrade during the first stage using alternative 3. The reason underlying the need for these upgrade plans is to allow these feeders (with the help of other system feeders) to pick up the loads disconnected due to the contingency by alleviating the thermal overloading of the feeder that would occur when the restoration process is applied. A comparison of this case study with the previous one (case 1) reveals that the number of tie lines required is reduced by one due to the increased generation sources from the renewables, which enable more successful islanding modes. Since the CDG at bus 37 is installed during the second stage, as shown in Table 4-4, feeders n104-30, 30-43, 37-43, and 31-37 must be upgraded during the first stage so as to accommodate the loads transferred when an outage occurs at circuit one. These circumstances explain the need for more feeder upgrades in this case study than in the first case. Figure 4-17 shows the system topology after reliability-based reinforcement planning is applied for case 2, and Table 4-7 presents all of the installation and upgrade plans required for case 2.

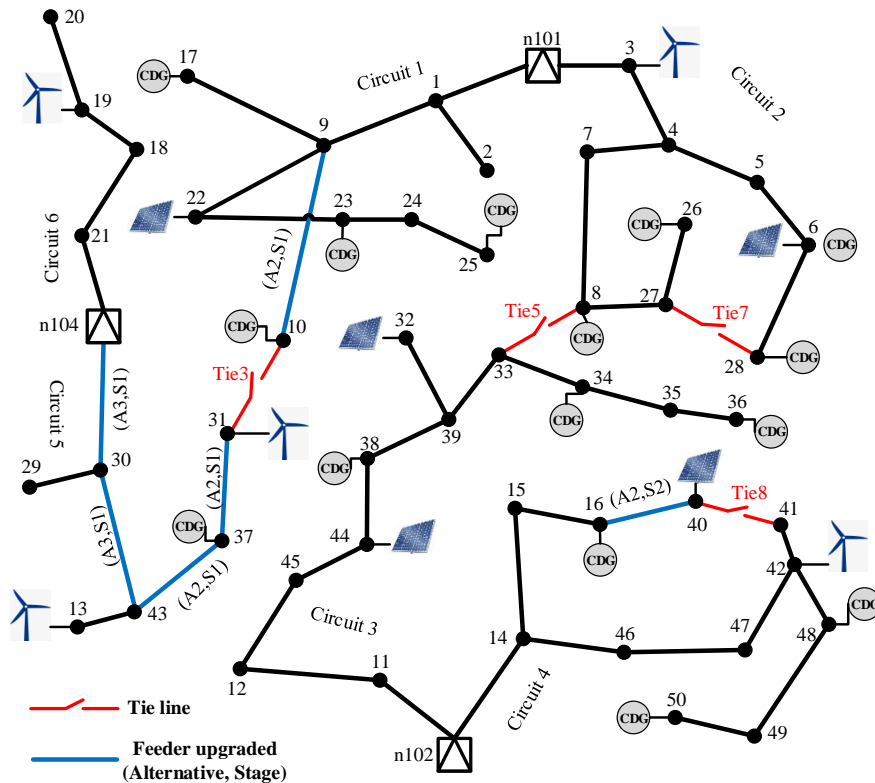


Figure 4-17 System topology after reliability-based reinforcement planning for case 2

Table 4-7 Investment Plans Required for Case Study 2

Tie lines and NO Switches to be Installed	System Assets to be Upgraded
Tie 3	Feeder 9-10 (A2, S1)
Tie 5	Feeder 31-37 (A2, S1)
Tie 7	Feeder 37-43 (A2, S1)
Tie 8	Feeder 30-43 (A3, S1)
	Feeder n104-30 (A3, S1)
	Feeder 16-40 (A2, S2)

The optimal corrective actions for three different contingencies are depicted in Figure 4-18. When an outage occurs in feeder 9-22, the optimal way to restore the buses affected is to isolate these buses from the grid and to feed the demand through the generation sources located inside this area (i.e., CDG at buses 23 and 25 and PVDG at bus 22). If the fault takes place in feeder 7-8, the affected load points can be restored by closing the tie line between bus 27 and bus 28 and by opening the switches at feeder 7-8. This corrective action would create a successful restoration mode since none of the operational system security limits would be violated.

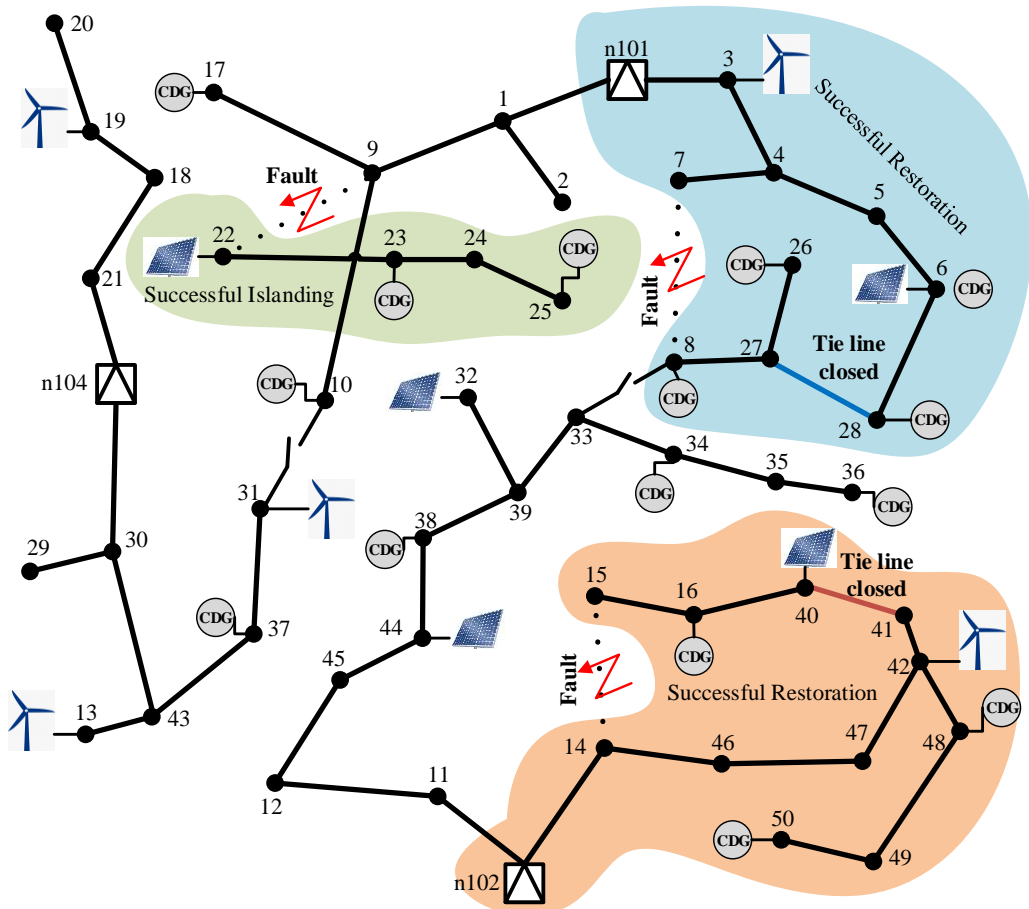


Figure 4-18 Optimal restoration process for three different contingencies in case 2

Figure 4-19 and Figure 4-20 indicate the SAIDIs for each bus in the network before and after the proposed reliability reinforcement planning for case 2, respectively. As can be seen, some of the system buses did not adhere to the reliability restrictions. However, when only four tie lines are placed properly and the required feeder upgrade plans are placed as shown in Table 4-7, the SAIDI at each bus in the system and at each planning stage is reduced substantially and maintained below the regulatory standard, as indicated in Figure 4-20. In addition, the SAIDIs of the primary feeders are reduced significantly as a result of the reduction in the SAIDIs at all system buses. Figure 4-21 illustrates the main feeder SAIDIs following reinforcement planning.

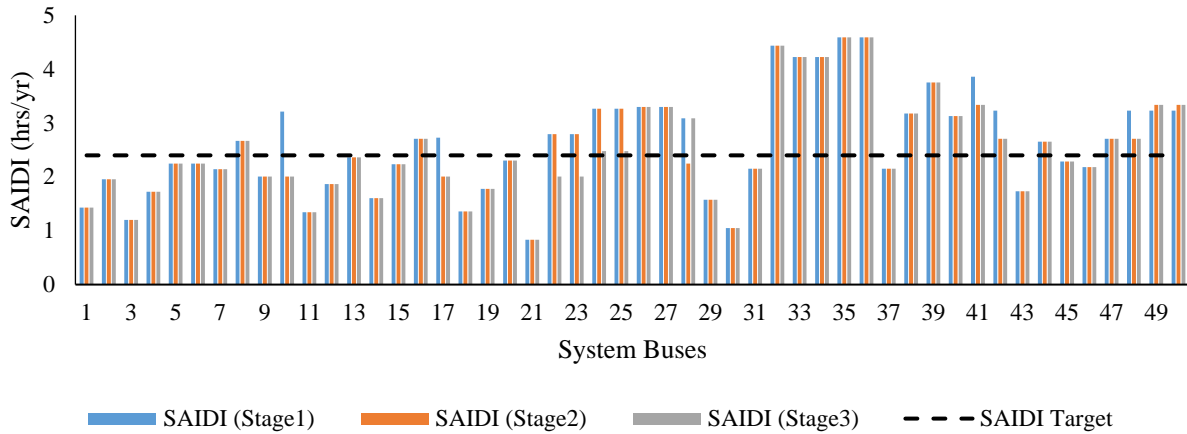


Figure 4-19 SAIDIs for each bus prior to reliability planning for case 2

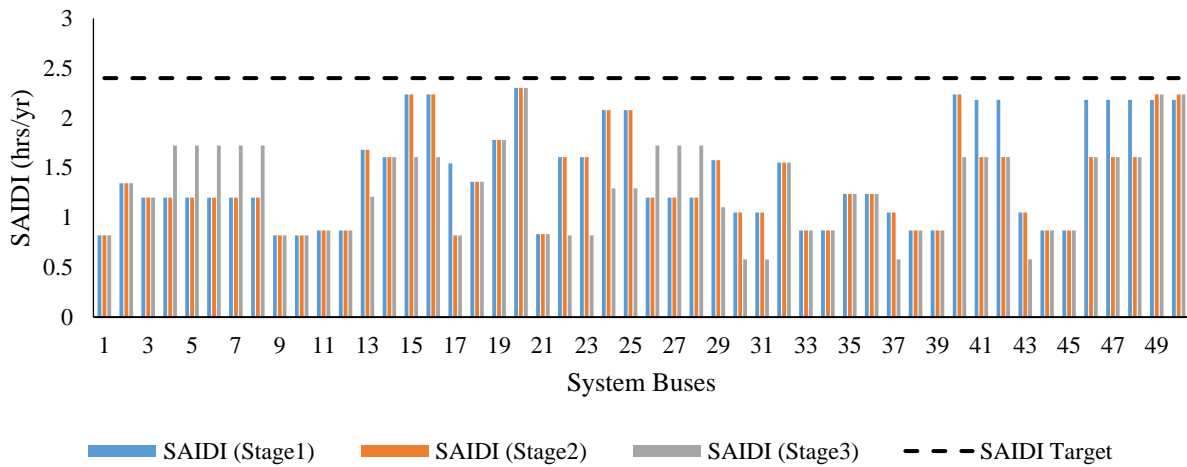


Figure 4-20 SAIDIs for each bus following reliability planning for case 2

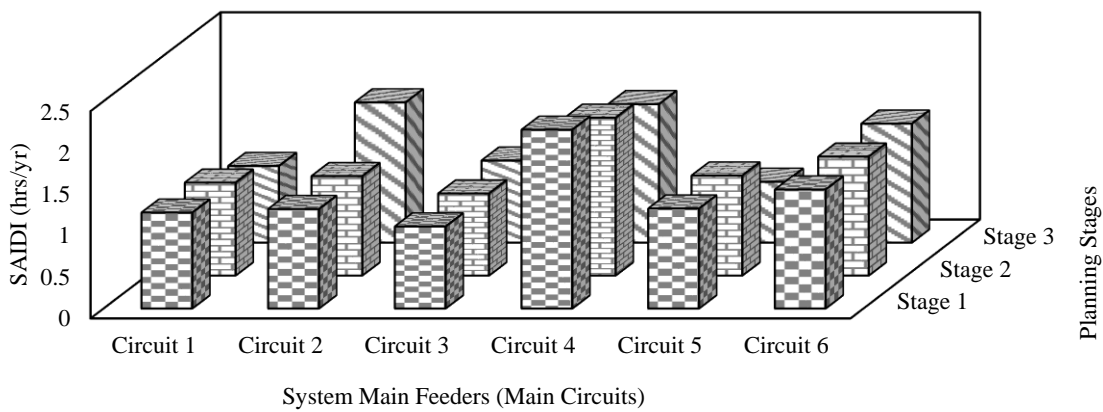


Figure 4-21 SAIDIs for the main feeders following reliability planning for case 2

Figure 4-22 indicates the expected ENS at each stage before and after the planning for case 2. It can be seen that the expected ENS is substantially reduced after the implementation of the proposed planning model. The ENS is decreased from 91.5 MWh/yr to 48.9 MWh/yr for stage 1. For stage 2, the ENS is reduced from 99.7 MWh/yr to 52.9 MWh/yr. The ENS is also decreased for stage 3: from 109.7 MWh/yr to 56 MWh/yr. The average reduction in the ENS for all planning stages is 52 %. The cost of the ENS drops from  $1.48 \times 10^6$  US\$ to  $7.84 \times 10^5$  US\$. Figure 4-23 and Figure 4-24 show the ENS for each bus during each stage prior to and following the planning, respectively.

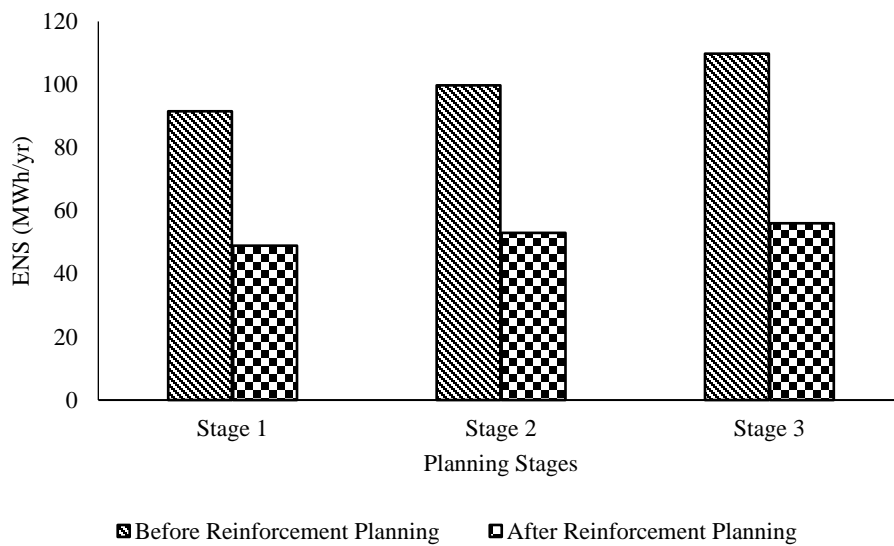


Figure 4-22 Expected ENS at each stage before and after reliability planning for case 2

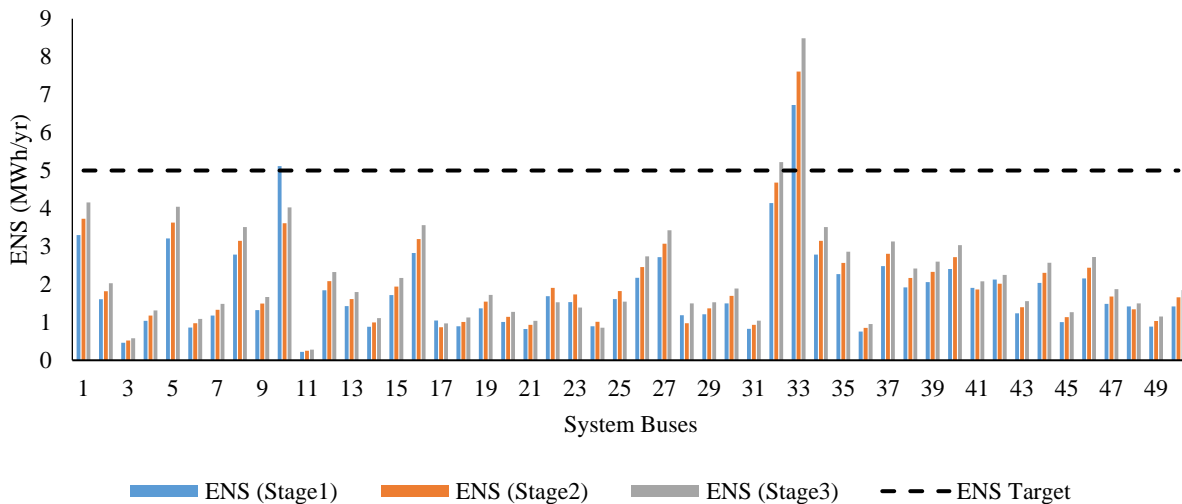


Figure 4-23 ENS for each bus prior to reliability planning for case 2

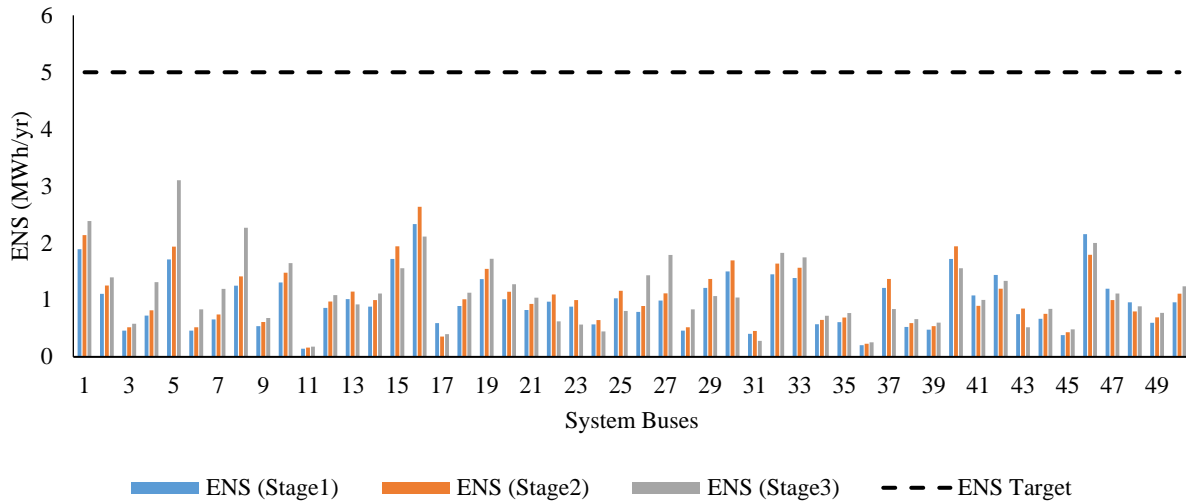


Figure 4-24 ENS for each bus following reliability planning for case 2

The results of this case study reveal that the NPV of the total reliability planning investment cost is equal to  $9.14 \times 10^6$  US\$. Almost 64.2 % of the total cost is for the installation of the tie lines, which represents the largest share of the total expenditure cost. Of the total cost, 27 % goes toward upgrading some of the system feeders. The NPV of the total CENS for the planning horizon represents roughly 8.5 % of the total cost. The cost of NO switches is equal to  $18.8 \times 10^3$  US\$. Table 4-8 lists the NPV of the total planning cost and of all of the costs associated with the reinforcement process.

Table 4-8 NPV of the Associated Planning Costs for Case 2

<b>Reinforcement Planning Costs Breakdown</b>	<b>Cost in dollars (\$)</b>
Cost of energy not served (CENS)	784,010
Cost of tie lines (CTL)	5,868,000
Cost of normally open switches (CNOS)	18,800
Cost of feeder and substation upgrades (CUPG)	2,469,491.9
<b>NPV of total reinforcement planning cost</b>	<b>9,140,302</b>

Compared to case 1, the NPV of this case study is slightly higher than the planning cost for case 1, a discrepancy that can be attributed to the need for several feeder upgrade plans to accommodate the transferred loads. The CDG capacities are somewhat lower in case 2 due to the presence of non-dispatchable DGs and the fact that variations in the power generated from the wind- and PV-based DGs during the restoration process would cause thermal overload for some feeders, especially when the power generated

is low. Even though fewer tie lines and switches are needed in case 2 than in case 1, the higher investments required for line upgrades increase the planning costs in case 2.

#### 4.4.3 Composite Planning Results

The reinforcement planning proposed in this chapter represents an extension of the proposed incentive-based planning model described in Chapter 3, with both components together forming the general planning framework for smart distribution systems as can be seen in Figure 4-1. This section explains the total planning cost for the general planning framework, including the incentive-based planning outlined in the previous chapter and the reliability planning described in this chapter. The total planning cost for case 1 is equal to  $98.27 \times 10^6$  US\$, and the total planning cost for case 2 is equal to  $113.88 \times 10^6$  US\$. Table 4-9 presents the total cost breakdown for the general planning framework.

Table 4-9 Total Planning Cost for the General Planning Framework

<b>NPV of the Required Plan Investments and Planning Costs</b>		<b>Case 1 (Cost in M\$)</b>	<b>Case 2 (Cost in M\$)</b>
<b>Incentive-Based Planning (Chapter 3)</b>	Investment in S/S	0	6.169
	Operation of S/S	0.985	0.892
	Investment in lines	0.552	1.641
	Energy losses cost	0.39	0.35
	Energy purchased from S/S	41.455	39.68
	Energy purchased from CDG	46.047	42.954
	Energy purchased from WDG	0	5.992
	Energy purchased from PVDG	0	7.064
<b>Reliability Planning (Chapter 4)</b>	Cost of energy not served	0.793	0.784
	Cost of tie lines	6.992	5.868
	Cost of normally open switches	0.024	0.019
	Cost of feeder upgrade and substation	1.037	2.469
<b>Total NPV of Planning Cost</b>		<b>98.274</b>	<b>113.88</b>

#### 4.5 Summary

This chapter has presented a reinforcement planning model that will enable distribution systems to enhance their overall system reliability while adhering to regulatory restrictions. The proposed model uses several alternatives including tie lines, NO switches, and feeder and substation upgrade plans in order to improve the nodal reliability indices in the presence of renewable and non-renewable generation sources. Three modes of operation during a contingency are proposed in the model. A successful restoration mode is achieved if at least one restoration path reconnects the disconnected loads with the source without causing any violations of the operational security limits. If the successful restoration mode is not achieved,

successful islanding mode is then assessed based on the requirement that the total generation in the affected area must match the total demand and losses. Failure mode occurs when the conditions for the previous operation modes are unmet. To accommodate the large number of potential system topologies during a contingency, the optimization model is solved using a GA-based metaheuristic technique. The results of the case studies conducted demonstrate the effectiveness of the proposed model with respect to enhancing system reliability and maintaining the reliability indices within permissible boundaries. The dual operation modes during a contingency also provide a more effective contribution to a reduction in the investments required for reliability enhancement.

## **Chapter 5**

# **Distribution System Planning with Reliability Considering Generation Sufficiency for Virtual Dynamic System Zones**

### **5.1 Introduction**

The primary concern of a distribution system planner is to investigate multiple planning options in order to ensure the economical and reliable delivery of power to customers. Because most distributed generation units (DGs) are run by private investors, additional effort is required for the development of innovative models that promote collaboration between those investors and the local distribution company (LDC). As discussed in chapter 3, incentives are a proven strategy for encouraging the positive participation of investors in the planning process. As explained in that chapter, deferment of required asset upgrades, minimization of the total costs of purchased energy, and minimization of operation and maintenance costs comprise the main drivers prompting an LDC to incentivize DG investors. However, the inclusion of system reliability in the planning process would play a key role in determining appropriate DG sizes and locations as well as in establishing new incentives to be offered to investors. Some of the system buses that have proven economically unfeasible for the integration of DGs in previous planning (i.e., the type of planning described in chapter 3) might now become the most favorable locations for DG placement when reliability becomes the main drive for the system planning. Moreover, some system buses would be associated with higher incentives because of their greater contribution to improvements in reliability. For these reasons, this chapter proposes a novel planning model and methodology for addressing the problem of smart distribution system expansion. The new technique includes consideration of system reliability as a main component in the setting of incentivized prices for DG owners.

The aim of the proposed planning model is to maintain reliability measures within allowable limits while minimizing the total planning cost, which comprises the cost of incentivizing DG investors, the cost of substation and feeder upgrades, the cost of energy purchased from the upstream market, and the cost of system operation. For the work presented in this chapter, the enhancement of distribution system reliability is considered to be achieved through increased DG penetration levels (i.e., generation capacity) in the system. An iteration-based methodology has thus been developed with the goal of increasing generation sufficiency in some virtual zones in the system that are subject to reliability issues. This proposed method enables the affected zones to become independent of the main generation sources (i.e., substations) during disturbance events and allows them to operate in islanded mode. The uncertainty caused by variable demand, random DG power output, and unpredicted equipment failure events is addressed and incorporated within the model. Distribution system reliability is assessed through the application of the proposed work

presented in the previous chapter and with consideration of islanded mode of operation during contingencies.

The following are the main contributions of the work presented in this chapter:

- 1- A new iteration-based optimization model is proposed for minimizing the total planning cost for distribution systems while achieving a satisfactory level of reliability.
- 2- A virtual dynamic zoning method is proposed for identifying the areas in the system that provide low levels of service reliability, and for establishing an economical way to overcome this issue through the incentivization of DG investors in order to increase DG penetration and ensure generation sufficiency during outages.
- 3- A new approach for handling DGs in a planning process that includes reliability. This approach is proposed in order to avoid any contravention of operational security boundaries.
- 4- A method for evaluating distribution system reliability that takes into account islanded operation mode during unplanned outages is introduced.

The following sections describe the proposed general planning framework; the problem formulation; the approach to reliability evaluation; and a case study, along with its results. The chapter ends with concluding remarks.

## **5.2 Proposed Distribution System Planning Framework That Includes Consideration of Reliability**

The main goal of the proposed planning framework is to increase DG penetration in a way that benefits the overall system by minimizing the total planning cost while maintaining the reliability indices within regulatory standards. This objective can be achieved if the system is provided with a sufficient generation reserve capacity to enable some load points in the system to operate in islanded mode during a contingency occurrence. However, continuing to increase DG penetration might contravene operational system security boundaries during normal operating states (i.e., causing a high reverse power flow, violating the upper voltage limit, or overloading system feeders). DG capacity is therefore represented by two components: DG capacity for normal operation and DG reserve capacity. Normal-operation DG capacity is the capacity committed to from DGs during the normal state of operation during which no disturbance events occur. DG reserve capacity represents the added capacity required to meet system demand during disturbance events. The total DG capacity installed in the system is thus equal to the summation of the normal-operation DG capacity and the DG reserve capacity. DG variations with respect to discrepancies in the reserve capacity required from each DG results in different incentive prices for DG owners. For reliability enhancement, DG projects with greater reserve capacities are considered more beneficial than others and would therefore

receive higher incentive prices as compensation for their loss of revenue due to their unused capacity during normal operation. As a result, the financial feasibility of a project is guaranteed by the achievement of the minimum acceptable rate of return (MARR) required for each DG project.

The proposed planning framework involves the implementation of a number of steps and models. It begins with the initial planning by solving the optimization model proposed in Chapter 3 in order to obtain the system configuration; the initial asset upgrade plans (i.e., feeder and substation upgrades); and the initial DG locations, sizes, and incentives. It is important to note that only in the initial planning step is DG reserve capacity not considered (i.e., system reserve = 0). Next, the overall reliability of the distribution system is assessed based on consideration of the planning decisions derived from the optimization model. The reliability indices obtained are compared against the reliability threshold enforced by the regulator. If the reliability measures meet the standard limits, the algorithm stops and records the results, meaning that the planning decisions obtained have achieved the minimum planning cost while adhering to the reliability regulations. Otherwise, the model creates virtual system zones that contain only the system buses that fail to meet reliability standards. Any adjacent buses that also violate the reliability limits are included to form one virtual zone. The DG penetration level (i.e., total DG capacity) for each virtual zone is forced to increase by incremental steps through the imposition of penetration-reserve constraints in the planning model. At the same time, the capacity of each DG located outside the virtual zone is fixed based on a fixed DG constraint. The new modified optimization model is executed then; following which, the reliability of the system is re-evaluated. This iterative process is repeated, and the size of each virtual zone (i.e., the total number of buses inside the zone) continues to shrink until the necessary reliability level is achieved for all planning stages. It must be noted that the determination of virtual zones is carried out for each planning stage, which means that these virtual zones might vary from one stage to another depending on the demand and the generation associated with each planning stage. Figure 5-1 presents the flowchart for the proposed planning model that incorporates reliability. It is worth mentioning that due to the variability of wind- and PV-based DG output power, relying on these sources to provide the required reserve when it is needed is impractical; the required reserve capacity is therefore to be furnished by controllable DGs.

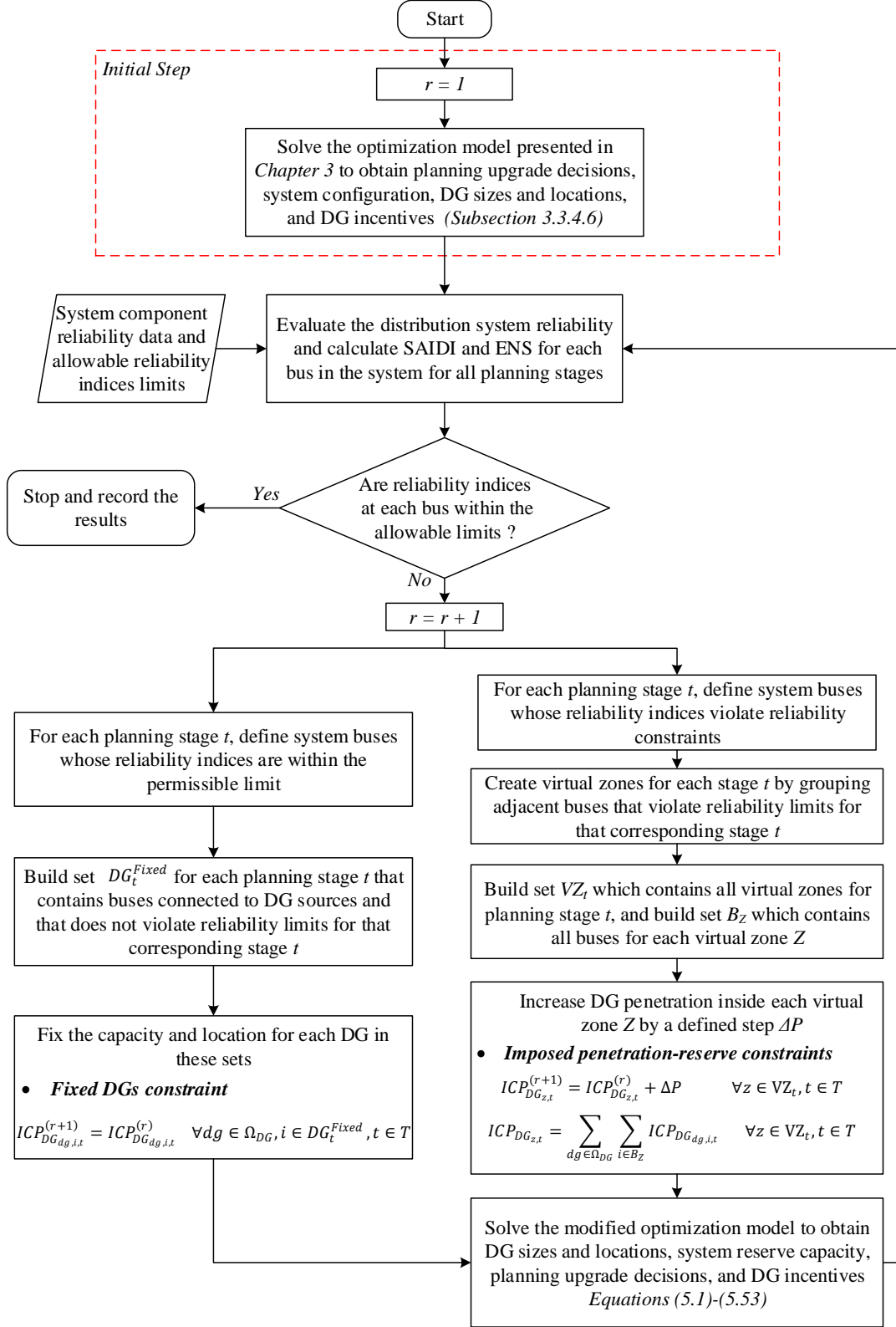


Figure 5-1 Flowchart of the proposed planning model that incorporates reliability

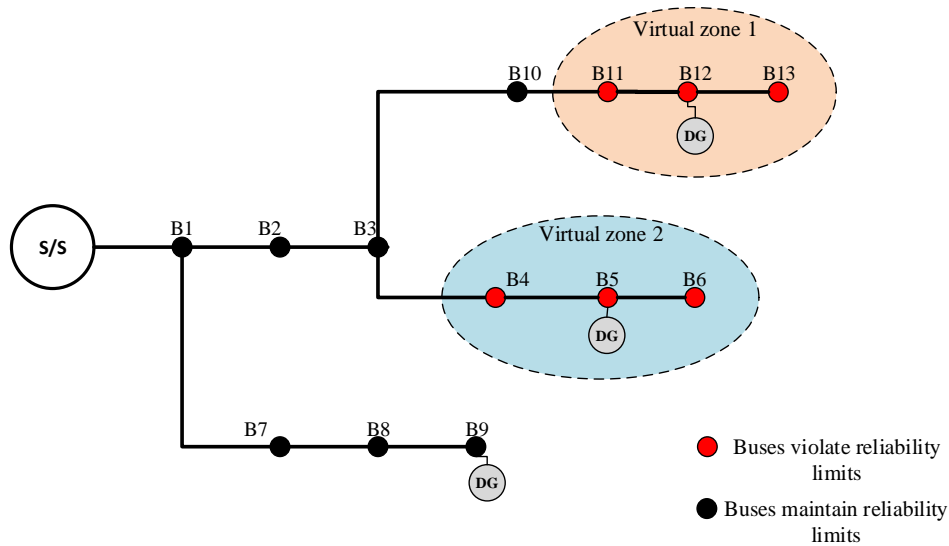


Figure 5-2 Illustrative example of a 13-bus system with virtual zones

The following illustrative example provides a better understating of the way the main sets in the planning model are created. Consider the 13-bus distribution system presented in Figure 5-2. Three DGs are installed after the initial planning model is implemented without consideration of reliability. However, following the execution of the reliability assessment algorithm “not reliability-based planning”, it can be seen that six buses do not comply with the reliability standards. Two virtual zones are therefore created:  $VZ = \{Z1, Z2\}$ . Two new sets are also constructed, each of which contains the buses located in their corresponding virtual zone  $Z$ :  $B_{Z1} = \{B11, B12, B13\}$  and  $B_{Z2} = \{B4, B5, B6\}$ . Any DG connected to those buses is subject to reallocation and/or resizing inside its corresponding zone  $Z$  during the next planning iteration, as mandated by equations (5.32) and (5.33). Another set called  $DG^{Fixed}$  is generated so that it includes the buses that are not subject to resizing and/or reallocation:  $DG^{Fixed} = \{B9\}$ . The DG capacity and location for each bus in this set is fixed during the next iteration of the planning process. If these DG capacities and locations are not fixed, their capacities and locations might change during the next iteration, which would have a negative effect on reliability at those buses and create new virtual zones.

The next sections present the iteration-based optimization model along with the methodology for calculating the system reliability indices.

### 5.3 Mathematical Formulation of Distribution System Planning

This section introduces a linearized distribution system planning model for minimizing the total planning cost. The model comprises the objective function and all of the planning constraints and also includes the reserve capacity required from each DG in order to enhance the reliability indices.

### 5.3.1 The Objective Function

The goal of the planning model is to minimize the total planning cost, including the substation investment (IS), the line investment (IL), the substation operating cost (OS), the cost of energy losses (EL), the cost of energy purchased from the market (PSP), and the cost of energy purchased from the DG investors (PPDG). The mathematical formulation of the objective function is as follows:

$$\text{Min} \sum_{t \in T} \left[ \frac{IS(t) + IL(t) + OS(t) + EL(t) + PSP(t) + PPDG(t)}{(1 + \tau)^{(t-1)K}} \right] \quad (5.1)$$

The detailed mathematical formulations for the components of the objective function are indicated in (5.2) to (5.7).

$$IS(t) = \sum_{i \in \Omega_{BS}} \sum_{u \in \Omega_U} (C_u^{US} \sigma_{i,u,t}) \quad (5.2)$$

$$IL(t) = \sum_{ij \in \Omega_{EL}} \sum_{a \in \Omega_a} C_a^{UF} L_{ij} \beta_{ij,a,t} \quad (5.3)$$

$$OS(t) = \sum_{i \in \Omega_{BS}} \sum_{e \in \Omega_{se}} (S_{G_{i,e,t}}^{Sqr} \alpha_e \varphi \omega) f(\tau, K) \quad (5.4)$$

$$EL(t) = \sum_{ij \in \Omega_{EL}} \sum_{e \in \Omega_{se}} (Pl_{ij,e,t} \alpha_e \varphi \varepsilon) f(\tau, K) \quad (5.5)$$

$$PSP(t) = \sum_{i \in \Omega_{BS}} \sum_{e \in \Omega_{se}} (P_{G_{i,e,t}} \alpha_e \varphi C_{e,t}^E) f(\tau, K) \quad (5.6)$$

$$PPDG(t) = \sum_{dg \in \Omega_{DG}} \sum_{i \in \Omega_N} \sum_{e \in \Omega_{se}} \rho_{dg} (INC_{dg,i,t} OP_{dg,e} \alpha_e \varphi) f(\tau, K) \quad (5.7)$$

The function  $f(\tau, K) = \left( \frac{1 - (1 + \tau)^{-K}}{\tau} \right)$  represents the present value of the annuity function, which calculates the present value of a series of future constant annualized payments at any given time.

### 5.3.2 Planning Model Constraints

The following equations represent the constraints that govern the proposed planning model.

1) **Power Conservation Constraints:** The active and reactive power flow must be balanced at each bus in the system, as expressed in (5.8) and (5.9). The parameter  $\epsilon_{dg} = \left( \frac{\sin(\arccos(pf_{dg}))}{pf_{dg}} \right)$  in (5.9) is used for calculating the DG reactive power as a function of the DG active power based on the DG power factor ( $pf_{dg}$ ).

$$P_{G_{i,e,t}} + \sum_{dg \in \Omega_{DG}} \rho_{dg} O P_{dg,e} P_{DG_{dg,i,t}} - DL_e P_{D_{i,t}} - \sum_{ij \in \Omega_L} P_{ij,e,t} + \sum_{ki \in \Omega_L} P_{ki,e,t} - \sum_{ij \in \Omega_L} Pl_{ij,e,t} = 0 \quad \forall i \in \Omega_N, e \in \Omega_{se}, t \in T \quad (5.8)$$

$$Q_{G_{i,e,t}} + \sum_{dg \in \Omega_{DG}} \rho_{dg} O P_{dg,e} \epsilon_{dg} P_{DG_{dg,i,t}} - DL_e Q_{D_{i,t}} - \sum_{ij \in \Omega_L} Q_{ij,e,t} + \sum_{ki \in \Omega_L} Q_{ki,e,t} - \sum_{ij \in \Omega_L} Ql_{ij,e,t} = 0 \quad \forall i \in \Omega_N, e \in \Omega_{se}, t \in T \quad (5.9)$$

2) **Line Power Flow and Losses Equations:** Equations (5.10) and (5.11) represent the linearized form of active and reactive power flows associated with line  $ij$  as a function of the nodal voltages and nodal voltage angles.

$$P_{ij,e,t} \cong (\Delta V_{i,e,t} - \Delta V_{j,e,t}) G_{ij} - (\delta_{i,e,t} - \delta_{j,e,t}) B_{ij} \quad \forall ij \in \Omega_L, e \in \Omega_{se}, t \in T \quad (5.10)$$

$$Q_{ij,e,t} \cong -(\Delta V_{i,e,t} - \Delta V_{j,e,t}) B_{ij} - (\delta_{i,e,t} - \delta_{j,e,t}) G_{ij} \quad \forall ij \in \Omega_L, e \in \Omega_{se}, t \in T \quad (5.11)$$

The active and reactive power losses in line  $ij$  are computed using equations (5.12) and (5.13), respectively.

$$Pl_{ij,e,t} = R_{ij} S_{ij,e,t}^{sqr} \quad \forall ij \in \Omega_L, e \in \Omega_{se}, t \in T \quad (5.12)$$

$$Ql_{ij,e,t} = X_{ij} S_{ij,e,t}^{sqr} \quad \forall ij \in \Omega_L, e \in \Omega_{se}, t \in T \quad (5.13)$$

3) **Substation Capacity Constraints:** Equation (5.14) ensures that the square of the apparent power drawn from the existing substation is less than or equal to the existing substation capacity plus the results of substation upgrade decisions. The quadratic expressions of the square of the active and reactive power drawn from the substation are linearized using piecewise linearization with sufficient linear segments or  $Y$  blocks as in (5.15). The active and reactive powers drawn from the substations are expressed as sum of series of linear segments  $\Delta P_{G_{i,e,t,y}}$  and  $\Delta Q_{G_{i,e,t,y}}$ , respectively, as shown in (5.16) and (5.17). The discretization variables for the active and reactive power are constrained as indicated in (5.18) and (5.19), while equation (5.20) defines the value used for discretization.

$$S_{G_{i,e,t}}^{sqr} \leq (\overline{S_{G_i}^{max}})^2 + \sum_{u \in \Omega_U} \sum_{t'=1}^t (S_u^{US})^2 \sigma_{i,u,t} \quad \forall i \in \Omega_{ES}, e \in \Omega_{se}, t \in T \quad (5.14)$$

$$S_{G_{i,e,t}}^{sqr} \cong \sum_{y=1}^Y (2y-1) \bar{\Delta}^G \Delta P_{G_{i,e,t,y}} + \sum_{y=1}^Y (2y-1) \bar{\Delta}^G \Delta Q_{G_{i,e,t,y}} \quad \forall i \in \Omega_{SS}, e \in \Omega_{se}, t \in T \quad (5.15)$$

$$P_{G_{i,e,t}} = \sum_{y=1}^Y \Delta P_{G_{i,e,t,y}} \quad \forall i \in \Omega_{SS}, e \in \Omega_{se}, t \in T \quad (5.16)$$

$$Q_{G_{i,e,t}} = \sum_{y=1}^Y \Delta Q_{G_{i,e,t,y}} \quad \forall i \in \Omega_{SS}, e \in \Omega_{se}, t \in T \quad (5.17)$$

$$\Delta P_{G_{i,e,t,y}} \leq \bar{\Delta}^G \quad \forall i \in \Omega_{SS}, e \in \Omega_{se}, t \in T, y \in Y \quad (5.18)$$

$$\Delta Q_{G_{i,e,t,y}} \leq \bar{\Delta}^G \quad \forall i \in \Omega_{SS}, e \in \Omega_{se}, t \in T, y \in Y \quad (5.19)$$

$$\bar{\Delta}^G = \frac{\overline{V}^{Max}}{Y} \max\{S_u^{US}, u \in \Omega_U\} \quad (5.20)$$

4) **Feeder Flow and Thermal Capacity Limits:** Equation (5.21) ensures that the current flow in the feeder is within the thermal capacity of the feeder. If upgrading this feeder is essential, the second term on the right side of (5.21) covers that contingency by replacing the old feeder with the new one. The quadratic expressions of the square of the active and reactive power flow in line  $ij$  are linearized using piecewise linearization with sufficient linear segments or  $Y$  blocks, as in (5.22). The active and reactive power flows in the feeder are expressed using non-negative auxiliary variables in order to obtain their absolute values, as in (5.23) and (5.24). The active and reactive power flows in feeder  $ij$  are also expressed as sum of series of linear segments  $\Delta P_{ij,e,t,y}$  and  $\Delta Q_{ij,e,t,y}$ , respectively, as shown in (5.25) and (5.26). The discretization variables are constrained as indicated in (5.27) and (5.28), while equation (5.29) defines the value used for discretization.

$$S_{ij,e,t}^{sqr} \leq (\overline{S_{ij}^{max}})^2 \left( 1 - \sum_{a \in \Omega_a} \sum_{t'=1}^t \beta_{ij,a,t} \right) + \sum_{a \in \Omega_a} \sum_{t'=1}^t (S_a^P)^2 \beta_{ij,a,t} \quad \forall ij \in \Omega_{EL}, e \in \Omega_{se}, t \in T \quad (5.21)$$

$$S_{ij,e,t}^{sqr} \cong \sum_{y=1}^Y (2y-1) \bar{\Delta}^L \Delta P_{ij,e,t,y} + \sum_{y=1}^Y (2y-1) \bar{\Delta}^L \Delta Q_{ij,e,t,y} \quad \forall ij \in \Omega_L, e \in \Omega_{se}, t \in T \quad (5.22)$$

$$P_{ij,e,t} = P_{ij,e,t}^+ - P_{ij,e,t}^- \quad \forall ij \in \Omega_L, e \in \Omega_{se}, t \in T \quad (5.23)$$

$$Q_{ij,e,t} = Q_{ij,e,t}^+ - Q_{ij,e,t}^- \quad \forall ij \in \Omega_L, e \in \Omega_{se}, t \in T \quad (5.24)$$

$$P_{ij,e,t}^+ + P_{ij,e,t}^- = \sum_{y=1}^Y \Delta P_{ij,e,t,y} \quad \forall ij \in \Omega_L, e \in \Omega_{se}, t \in T \quad (5.25)$$

$$Q_{ij,e,t}^+ + Q_{ij,e,t}^- = \sum_{y=1}^Y \Delta Q_{ij,e,t,y} \quad \forall ij \in \Omega_L, e \in \Omega_{se}, t \in T \quad (5.26)$$

$$0 \leq \Delta P_{ij,e,t,y} \leq \bar{\Delta}^L \quad \forall ij \in \Omega_L, e \in \Omega_{se}, t \in T, y \in Y \quad (5.27)$$

$$0 \leq \Delta Q_{ij,e,t,y} \leq \bar{\Delta}^L \quad \forall ij \in \Omega_L, e \in \Omega_{se}, t \in T, y \in Y \quad (5.28)$$

$$\bar{\Delta}^L = \frac{\bar{V}^{Max}}{Y} \max\{S_a^P, a \in \Omega_a\} \quad (5.29)$$

5) **Bus Voltage Constraint:** The deviation of the voltage magnitude from the nominal voltage in each bus must be kept within permissible voltage limits (-0.05,0.05), as set out in (5.30):

$$\underline{\Delta V_i}^{Min} \leq \Delta V_{i,e,t} \leq \bar{\Delta V_i}^{Max} \quad \forall i \in \Omega_N, e \in \Omega_{se}, t \in T \quad (5.30)$$

6) **DG Penetration-Reserve Constraints:** Equation (5.31) defines the total installed capacity of the DG where the first term presents the DG capacity committed for normal operation, and the second term represents the reserve capacity required.

$$ICP_{DG_{dg,i,t}} = P_{DG_{dg,i,t}} + P_{DG_{dg,i,t}}^{Res} \quad \forall dg \in \Omega_{DG}, i \in \Omega_N, t \in T \quad (5.31)$$

Because the proposed planning model is an iteration-based model, during the next iteration  $r+1$ , the total installed DG capacity at each virtual zone  $Z$  must be equal to the total DG capacity in that zone  $Z$  for the current iteration  $r$  plus a predefined incremental step  $\Delta P$ , as mandated by (5.32).  $\Delta P$  is assumed to be 0.1 MW. The total DG capacity for a virtual zone  $Z$  is equal to the summation of the installed DG capacities for all buses located in that corresponding virtual zone  $Z$ , as described in equation (5.33).

$$ICP_{DG_{z,t}}^{(r+1)} = ICP_{DG_{z,t}}^{(r)} + \Delta P \quad \forall z \in VZ_t, t \in T \quad (5.32)$$

$$ICP_{DG_{z,t}} = \sum_{dg \in \Omega_{DG}} \sum_{i \in B_Z} ICP_{DG_{dg,i,t}} \quad \forall z \in VZ_t, t \in T \quad (5.33)$$

Set  $VZ_t$  contains the virtual zones for stage  $t$ . Therefore, for example, if the planning stages are chosen to be three as is the case in this work, three virtual sets are then constructed, one for each stage:  $VZ_1, VZ_2$ , and  $VZ_3$ .  $B_z$  is a set that contains the buses located in zone  $z$  in which  $z \in VZ_t$ .

Due to the variability of wind- and PV-based DG output power, relying on these sources to provide the required reserve when it is needed is impractical; therefore, the required reserve capacity is furnished by controllable DGs, as set out in (5.34).

$$ICP_{DG_{dg,z,t}}^{(r+1)} = ICP_{DG_{dg,z,t}}^{(r)} + \Delta P \quad \forall dg = CDG, z \in VZ_t, t \in T \quad (5.34)$$

7) **Fixed DG Capacity Constraint:** The capacity and location of DGs for any bus located outside the virtual zones must be fixed for the next iteration, as prescribed by (5.35). If these DG capacities and locations are not fixed, their capacities and locations might change during the next iteration, which would negatively affect reliability at these buses and create new virtual zones.

$$ICP_{DG_{dg,i,t}}^{(r+1)} = ICP_{DG_{dg,i,t}}^{(r)} \quad \forall dg \in \Omega_{DG}, i \in DG_t^{Fixed}, t \in T \quad (5.35)$$

8) **Total DG Penetration Constraints:** The maximum DG capacity that can be connected to any bus in the network is constrained as specified in (5.36). Equation (5.37) ensures that the penetration level of each renewable-based DG conforms with environmental regulatory requirements.

$$\sum_{dg \in \Omega_{DG}} \rho_{dg} ICP_{DG_{dg,i,t}} \leq \overline{DG}_i \quad \forall i \in \Omega_N, t \in T \quad (5.36)$$

$$\sum_{dg \in \Omega_{DG} \setminus \{CDG\}} \sum_{i \in \Omega_N} \rho_{dg} ICP_{DG_{dg,i,t}} \geq \mu \sum_{i \in \Omega_N} P_{D,i,t} \quad \forall t = LT \quad (5.37)$$

9) **DG Dynamic Constraint:** The dynamic constraint denoted in (5.38) governs cumulative DG capacities between planning stages:

$$ICP_{DG_{dg,i,t}} - ICP_{DG_{dg,i,t+1}} \leq 0 \quad \forall dg \in \Omega_{DG}, i \in \Omega_N, t \in T \quad (5.38)$$

10) **DG Discretization Constraints:** DGs are most often sized in a discrete manner to represent the capacities available in the market. Equation (5.39) defines DG capacity as a multiplication of an integer variable by the available DG sizes. The available DG unit ratings are assumed to be set out in 0.1 MW steps.

$$ICP_{DG_{dg,i,t}} = n_{dg,i,t} \times 0.1MW \quad \forall dg \in \Omega_{DG}, i \in \Omega_N, t \in T \quad (5.39)$$

where  $n_{dg,i,t}$  is an integer variable.

11) **DG Investment and Utilization Constraints:** Equations (5.40) and (5.41) determine the total DG investment and operating costs, and equation (5.42) calculates the total benefit accruing to the DG investors when they sell the energy produced at the incentive price.

$$INVC_{dg,i,t}^{DG} = \rho_{dg} \left( ICP_{DG_{dg,i,t}} - ICP_{DG_{dg,i,t-1}} \right) C_{dg}^{IDG} \quad \forall dg \in \Omega_{DG}, i \in \Omega_N, t \in T \quad (5.40)$$

$$OPC_{dg,i,e,t}^{DG} = \rho_{dg} \left( OP_{dg,e} P_{DG_{dg,i,t}} C_{dg}^{ODG} \alpha_e \varphi \right) f(IRR_{dg,i}, K) \quad \forall dg \in \Omega_{DG}, i \in \Omega_N, e \in \Omega_{se}, t \in T \quad (5.41)$$

$$BEN_{dg,i,e,t}^{DG} = \rho_{dg} \left( OP_{dg,e} INC_{dg,i,t} \alpha_e \varphi \right) f(IRR_{dg,i}, K) \quad \forall dg \in \Omega_{DG}, i \in \Omega_N, e \in \Omega_{se}, t \in T \quad (5.42)$$

The incentive cost  $INC_{dg,i,t}$  is formulated as a product of DG output power during normal operation and the bus-wise incentive price (BWIP). This non-linear form is linearized using the binary expansion method, as in (5.43) to (5.45):

$$INC_{dg,i,t} = \underline{\gamma} P_{DG_{dg,i,t}} + \Delta\gamma \sum_{h=1}^{H+1} 2^{(h-1)} d_{h,dg,i,t} \quad \forall dg \in \Omega_{DG}, i \in \Omega_N, t \in T \quad (5.43)$$

$$0 \leq P_{DG_{dg,i,t}} - d_{h,dg,i,t} \leq M(1 - v_{h,dg,i}) \quad \forall dg \in \Omega_{DG}, i \in \Omega_N, t \in T, h = 1, 2, \dots, H+1 \quad (5.44)$$

$$0 \leq d_{h,dg,i,t} \leq M v_{h,dg,i} \quad \forall dg \in \Omega_{DG}, i \in \Omega_N, t \in T, h = 1, 2, \dots, H+1 \quad (5.45)$$

where  $v_{h,dg,i}$  is a binary variable;  $\Delta\gamma = \frac{\bar{\gamma} - \underline{\gamma}}{W}$ ,  $W = 2^H$  for some non-negative integer value  $H$ ; and  $\bar{\gamma}$  and  $\underline{\gamma}$  are the maximum and minimum incentive prices, respectively.

Equations (5.46) to (5.48) compute the present values of DG installation and operating costs as well as the DG benefit at each bus in the network. These values are then used for calculating the economic metrics of the DG projects.

$$PVINV_{dg,i}^{DG} = \sum_{t \in T} INVC_{dg,i,t}^{DG} (1 + IRR_{dg,i})^{-(t-1)K} \quad \forall dg \in \Omega_{DG}, i \in \Omega_N \quad (5.46)$$

$$PVOPE_{dg,i}^{DG} = \sum_{t \in T} \sum_{e \in \Omega_{se}} OPC_{dg,i,e,t}^{DG} (1 + IRR_{dg,i})^{-(t-1)K} \quad \forall dg \in \Omega_{DG}, i \in \Omega_N \quad (5.47)$$

$$PVBEN_{dg,i}^{DG} = \sum_{t \in T} \sum_{e \in \Omega_{se}} BEN_{dg,i,e,t}^{DG} (1 + IRR_{dg,i})^{-(t-1)K} \quad \forall dg \in \Omega_{DG}, i \in \Omega_N \quad (5.48)$$

To guarantee the financial feasibility of a project, equation (5.49) ensures that the net present value (NPV) of all cash flows equals zero, given that the internal rate of return (IRR) of each project is equal to the MARR of that corresponding project.

$$PVINV_{dg,i}^{DG} + PVOPE_{dg,i}^{DG} - PVBEN_{dg,i}^{DG} = 0 \quad \forall dg \in \Omega_{DG}, i \in \Omega_N \quad (5.49)$$

12) **LDC Investment Decision Constraints:** Equations (5.50) and (5.51) ensure that any upgrade or construction decision for a feeder/substation must be executed once over the planning horizon.

$$\sum_{u \in \Omega_U} \sum_{t \in T} \sigma_{i,u,t} \leq 1 \quad \forall i \in \Omega_{ES} \quad (5.50)$$

$$\sum_{a \in \Omega_a} \sum_{t \in T} \beta_{ij,a,t} \leq 1 \quad \forall ij \in \Omega_{EL} \quad (5.51)$$

13) **Binary Variables Constraints:**

$$\sigma_{i,u,t} \in \{0,1\} \quad \forall i \in \Omega_{ES}, u \in \Omega_U, t \in T \quad (5.52)$$

$$\beta_{ij,a,t} \in \{0,1\} \quad \forall ij \in \Omega_{EL}, a \in \Omega_a, t \in T \quad (5.53)$$

## 5.4 Distribution System Reliability Evaluation

This section explains the calculation of the distribution system reliability indices, which must fall within regulatory reliability thresholds. After the planning decisions have been determined from each iteration the reliability assessment must be performed. In the work presented in this chapter, the way that this assessment is applied in order to restore any disconnected load due to any contingency is to isolate the buses located downstream from the faulty part and to permit islanded operation mode. If the generation units inside the islanded area are capable of matching the demand and losses of that island, then the islanding process succeeds, thus improving system reliability. N-1 contingency analysis is implemented in order to evaluate system performance and behavior under any contingency and then to calculate the reliability measures. Algorithm 1 demonstrates the main steps to be performed for the computation of the system reliability indices when DGs are incorporated.

---

**Algorithm 1** Distribution System Reliability Assessment with DGs

---

- 1: Set  $S$  counter to 1.
- 2: Set  $C$  counter to 1.
- 3: Isolate the buses located downstream from the faulty section due to contingency  $C$ .
- 4: For current scenario  $S$ , check whether the generation units in this created island  $I$  (if any) meet the island demand and losses  $\{P_{DG_I} \geq P_{D_I} + P_{l_I}\}$ .
- 5: Set index  $I_{SI_{i,S,C}} = 1$  for all buses located in the formed island  $I$  if the condition in **Step 4** is fulfilled. Otherwise, set  $I_{SI_{i,S,C}} = 0$ .
- 6: If all contingencies are examined ( $C = TC$ ), go to **Step 7**. Otherwise, set  $C = C+I$ , and go to **step 3**.
- 7: If all scenarios are evaluated ( $S = TS$ ), go to **Step 8**. Otherwise, set  $S = S+I$ , and go to **Step 2**.
- 8: Calculate reliability indices using equations (5.54) to (5.61).

**End**

---

#### 5.4.1 Calculating the Probability of Success in Islanded Operation Mode

The probability of a load point  $i$  to be in isolated mode due to contingency  $c$  is calculated as follows:

$$P_{i,c}^{isolated} = \begin{cases} \frac{\lambda_c r_c}{NH} & \text{if } c \in SP_i \\ 0 & \text{if } c \notin SP_i \end{cases} \quad (5.54)$$

where the set  $SP_i$  contains all the components in the series path between the load point  $i$  and the main source (i.e., distribution substation),  $\lambda_c$  is the failure rate of component  $c$ ,  $r_c$  is the repair rate of component  $c$ , and  $NH$  is the total hours in a calendar year (i.e.,  $NH = 8760$ ).

The probability of load point  $i$  to be working in a successful operating mode after contingency  $c$  has taken place is dependent mainly on the probability of load point  $i$  to be in isolated mode due to contingency  $c$  and the probability of successful islanding for that contingency  $c$ . Given that the probability of a load point being in isolated mode and the probability of a successful operating mode are independent, the probability of a successful operating mode for bus  $i$  due to contingency  $c$  can be calculated by multiplying these two probabilities, as expressed in the following equation.

$$P_{i,c}^{success} = P_{i,c}^{isolated} \times P_{i,c}^{SI} \quad (5.55)$$

where  $P_{i,c}^{SI}$  is the probability of successful islanding for bus  $i$  due to contingency  $c$ .

The probability of successful islanding  $P_{i,c}^{SI}$  is dependent primarily on the probability of the scenario that

incorporates renewable-based DG output power and power demand. For an operating scenario  $s$ , if the generation units inside the formed island are able to match the demand and losses of that island, then probability of this scenario will participate for reducing the unavailability time of the load points inside this island. Therefore,  $P_{i,c}^{SI}$  is equal to the summation of the probabilities of occurrence for the scenarios in which the islanding condition is satisfied; otherwise, the probability is considered to be zero.

$$P_{i,c}^{SI} = \sum_{s=1}^{Ts} P_s I_{SI_{i,s,c}} \quad (5.56)$$

where  $I_{SI_{i,s,c}}$  is an index for the successful islanding of bus  $i$  due to contingency  $c$  in operating scenario  $s$ ,  $P_s$  is the probability of occurrence of scenario  $s$ , and  $Ts$  is the total number of operating scenarios.

#### 5.4.1 Calculating the Unavailability of Load Points and the Reliability Indices

Following the calculation of the probability of a successful operating mode for each load point  $i$  due to any contingency  $c$ , the unavailability of load point  $i$  is calculated using the following equation:

$$U_i = \sum_{c \in SP_i} (\lambda_c r_c - P_{i,c}^{success} \times NH) \quad (5.57)$$

The improvement in the annual unavailability of load point  $i$  due to successful islanding is represented by the second part of the above equation:  $(P_{i,c}^{success} \times NH)$ .

Total reliability indices for each bus in the system can be calculated using the following equations:

$$SAIDI_i = \sum_{c \in SP_i} (\lambda_c r_c - P_{i,c}^{success} \times NH) \quad (5.58)$$

$$ENS_i = L_{a(i)} \sum_{c \in SP_i} (\lambda_c r_c - P_{i,c}^{success} \times NH) \quad (5.59)$$

Distribution system reliability indices are then calculated from the following equations:

$$SAIDI = \frac{\sum_i U_i N_i}{\sum_i N_i} \quad (5.60)$$

$$ENS = \sum_i L_{a(i)} U_i \quad (5.61)$$

where  $N_i$  is the number of customers at load point  $i$ ,  $L_{a(i)}$  is the average load connected to load point  $i$ , and  $NH$  is the number of hours in a calendar year ( $NH = 8760$ ).

## 5.5 Case Study and Numerical Results

To verify the efficacy of the proposed planning model, a case study was conducted. The details and results of the study are provided in this section.

### 5.5.1 Distribution System Under Study

The full data for the system used in this study and all of the planning parameters are reported in section 3.4.1; all of the reliability data employed are reported in section 4.4.1.

### 5.5.2 Results and Discussion

The case study addressed in this chapter involves both controllable and renewable-based DGs (i.e., wind DGs (WDGs) and photo-voltaic DG (PVDG) systems). The planning outcome from the first iteration results in the allocation and sizing of the CDGs at 15 buses in the system. As well, WDGs and PVDGs are allocated at 10 different buses: five buses for each type. However, after the overall reliability of the system has been calculated, it can be observed that 26 buses in stage 1, 24 buses in stage 2, and 22 buses in stage 3 fail to comply with the reliability standard: their system average interruption duration indices (SAIDIs) are higher than 2.5 h/yr, as shown in Figure 5-3. As a result, these buses that violate reliability limits create eight virtual zones in stage 1 and six virtual zones each in stages 2 and 3. During the next planning iteration, the total DG capacity inside each virtual zone is thus enforced to increase in order to enhance the reliability of those zones. It can be observed that located outside these zones are six DGs, whose capacities are therefore fixed during the following iteration. Figure 5-3 indicates the SAIDI at each node in the system for all planning stages. Figure 5-4, Figure 5-5, and Figure 5-6 illustrate the creation of virtual zones during stage 1, stage 2, and stage 3, respectively.

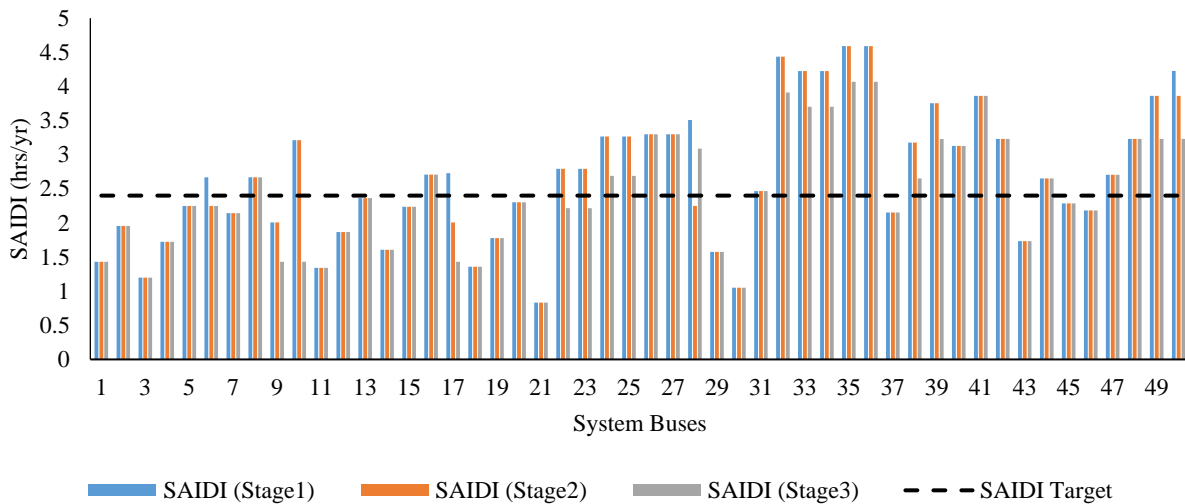


Figure 5-3 SAIDI at each bus in the system following the initial planning

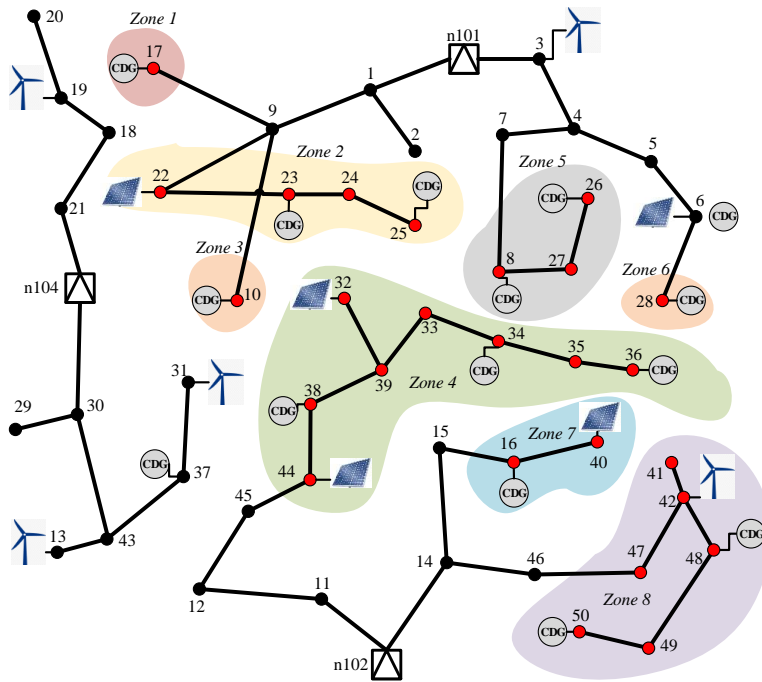


Figure 5-4 Zones formed during stage 1 for buses not adhering to reliability standards

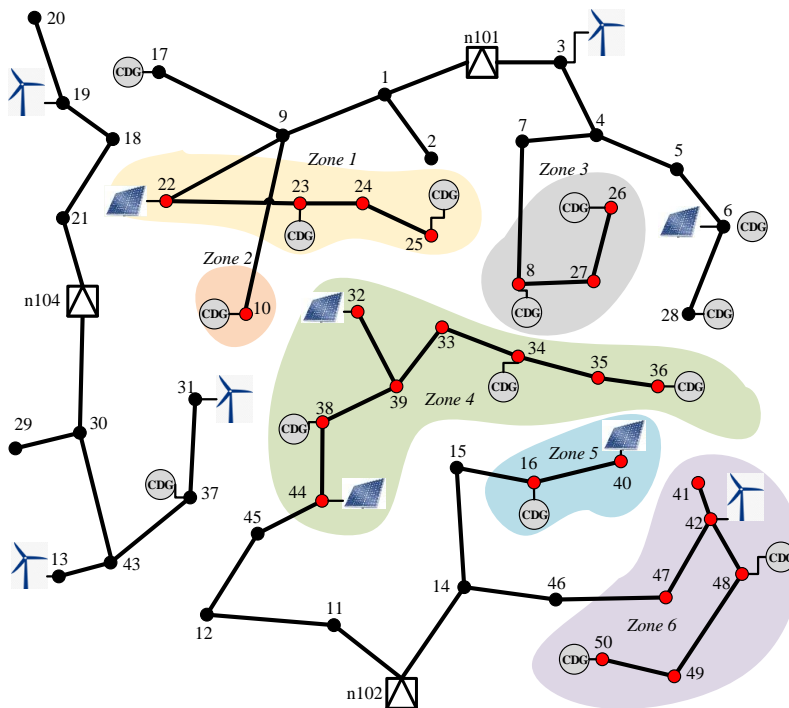


Figure 5-5 Zones formed during stage 2 for buses not adhering to reliability standards

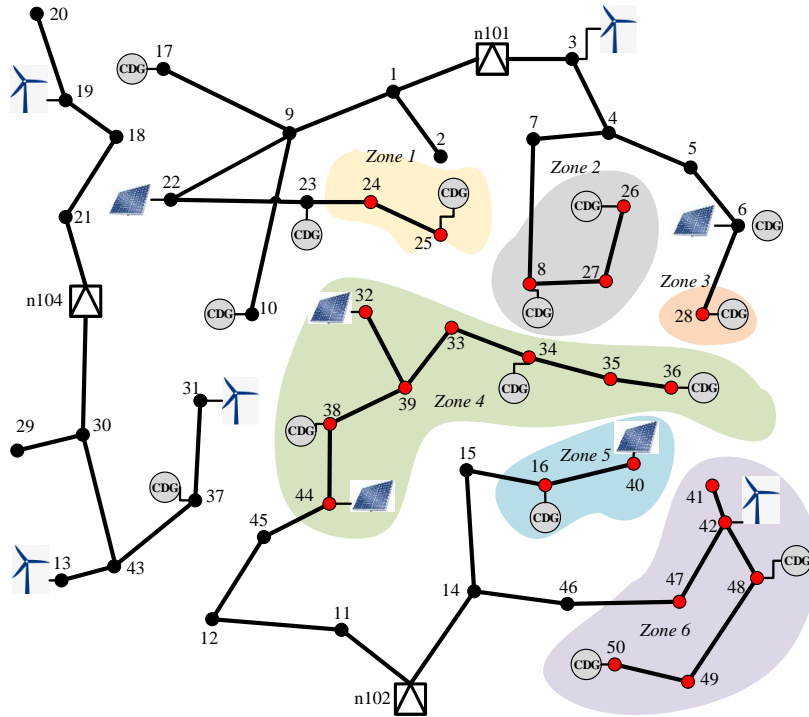


Figure 5-6 Zones formed during stage 3 for buses not adhering to reliability standards

Table 5-1 lists sample iterations of the planning process and the generated sets to be fed into the updated optimization planning model for stage 1 only. It can be seen that, for the first iteration, all eight zones are included in the set of virtual zones and that all six DGs located outside the zones are fixed and included in the  $DG_1^{Fixed}$  set. As is evident from Table 5-1, the reliability issues associated with Z3 and Z6 are resolved during the third iteration when the DG penetration level inside each of these zones is increased by 0.2 MW. Z3 and Z6 are therefore excluded from the set of virtual zones at the beginning of iteration 4, and the DG capacities at buses 10 and 28 are fixed and included in the set  $DG_1^{Fixed}$  for the fourth iteration. Table 5-1 and Figure 5-7 also reveal that the size of Z2 is truncated following the fourth planning iteration, when the SAIDI and energy not supplied (ENS) at buses 22 and 23 are reduced and kept within the limit. The size of the DG located at bus 23 is consequently fixed and added to the  $DG_1^{Fixed}$  set, and buses 22 and 23 are removed from the  $B_{Z2}$  set for the fifth iteration. As can be seen in Figure 5-7, after the implementation of 23 iterations, no additional virtual zones are created since all of the reliability targets have been achieved.

Table 5-1 Sample Iterations of the Planning Process and the Sets Created for Stage 1 Only

Iter.#	$VZ_1$	$B_Z$	$DG_1^{Fixed}$
1	{Z1,Z2,Z3,Z4,Z5,Z6,Z7,Z8}	$B_{Z1}=\{17\}$ , $B_{Z2}=\{22,23,24,25\}$ , $B_{Z3}=\{10\}$ , $B_{Z4}=\{44,38,39,32,33,34,35,36\}$ , $B_{Z5}=\{8,27,26\}$ , $B_{Z6}=\{28\}$ , $B_{Z7}=\{16,40\}$ , $B_{Z8}=\{47,41,42,48,49,50\}$	{3,6,13,19,31,37}
4	{Z1,Z2,Z4,Z5,Z7,Z8}	$B_{Z1}=\{17\}$ , $B_{Z2}=\{22,23,24,25\}$ , $B_{Z4}=\{44,38,39,32,33,34,35,36\}$ , $B_{Z5}=\{8,27,26\}$ , $B_{Z7}=\{16,40\}$ , $B_{Z8}=\{47,41,42,48,49,50\}$	{3,6,13,19,31,37,10,28}
5	{Z1,Z2,Z4,Z5,Z7,Z8}	$B_{Z1}=\{17\}$ , $B_{Z2}=\{24,25\}$ , $B_{Z4}=\{44,38,39,32,33,34,35,36\}$ , $B_{Z5}=\{8,27,26\}$ , $B_{Z7}=\{16,40\}$ , $B_{Z8}=\{47,41,42,48,49,50\}$	{3,6,13,19,31,37,10,28,23}
7	{Z4,Z5,Z7,Z8}	$B_{Z4}=\{44,38,39,32,33,34,35,36\}$ , $B_{Z5}=\{8,27,26\}$ , $B_{Z7}=\{16,40\}$ , $B_{Z8}=\{47,41,42,48,49,50\}$	{3,6,13,19,31,37,10,28,23,17,25}
10	{Z4,Z5,Z7,Z8}	$B_{Z4}=\{44,38,39,32,33,34,35,36\}$ , $B_{Z5}=\{26\}$ , $B_{Z7}=\{16,40\}$ , $B_{Z8}=\{47,41,42,48,49,50\}$	{3,6,13,19,31,37,10,28,23,17,25,8}
11	{Z4,Z7,Z8}	$B_{Z4}=\{44,38,39,32,33,34,35,36\}$ , $B_{Z7}=\{16,40\}$ , $B_{Z8}=\{47,41,42,48,49,50\}$	{3,6,13,19,31,37,10,28,23,17,25,8,26}
15	{Z4,Z7,Z8}	$B_{Z4}=\{44,38,39,32,33,34,35,36\}$ , $B_{Z7}=\{16,40\}$ , $B_{Z8}=\{49,50\}$	{3,6,13,19,31,37,10,28,23,17,25,8,26,48}
17	{Z4,Z7}	$B_{Z4}=\{39,32,33,34,35,36\}$ , $B_{Z7}=\{16,40\}$	{3,6,13,19,31,37,10,28,23,17,25,8,26,48,38,50}
21	{Z4,Z7}	$B_{Z4}=\{35,36\}$ , $B_{Z7}=\{16,40\}$	{3,6,13,19,31,37,10,28,23,17,25,8,26,48,38,50,34}
23	{Z7}	$B_{Z7}=\{16,40\}$	{3,6,13,19,31,37,10,28,23,17,25,8,26,48,38,50,34,36}
24	{ $\varphi$ }	NA	{3,6,13,19,31,37,10,28,23,17,25,8,26,48,38,50,34,36,16}

Figure 5-7 presents a graphical representation of the changes in the dimensions of the virtual zones for the different iterations only for stage 1 of the planning horizon. Z1 and Z2 conform to the reliability limits following the sixth planning iteration whereas 22 iterations are required for the reliability issues in zone Z4 to be resolved. The dimension, or size, of Z4 is truncated after iterations 5 and 20. Twenty-three iterations are needed for the problem in Z7 to be resolved, which is attributable to the small DG capacity obtained during the initial planning iteration.

	Z1	Z2	Z3	Z4	Z5	Z6	Z7	Z8
Iter.# 1	17	22 23 24 25	10	44 38 32 39 33 34 35 36	8 27 26	28	16 40	47 41 42 48 49 50
Iter.# 4	17	22 23 24 25	10	44 38 32 39 33 34 35 36	8 27 26	28	16 40	47 41 42 48 49 50
Iter.# 5	17	22 23 24 25	10	44 38 32 39 33 34 35 36	8 27 26	28	16 40	47 41 42 48 49 50
Iter.# 7	17	22 23 24 25	10	44 38 32 39 33 34 35 36	8 27 26	28	16 40	47 41 42 48 49 50
Iter.# 10	17	22 23 24 25	10	44 38 32 39 33 34 35 36	8 27 26	28	16 40	47 41 42 48 49 50
Iter.# 11	17	22 23 24 25	10	44 38 32 39 33 34 35 36	8 27 26	28	16 40	47 41 42 48 49 50
Iter.# 15	17	22 23 24 25	10	44 38 32 39 33 34 35 36	8 27 26	28	16 40	47 41 42 48 49 50
Iter.# 17	17	22 23 24 25	10	44 38 32 39 33 34 35 36	8 27 26	28	16 40	47 41 42 48 49 50
Iter.# 21	17	22 23 24 25	10	44 38 32 39 33 34 35 36	8 27 26	28	16 40	47 41 42 48 49 50
Iter.# 23	17	22 23 24 25	10	44 38 32 39 33 34 35 36	8 27 26	28	16 40	47 41 42 48 49 50
Iter.# 24	17	22 23 24 25	10	44 38 32 39 33 34 35 36	8 27 26	28	16 40	47 41 42 48 49 50

Figure 5-7 Graphical representation of the changes in zone dimensions during different iterations

Figure 5-8, Figure 5-9, and Figure 5-10 indicate the CDG locations, normal operation capacity, and reserve capacity at each planning stage, and Table 5-2 shows the total cumulative installed CDG capacity at each bus for each planning stage along with the incentive prices offered to CDG owners. Because the CDGs at buses 16 and 34 have the greatest capacities and the highest reserve margin, these two DGs receive higher incentive pricing than other DGs. The incentive prices vary depending on the reserve capacity required from each CDG. Buses that have a lower reserve capacity would receive smaller incentives than ones with a higher reserve capacity. It can be observed that the model attempts to increase utilization of a DG during normal operation as much as possible (by increasing normal DG commitment during normal operation and minimizing the reserve) in order to reduce the incentive costs, unless such an increase contravenes operation limits or has a negative effect on the objective function by increasing losses and feeder upgrade investments. Since the DGs at buses 6 and 37 are located outside the virtual zones for all stages, no reserve capacity is provided from these DGs, as indicated in Figure 5-8, Figure 5-9, and Figure 5-10. Bus 28 violates the reliability limits during two time stages (i.e., stage 1 and stage 3), and therefore the reserve capacity of the CDG connected to this bus is obtained for these two stages only.

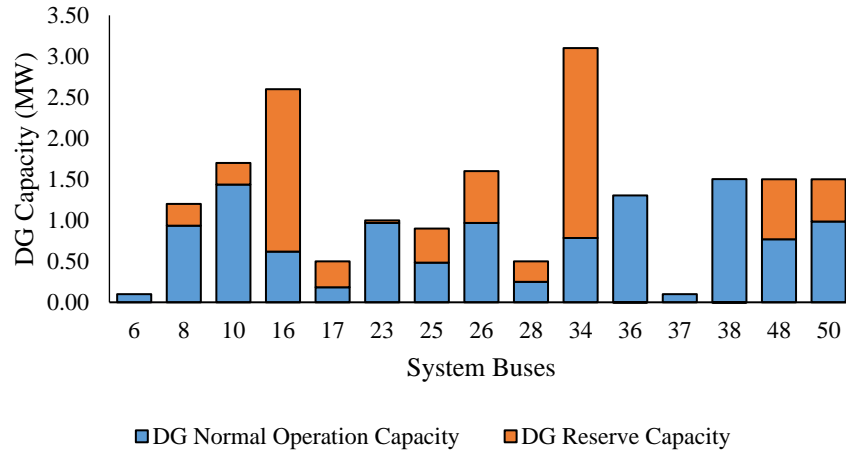


Figure 5-8 Total DG capacity including both normal operating and reserve capacities for stage 1

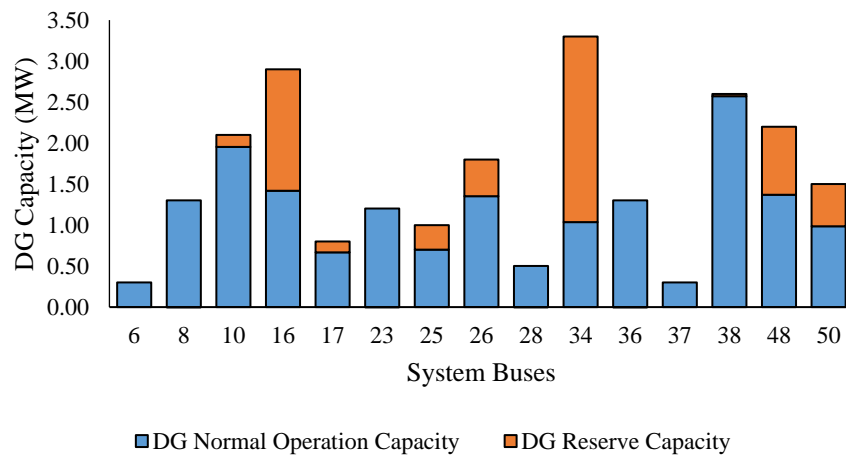


Figure 5-9 Total DG capacity including both normal operating and reserve capacities for stage 2

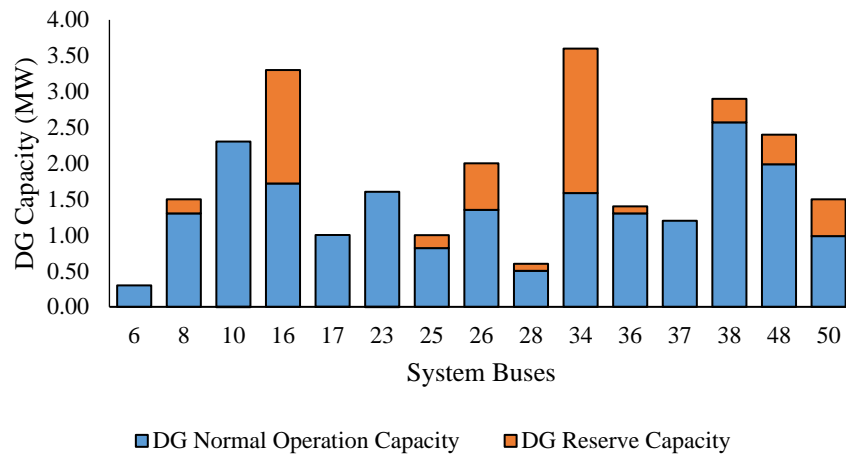


Figure 5-10 Total DG capacity including both normal operating and reserve capacities for stage 3

The CDG upgrade capacity required for the second and third stages also affects the determination of the incentives. When the installed capacity of the CDGs increases during the final stages, incentive prices increase, as can be observed with respect to buses 6 and 37. Neither CDG in these buses has a reserve capacity, yet the installed capacity for bus 37 in the last stage is increased by 0.9 MW compared to the second stage. The incentive price at bus 37 is therefore increased to ensure the feasibility of the project.

Table 5-2 Cumulative CDG Capacity at Each Bus and the Corresponding Incentive

Bus	6	8	10	16	17	23	25	26	28	34	36	37	38	48	50	
DG Installed Capacity (MW)	Stage 1	0.1	1.2	1.7	2.6	0.5	1	0.9	1.6	0.5	3.1	1.3	0.1	1.5	1.5	1.5
	Stage 2	0.3	1.3	2.1	2.9	0.8	1.2	1	1.8	0.5	3.3	1.3	0.3	2.6	2.2	1.5
	Stage 3	0.3	1.5	2.3	3.3	1	1.6	1	2	0.6	3.6	1.4	1.2	2.9	2.4	1.5
Incentive (\$/MWh)	44.5	45	44.3	64	49.3	44	49.4	49.3	48	71	43.4	45.9	45.6	51.1	49	

Table 5-3 lists the installed capacity of renewable-based DGs for all stages along with the incentive prices. All wind- and PV-based DGs are installed during stage 1, which means that the capacities for all planning stages remain the same. By the last stage, the total renewable-based DG penetration is almost 15 % of the demand. It was found that WDG owners would receive 67.4 \$ for each MWh generated, based on which, the MARRs of their projects are guaranteed. In the case of PVDG owners, 87.5 \$ for each MWh generated would ensure the profitability of their projects.

Table 5-3 Installed Capacities of Renewable-Based DGs and the Associated Incentives

Bus	3	13	19	31	42	Bus	6	22	32	40	44
WDG Installed Capacity* (MW)	0.1	1.3	1.0	1.9	0.3	PVDG Installed Capacity* (MW)	2.0	0.6	1.2	0.8	0.1
Incentive (\$/MWh)	67.4	67.4	67.4	67.4	67.4	Incentive (\$/MWh)	87.5	87.5	87.5	87.5	87.5

\* The capacity installed for each bus is equal at all planning stages.

Figure 5-11 illustrates the total CDG capacity for normal operation and the reserve required for each planning stage. It can be noted that CDG penetration increases following the increase in demand at each stage. The total required reserve capacities from CDGs for stage 1, stage 2, and stage 3 are 7.7 MW, 6.2 MW, 6.1 MW, respectively. These reserve capacities, which are in line with normal CDG operating capacities, are required in order to stay within system reliability limits.

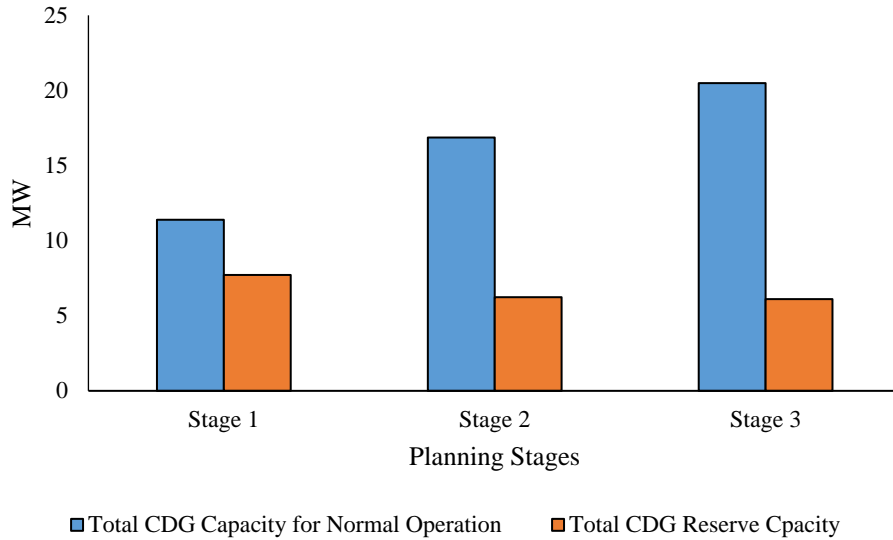


Figure 5-11 Total CDG installed capacity at the end each planning stage

Table 5-4 shows the required upgrade plans for each stage. The LDC should upgrade feeder 30-43 using alternative A3 and should upgrade feeder 37-43 using alternative A2, both in stage 1. Most of the upgrade plans are deferred to the final stage, as indicated in Table 5-4. Using transformer alternative U1, substations S1 and S2 must be upgraded during stage 3. Feeders S1-1 and 18-21 should also be upgraded using alternative A3, and feeder 18-19 requires an upgrade during the final stage with feeder alternative A3 in order to handle the increased power drawn from substation S1 during the last stage.

Table 5-4 LDC Investment Upgrade Plans for Each Stage

Stage	LDC Upgrade Plans
1	30-43 (A3), 37-43 (A2)
2	NA
3	S1 (U1), S2 (U1), S1-1 (A3), 18-19 (A2), 18-21 (A3)

As can be observed from Figure 5-12 and Figure 5-13, the SAIDI and ENS at each bus in the system are reduced and kept within the reliability obligations since the SAIDIs do not exceed the threshold of 2.5 h/yr, and the ENSs are lower than 5 MWh/yr for all planning time stages. Figure 5-14 presents the total ENS for the system for all planning stages both before and after reliability is taken into account. The planning model achieved almost a 23 % reduction in the total ENS at each stage of the planning period.

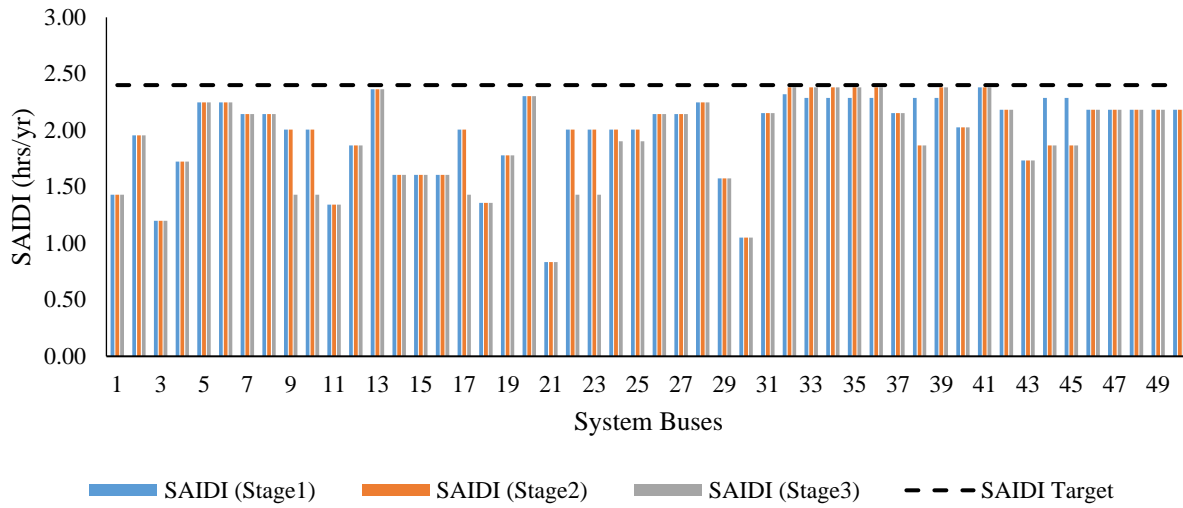


Figure 5-12 SAIDI at each bus following planning that includes consideration of reliability

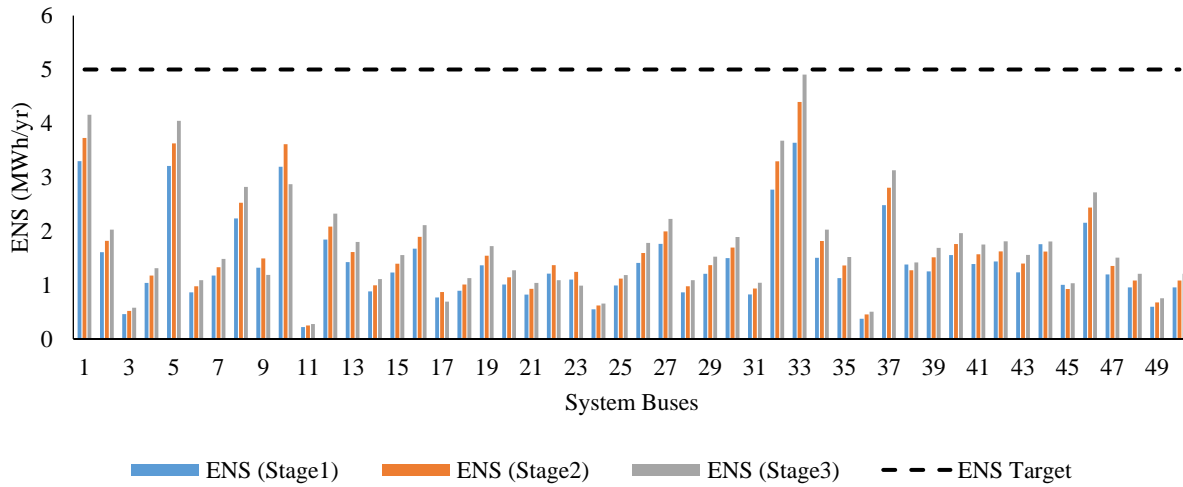


Figure 5-13 ENS at each bus following planning that includes consideration of reliability

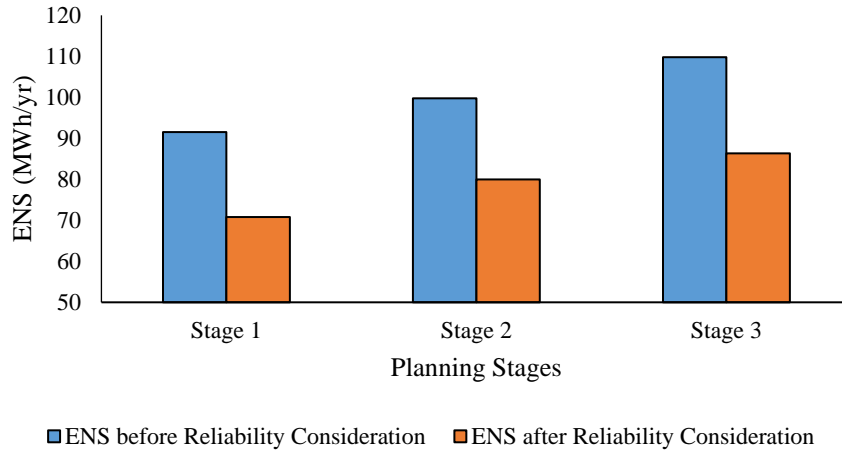


Figure 5-14 ENS before and after consideration of reliability

Figure 5-15 illustrates the differences between the incentives provided to DG owners prior to and following consideration of reliability. It has been observed that DGs that participate extensively in the enhancement of system reliability (in terms of providing a high generation reserve capacity in the system) would receive higher incentive prices, as in the case of buses 16 and 34. Incentive prices for buses 6 and 37 remain unchanged since they have no reserve capacity, and their entire DG capacity will be dispatched during normal operation.

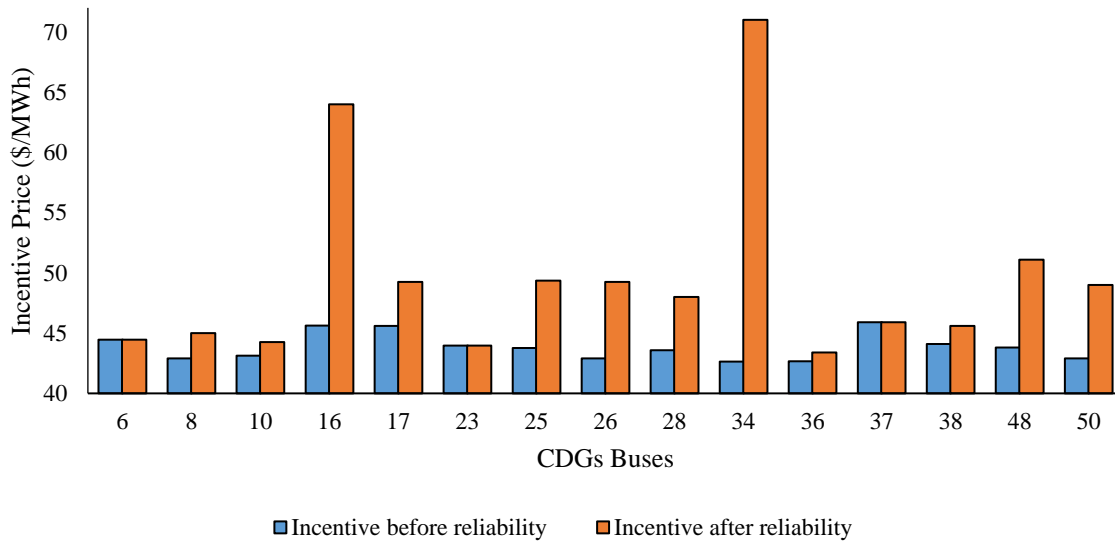


Figure 5-15 Incentives provided to DG owners before and after consideration of reliability

The results reveal that the NPV of the total planning cost when system reliability is considered is  $111.3 \times 10^6$  US\$. Table 5-5 indicates the NPV of the total planning cost incurred by the LDC, with a breakdown of all associated installation and operation costs. Almost 43.5 % of the planning cost represents the cost of purchasing energy from CDG owners. It can be seen that the cost of purchasing power from CDG owners increased by  $5.55 \times 10^6$  US\$ compared to the solution produced from the first iteration, a result that can be attributed to the presence of the reserve capacity in the system. This incremented cost (i.e.,  $5.55 \times 10^6$  US\$) must therefore be distributed to the CDG owners in order to compensate them for their power unutilized during normal operation so as to assure the profitability of their projects. The cost of purchasing power from the market represents approximately 35.6 % of the total cost, and almost 11.7 % of the total planning cost is paid to incentivize renewable-based DG owners. The NPV of the substation upgrades and feeder investment plans is  $7.655 \times 10^6$  US\$. The ENS cost is reduced from the  $1.48 \times 10^6$  US\$ indicated in the initial planning results to  $1.17 \times 10^6$  US\$.

Table 5-5 NPV of the Required Plan Investments and Planning Costs

<b>Breakdown of Planning Costs</b>	<b>(Cost in M\$)</b>
Investment in S/S	6.169
Operation of S/S	0.891
Investment in lines	1.486
Energy losses cost	0.356
Energy purchased from S/S	39.663
Energy purchased from CDG	48.509
Energy purchased from WDG	5.992
Energy purchased from PVDG	7.064
Cost of ENS	1.17
<b>Total NPV of Planning Costs</b>	<b>111.303</b>

## 5.6 Summary

This chapter has proposed an iteration-based optimization model for distribution system planning that includes consideration of reliability. The model is targeted at minimizing the total planning costs incurred by the LDC, which comprises substation and feeder upgrade investments, the cost of energy purchased from the market, the costs of energy purchased from DG owners, the cost of energy losses, and operating costs. The model also produces results that improve system reliability by ensuring that the reliability indices (i.e., SAIDI and ENS) at each system bus remain within the regulatory permissible limits. The chapter also introduced the proposed concept of dynamic virtual zones as a means of increasing DG penetration in

specific zones in the system that exhibit reliability issues, thereby enhancing reliability in those weak areas. The DG capacity is split into two components: normal DG operating capacity and reserve DG capacity, so that any contravention of the operational security limits can be avoided when DG penetration increases. The proposed model has been tested using a 53-bus distribution system; the results confirm its usefulness and effectiveness. The model minimizes total planning costs while achieving the required level of system reliability. The incentive prices offered to the DG owners guarantee the profitability of their projects. To compensate them for their energy unutilized during normal operation, DGs with a greater reserve capacity receive higher incentive prices than ones that have a lower reserve capacity. Employing the proposed model results in lower planning costs for enhanced system reliability compared to the use of the conventional alternatives discussed in Chapter 4.

## Chapter 6

### Concluding Remarks

#### 6.1 Summary and Conclusions

The significant paradigm shift toward smart grids in recent years and the accompanying myriad technologies and regulations have made distribution system planning a very complex and challenging undertaking. The primary goal of the work presented in this thesis was to develop new planning and reliability models that can help distribution systems respond to these changes and provide local distribution companies (LDCs) with economical and reliable solutions. The motivation behind the work presented in this thesis and the research objectives are discussed thoroughly in Chapter 1.

Chapter 2 has provided a review of the fundamentals of power distribution systems, the primary purpose of power distribution planning, and the factors that affect the planning process. Traditional planning is compared with modern distribution system planning, which encompasses distributed generation units (DGs) and includes consideration of reliability. The review also summarizes the literature that addresses both traditional and modern models and techniques employed for handling the distribution planning problem. Definitions of DGs and their power scales as well as an overview of wind and PV technologies are presented. The chapter closes with an introduction to the evaluation of reliability in distribution systems.

Chapter 3 has presented a novel incentive-based distribution system planning (IDSP) model that incorporates the active participation of DG investors in the expansion problem. The proposed model establishes a bus-wise incentive program (BWIP), and based on several economic indices, determines appropriate incentives for the LDC to offer DG investors so that the profitability of their investments will be ensured. Using the proposed IDSP, the LDC can identify the least costly solution from a combination of the proposed BWIP and traditional expansion options, which enables the LDC to coordinate future expansion projects effectively with DG investors. The uncertainty associated with the intermittent nature of wind speed, solar irradiance, and system demand is discussed in this chapter; this issue is treated probabilistically in the model. A number of linearization methods are examined with respect to their suitability for converting the IDSP into a mixed integer linear programming (MILP) model.

A reinforcement planning model that enables a distribution system to enhance its overall system reliability while adhering to regulatory restrictions has been introduced in Chapter 4. The proposed model looks at several alternatives, including tie lines, normally open (NO) switches, and feeder and substation upgrade plans as a way of improving nodal reliability indices in the presence of renewable and non-renewable generation sources. Three modes of operation during contingencies are analyzed and incorporated into the

reliability assessment model. Due to the complexity inherent in the nature of the problem, the proposed model is solved using a GA-based metaheuristic technique that can accommodate the large number of potential system topologies associated with the occurrence of a contingency.

Chapter 5 has described an iteration-based optimization model for distribution system planning that includes consideration of reliability issues. The concept of dynamic virtual zones is proposed as a means of increasing DG penetration in specific system zones that exhibit reliability issues, thus enhancing reliability in those weak areas. The model minimizes the total planning cost to be incurred by the LDC, which comprises substation and feeder upgrade investments, the cost of purchasing energy from the market, the costs of purchasing energy from DG owners, the cost of energy losses, and operating costs. Reliability indices (i.e., the system average interruption duration index (SAIDI) and the energy not supplied (ENS)) at each system bus are kept within the permissible regulatory limits. To avoid any contraventions of the operational security limits in the event of increases in DG penetration, DG capacity is split into two components: normal DG operating capacity and reserve DG capacity.

The following are the main conclusions that can be drawn from the work presented here:

- It is more beneficial for LDCs to direct DG investors to integrate their projects at specific locations in the grid and to provide incentives for only those buses. Keeping the incentives identical for all system buses does not necessarily help LDCs reduce their planning costs because some system buses make no contribution to the deferment of upgrade plans or to the enhancement of reliability. Such buses should therefore be removed from the incentive programs.
- Since several factors hinder LDCs from investing in DGs, coordinated planning between LDCs and DG investors will always lead to a win-win resolution that satisfies all parties. Lack of coordination may result in the rejection of DG investors' applications or may affect their expected profitability. It can also lead to additional, avoidable expenditures on the part of the LDCs.
- Utilities are always concerned about financial liquidity. Purchasing and operating DGs will definitely reduce the amount of cash available to those utilities. The proposed incentive-based planning can be seen as enabling implicit purchases of DGs by the utilities through installment loans, which keep cash still available and reduce risk.
- The incentive-based planning model is sensitive to the minimum acceptable rate of return (MARR) required by DG investors. As long as the MARR increases, the costs for the LDC also increase accordingly. LDCs should therefore carefully design their system with an MARR that satisfies both parties.

- DGs have proven roles in providing a system with numerous technical and economic advantages; however, LDCs should not rely on DGs as the only planning alternative but should also investigate additional options for achieving the least-cost planning outcome.
- Of critical importance is the necessity of incorporating the stochastic nature of the system demand and the power output from renewable DGs. If these factors are not taken into account, the most likely operating scenarios for the system will fail to be investigated, resulting in the possibility of overestimated or underestimated investment plans.
- Observations include the fact that wind- and PV-based DGs would receive higher incentive prices than controllable DGs, a discrepancy that is due to the power fluctuations associated with these DGs which result in lower capacity factors. It is strongly recommended that incentive prices for wind- and PV-based DGs be increased in order to guarantee the feasibility of those types of projects.
- A number of factors affect the determination of incentive prices: the MARR required by the DG investors, the technology used for the DGs, and the installed capacities of these projects as well as the installation time needed.
- DGs play a key role in the enhancement of distribution system reliability because of their ability to mitigate or eliminate violations of system operational security constraints as a result of the restoration process and also because of their ability to feed all or part of the loads in the islands formed due to component failures.
- From a reliability perspective, designing the system with consideration of the reliability indices at each bus is more effective than designing the network to minimize the overall system indices. A design targeted at the overall system indices can mean that some system buses will still be subject to reliability issues. Higher design resolution is thus required.
- It is strongly recommended that any system reliability analysis address multiple operation modes under contingencies. Examining both the restoration process and islanding modes during outages increases the chance of minimizing the length of the unavailability time and hence of improving system reliability. Relying on only one of these modes can lead to greater expenditures for reinforcing the system.
- The proposed method of defining virtual zones that fail to adhere to reliability standards provides system planners with valuable insight that enables them to scrutinize these areas closely and investigate appropriate decisions for enhancing reliability. Further findings reveal that this process would reduce the computational burden and produce excellent results.
- The incorporation of reliability constraints engenders remarkable changes in the incentive prices offered to DG investors. DGs that contribute significantly to the enhancement of reliability indices

(because of having greater reserve capacities) would receive higher incentive prices than would those who provide a lesser contribution.

- It was found that increasing DG penetration in the grid with the goal of improving system reliability and that incentivizing DG investors with different prices depending on their contribution to reliability result in lower planning costs compared with employing traditional options. Using the proposed model described in Chapter 5 increases the reserve capacity in the system, which could then be used for other operational applications.
- During the planning process, splitting the DG capacity into two components, namely, DG normal operating capacity and DG reserve capacity, has a positive effect on the achievement of a feasible solution that also avoids any contraventions of the operational security limits when DG penetration is increased.

## 6.2 Research Contributions

The primary contributions of the research presented in this thesis can be summarized as follows:

- A novel IDSP model is proposed. The new model helps LDCs determine necessary expenditures while also implementing a bus-wise incentive program to encourage the integration of DG projects at specific buses that will benefit the system. The model determines the time, location, capacity, technology, and incentive price for each DG investment. It also identifies required upgrade plans to be undertaken by the LDC as well as their implementation time, including upgrading existing substations, constructing new substations, upgrading existing lines, building new lines, and/or modifying the network topology.
- The proposed incentive-based model can replace most regulations whose provisions apply identical incentive prices for all buses in order to help energy regulators and LDCs set up incentive programs based on their requirements and system needs. The proposed BWIP can replace the Feed-In Tariff (FIT) program, which is currently being phased out in Ontario.
- The most popular financial-based indicators for DG investors, including internal rate of return, profit investment ratio, and discounted payback period, are adopted in the proposed model so as to incorporate profitability analysis for DG investors. A number of linearization techniques are also presented for transforming the proposed model from a mixed integer nonlinear programming (MINLP) model into an MILP model, in which convergence to optimality is guaranteed.
- A comprehensive probabilistic methodology has been developed for modeling the intermittent behavior of both fluctuating demand and the variable power generated from wind- and PV-based DGs. The probabilistic model is treated in such a way that it can be incorporated into distribution system planning problems.

- A proposed planning methodology facilitates the determination of the optimal allocation of tie lines and NO switches so as to improve system reliability while maintaining reliability indices within permissible boundaries in the presence of controllable and renewable-based DGs. The required upgrade capacities of feeders and substations are also obtained. The proposed probabilistic mathematical model takes into account the variations in system demand and DG output power as well as the uncertainty associated with system components.
- For evaluating the reliability of distribution systems, the proposed two hierarchical levels for system operation under contingencies allow the load points affected by the fault to be restored from either restoration paths in the system or from an islanded operating mode. Analyzing both modes during outages increases the chances of reducing the downtime and thereby improving system reliability.
- Distribution system restoration algorithm is presented in this thesis that takes advantages of the existing DGs in the system and at the same time aims to meet certain reliability target.
- A new iteration-based optimization model is proposed for minimizing the total planning cost of distribution systems while achieving a satisfactory level of reliability. In the proposed model, a dynamic zoning method has been developed to ensure generation sufficiency in defined areas in the system that exhibit poor service reliability. A further proposal is an economical technique for overcoming this issue through the incentivization of DG investors. To avoid violations of the operational security limits, the model introduces a new representation of DG capacity.
- Also introduced is an analytical model for evaluating distribution system reliability with controllable and renewable-based DGs and with consideration of islanding and/or restoration modes of operation during unplanned outages.

### **6.3 Directions for Future Research**

The following studies can be conducted as an extension of the work presented in this thesis:

- The problem of incentive-based distribution system planning can be extended to include new parties, including energy storage system (ESS) owners and demand response (DR) aggregators. ESS and DR are new technologies in smart distribution systems that can provide substantial benefits for a system. These benefits should be quantified and explored.
- The adoption of plug-in electric vehicles (PEVs) in distribution systems and their impact on distribution system planning should be investigated. A PEV charging load is characterized by a high degree of uncertainty that should be analyzed and incorporated into planning models in order to identify the most economic and reliable solutions.

- The impact of PEVs and ESS on the reliability analysis of distribution systems should be examined. The model presented in Chapter 4 is efficient and can be utilized for quantifying the effect of these emerging technologies with respect to reliability indices.

## Bibliography

- [1] Annual Energy Outlook, "US Energy Information Administration; Washington. DC." 2013.
- [2] R. C. Lotero and J. Contreras, "Distribution system planning with reliability," *IEEE Trans. Power Del.*, vol. 26, (4), pp. 2552-2562, 2011.
- [3] International Renewable Energy Agency (IRENA), "Renewable capacity highlights," 2018.
- [4] Ontario Power Authority, "Supply mix advice and recommendations report," 2005.
- [5] Ontario Power Authority, "Feed-in tariff program," *Internet: [Http://Fit.Powerauthority.on.ca/what-Feed-Tariff-Program](http://Fit.Powerauthority.on.ca/what-Feed-Tariff-Program)*, 2010.
- [6] Ontario Power Authority, "Micro Feed-In Tariff Program: Program Overview," *Toronto, Ontario*, 2010.
- [7] Independent Electricity System Operator, "A progress report on contracted electricity supply: Q1-2018," IESO, June 16. 2018.
- [8] Independent Electricity System Operator (IESO), "Feed-in Tariff program," 2017.
- [9] G. W. Ault, C. E. Foote and J. R. McDonald, "Distribution system planning in focus," *IEEE Power Engineering Review*, vol. 22, (1), pp. 60-62, 2002.
- [10] A. A. Chowdhury and D. O. Koval, "Current practices and customer value-based distribution system reliability planning," *IEEE Trans. Ind. Appl.*, vol. 40, (5), pp. 1174-1182, 2004.
- [11] K. R. Larry Kaufmann, "SERVICE RELIABILITY STANDARDS IN ONTARIO: ANALYSIS OF OPTIONS," September, 2013.
- [12] I. Ziari *et al*, "Optimal distribution network reinforcement considering load growth, line loss, and reliability," *Power Systems, IEEE Transactions On*, vol. 28, (2), pp. 587-597, 2013.
- [13] R. E. Brown and M. Marshall, "Budget constrained planning to optimize power system reliability," *IEEE Trans. Power Syst.*, vol. 15, (2), pp. 887-892, 2000.
- [14] T. Lowder *et al*, "Historical and Current US Strategies for Boosting Distributed Generation," *Golden, CO: National Renewable Energy Laboratory*, 2015.
- [15] L. F. Ochoa and G. P. Harrison, "Minimizing energy losses: Optimal accommodation and smart operation of renewable distributed generation," *IEEE Trans. Power Syst.*, vol. 26, (1), pp. 198-205, 2011.
- [16] Ontario Energy Board, "Discussion paper on distributed generation (DG) and rate treatment of DG: Appendix B-survey of DG policy," 2007.
- [17] T. Gönen, *Electric Power Distribution System Engineering*. McGraw-Hill New York, 1986.
- [18] L. Aniti, "Electricity distribution investments rose over the past two decades. Today in Energy," October 24. 2014.

- [19] Guenther, O., Mandatova, P., Lorenz, G., "Electricity distribution investments: What regulatory framework do we need," May. 2014.
- [20] W. H. Kersting, *Distribution System Modeling and Analysis*. CRC press, 2012.
- [21] T. Ackermann, G. Andersson and L. Söder, "Distributed generation: a definition," *Electr. Power Syst. Res.*, vol. 57, (3), pp. 195-204, 2001.
- [22] R. Viral and D. Khatod, "Optimal planning of distributed generation systems in distribution system: A review," *Renewable and Sustainable Energy Reviews*, vol. 16, (7), pp. 5146-5165, 2012.
- [23] Y. Atwa, "Distribution system planning and reliability assessment under high DG penetration," 2010.
- [24] M. A. Alotaibi and M. Salama, "An Incentive-Based Multistage Expansion Planning Model for Smart Distribution Systems," *IEEE Trans. Power Syst.*, 2018.
- [25] Y. Atwa *et al.*, "Optimal renewable resources mix for distribution system energy loss minimization," *IEEE Trans. Power Syst.*, vol. 25, (1), pp. 360-370, 2010.
- [26] P. A. Lynn, *Electricity from Sunlight: An Introduction to Photovoltaics*. John Wiley & Sons, 2011.
- [27] W. El-Khattam, "Power delivery system planning implementing distributed generation," *University of Waterloo, Waterloo*, 2004.
- [28] H. Willis and J. Northcote-green, "Comparison of several computerized distribution planning methods," *IEEE Transactions on Power Apparatus and Systems*, vol. 1, (PAS-104), pp. 233-240, 1985.
- [29] G. L. Thompson and D. Wall, "A branch and bound model for choosing optimal substation locations," *Power Apparatus and Systems, IEEE Transactions On*, (5), pp. 2683-2688, 1981.
- [30] E. Míguez *et al.*, "An improved branch-exchange algorithm for large-scale distribution network planning," *Power Systems, IEEE Transactions On*, vol. 17, (4), pp. 931-936, 2002.
- [31] W. Ouyang *et al.*, "Distribution network planning considering distributed generation by genetic algorithm combined with graph theory," *Electric Power Components and Systems*, vol. 38, (3), pp. 325-339, 2010.
- [32] Ž Popović, V. D. Kerleta and D. Popović, "Hybrid simulated annealing and mixed integer linear programming algorithm for optimal planning of radial distribution networks with distributed generation," *Electr. Power Syst. Res.*, vol. 108, pp. 211-222, 2014.
- [33] A. Cossi *et al.*, "Primary power distribution systems planning taking into account reliability, operation and expansion costs," *Generation, Transmission & Distribution, IET*, vol. 6, (3), pp. 274-284, 2012.
- [34] H. Falaghi *et al.*, "DG integrated multistage distribution system expansion planning," *International Journal of Electrical Power & Energy Systems*, vol. 33, (8), pp. 1489-1497, 2011.

- [35] R. Adams and M. Laughton, "Optimal planning of power networks using mixed-integer programming. part 1: Static and time-phased network synthesis," *Electrical Engineers, Proceedings of the Institution Of*, vol. 121, (2), pp. 139-147, 1974.
- [36] E. Masud, "An interactive procedure for sizing and timing distribution substations using optimization techniques," *Power Apparatus and Systems, IEEE Transactions On*, (5), pp. 1281-1286, 1974.
- [37] D. M. Crawford and S. B. Holt Jr, "A mathematical optimization technique for locating and sizing distribution substations, and deriving their optimal service areas," *Power Apparatus and Systems, IEEE Transactions On*, vol. 94, (2), pp. 230-235, 1975.
- [38] K. Hindi and A. Brameller, "Design of low-voltage distribution networks: A mathematical programming method," in *Proceedings of the Institution of Electrical Engineers*, 1977, pp. 54-58.
- [39] M. Ponnavaikko and K. Rao, "Optimal distribution system planning," *Power Apparatus and Systems, IEEE Transactions On*, (6), pp. 2969-2977, 1981.
- [40] N. Ponnavaikko, K. Rao and S. Venkata, "Distribution system planning through a quadratic mixed integer programming approach," *Power Delivery, IEEE Transactions On*, vol. 2, (4), pp. 1157-1163, 1987.
- [41] T. Fawzi, K. Ali and S. El-Sobki, "A new planning model for distribution systems," *Power Apparatus and Systems, IEEE Transactions On*, (9), pp. 3010-3017, 1983.
- [42] B. Foote, "Distribution-system planning using mixed-integer programming," in *Generation, Transmission and Distribution, IEE Proceedings C*, 1981, pp. 70-79.
- [43] T. Gönen and I. Ramirez-Rosado, "Review of distribution system planning models: A model for optimal multistage planning," in *Generation, Transmission and Distribution, IEE Proceedings C*, 1986, pp. 397-408.
- [44] T. Gönen and I. J. Ramirez-Rosado, "Optimal multi-stage planning of power distribution systems," *Power Delivery, IEEE Transactions On*, vol. 2, (2), pp. 512-519, 1987.
- [45] M. El-Kady, "Computer-aided planning of distribution substation and primary feeders," *Power Apparatus and Systems, IEEE Transactions On*, (6), pp. 1183-1189, 1984.
- [46] D. Sun *et al*, "Optimal distribution substation and primary feeder planning via the fixed charge network formulation," *Power Apparatus and Systems, IEEE Transactions On*, (3), pp. 602-609, 1982.
- [47] I. J. Ramirez-Rosado and T. Gönen, "Pseudodynamic planning for expansion of power distribution systems," *Power Systems, IEEE Transactions On*, vol. 6, (1), pp. 245-254, 1991.
- [48] H. Temraz and M. Salama, "A comprehensive long-term power distribution system expansion planning model," *Electrical and Computer Engineering, Canadian Journal Of*, vol. 23, (4), pp. 147-153, 1998.
- [49] M. Blanchard *et al*, "Experience with optimization software for distribution system planning," *Power Systems, IEEE Transactions On*, vol. 11, (4), pp. 1891-1898, 1996.

- [50] E. Yeh and H. Tram, "Information integration in computerized distribution system planning," in *Transmission and Distribution Conference, 1996. Proceedings., 1996 IEEE*, 1996, pp. 602-607.
- [51] P. Paiva *et al*, "Integral planning of primary-secondary distribution systems using mixed integer linear programming," *Power Systems, IEEE Transactions On*, vol. 20, (2), pp. 1134-1143, 2005.
- [52] R. H. Fletcher and K. Strunz, "Optimal distribution system horizon planning–part I: formulation," *Power Systems, IEEE Transactions On*, vol. 22, (2), pp. 791-799, 2007.
- [53] K. Aoki *et al*, "New approximate optimization method for distribution system planning," *Power Systems, IEEE Transactions On*, vol. 5, (1), pp. 126-132, 1990.
- [54] K. Nara *et al*, "Multi-year expansion planning for distribution systems," *Power Systems, IEEE Transactions On*, vol. 6, (3), pp. 952-958, 1991.
- [55] K. Nara *et al*, "Distribution systems expansion planning by multi-stage branch exchange," *Power Systems, IEEE Transactions On*, vol. 7, (1), pp. 208-214, 1992.
- [56] V. Quintana, H. Temraz and K. Hipel, "Two-stage power-system-distribution-planning algorithm," in *Generation, Transmission and Distribution, IEE Proceedings C*, 1993, pp. 17-29.
- [57] S. Najafi *et al*, "A framework for optimal planning in large distribution networks," *Power Systems, IEEE Transactions On*, vol. 24, (2), pp. 1019-1028, 2009.
- [58] M. Lavorato *et al*, "A constructive heuristic algorithm for distribution system planning," *Power Systems, IEEE Transactions On*, vol. 25, (3), pp. 1734-1742, 2010.
- [59] A. Samui *et al*, "A direct approach to optimal feeder routing for radial distribution system," *Power Delivery, IEEE Transactions On*, vol. 27, (1), pp. 253-260, 2012.
- [60] H. L. Willis, *Power Distribution Planning Reference Book*. CRC press, 2004.
- [61] V. F. Martins and C. L. Borges, "Active distribution network integrated planning incorporating distributed generation and load response uncertainties," *Power Systems, IEEE Transactions On*, vol. 26, (4), pp. 2164-2172, 2011.
- [62] I. Ziari *et al*, "Integrated distribution systems planning to improve reliability under load growth," *Power Delivery, IEEE Transactions On*, vol. 27, (2), pp. 757-765, 2012.
- [63] E. Naderi, H. Seifi and M. S. Sepasian, "A dynamic approach for distribution system planning considering distributed generation," *Power Delivery, IEEE Transactions On*, vol. 27, (3), pp. 1313-1322, 2012.
- [64] B. Humayd, S. Abdullah and K. Bhattacharya, "Comprehensive multi-year distribution system planning using back-propagation approach," *Generation, Transmission & Distribution, IET*, vol. 7, (12), pp. 1415-1425, 2013.
- [65] S. Wong, K. Bhattacharya and J. D. Fuller, "Electric power distribution system design and planning in a deregulated environment," *IET Generation, Transmission & Distribution*, vol. 3, (12), pp. 1061, 2009.

- [66] G. Muñoz-Delgado, J. Contreras and J. M. Arroyo, "Joint expansion planning of distributed generation and distribution networks," *IEEE Trans. Power Syst.*, vol. 30, (5), pp. 2579-2590, 2015.
- [67] G. Muñoz-Delgado, J. Contreras and J. M. Arroyo, "Multistage generation and network expansion planning in distribution systems considering uncertainty and reliability," *IEEE Trans. Power Syst.*, vol. 31, (5), pp. 3715-3728, 2016.
- [68] G. Munoz-Delgado, J. Contreras and J. M. Arroyo, "Distribution Network Expansion Planning With an Explicit Formulation for Reliability Assessment," *IEEE Trans. Power Syst.*, vol. 33, (3), pp. 2583-2596, 2018.
- [69] A. Tabares *et al*, "Multistage Long-Term Expansion Planning of Electrical Distribution Systems Considering Multiple Alternatives," *IEEE Trans. Power Syst.*, vol. 31, (3), pp. 1900-1914, 2016.
- [70] R. Gholizadeh-Roshanagh, S. Najafi-Ravadanegh and S. Hosseinian, "A Framework for Optimal Coordinated Primary-Secondary Planning of Distribution Systems Considering MV Distributed Generation," *IEEE Transactions on Smart Grid*, 2016.
- [71] M. Ahmadigorji, N. Amjady and S. Dehghan, "A novel two-stage evolutionary optimization method for multiyear expansion planning of distribution systems in presence of distributed generation," *Applied Soft Computing*, vol. 52, pp. 1098-1115, 2017.
- [72] K. Zou *et al*, "Distribution system planning with incorporating DG reactive capability and system uncertainties," *IEEE Transactions on Sustainable Energy*, vol. 3, (1), pp. 112-123, 2012.
- [73] M. E. Samper and A. Vargas, "Investment decisions in distribution networks under uncertainty with distributed generation—Part I: Model formulation," *IEEE Trans. Power Syst.*, vol. 28, (3), pp. 2331-2340, 2013.
- [74] A. Zidan, M. F. Shaaban and E. F. El-Saadany, "Long-term multi-objective distribution network planning by DG allocation and feeders' reconfiguration," *Electr. Power Syst. Res.*, vol. 105, pp. 95-104, 2013.
- [75] M. Alvarez-Herault *et al*, "Optimizing traditional urban network architectures to increase distributed generation connection," *International Journal of Electrical Power & Energy Systems*, vol. 35, (1), pp. 148-157, 2012.
- [76] D. Kumar and S. Samantaray, "Design of an advanced electric power distribution systems using seeker optimization algorithm," *International Journal of Electrical Power & Energy Systems*, vol. 63, pp. 196-217, 2014.
- [77] E. G. Carrano *et al*, "Electric distribution network multiobjective design using a problem-specific genetic algorithm," *Power Delivery, IEEE Transactions On*, vol. 21, (2), pp. 995-1005, 2006.
- [78] P. Carvalho and L. A. Ferreira, "Distribution quality of service and reliability optimal design: individual standards and regulation effectiveness," *Power Systems, IEEE Transactions On*, vol. 20, (4), pp. 2086-2092, 2005.

- [79] G. Celli *et al*, "Optimal planning of active networks," in *16th Power Systems Computation Conference*, 2008, .
- [80] M. S. Nazar and M. R. Haghifam, "Multiobjective electric distribution system expansion planning using hybrid energy hub concept," *Electr. Power Syst. Res.*, vol. 79, (6), pp. 899-911, 2009.
- [81] J. E. Mendoza *et al*, "Low voltage distribution planning considering micro distributed generation," *Electr. Power Syst. Res.*, vol. 103, pp. 233-240, 2013.
- [82] D. Kumar, S. Samantaray and G. Joos, "A reliability assessment based graph theoretical approach for feeder routing in power distribution networks including distributed generations," *International Journal of Electrical Power & Energy Systems*, vol. 57, pp. 11-30, 2014.
- [83] N. Koutsoukis, P. Georgilakis and N. Hatziargyriou, "Active distribution network planning based on a hybrid genetic algorithm-nonlinear programming method," *CIREC-Open Access Proceedings Journal*, vol. 2017, (1), pp. 2065-2068, 2017.
- [84] N. C. Koutsoukis, P. S. Georgilakis and N. D. Hatziargyriou, "Multistage coordinated planning of active distribution networks," *IEEE Trans. Power Syst.*, vol. 33, (1), pp. 32-44, 2018.
- [85] S. Haffner *et al*, "Multistage model for distribution expansion planning with distributed generation—Part I: Problem formulation," *Power Delivery, IEEE Transactions On*, vol. 23, (2), pp. 915-923, 2008.
- [86] R. J. Millar *et al*, "Impact of MV connected microgrids on MV distribution planning," *IEEE Transactions on Smart Grid*, vol. 3, (4), pp. 2100-2108, 2012.
- [87] N. Amjady *et al*, "Adaptive Robust Expansion Planning for a Distribution Network With DERs," *IEEE Trans. Power Syst.*, vol. 33, (2), pp. 1698-1715, 2018.
- [88] A. Zare *et al*, "A Distributionally Robust Chance-Constrained MILP Model for Multistage Distribution System Planning with Uncertain Renewables and Loads," *IEEE Trans. Power Syst.*, 2018.
- [89] I. G. Sardou and E. Azad-Farsani, "Network expansion planning with microgrid aggregators under uncertainty," *IET Generation, Transmission & Distribution*, vol. 12, (9), pp. 2105-2114, 2018.
- [90] H. Haghghat and B. Zeng, "Stochastic and Chance-Constrained Conic Distribution System Expansion Planning Using Bilinear Benders Decomposition," *IEEE Trans. Power Syst.*, 2017.
- [91] P. Wang, "Reliability Cost/Worth Considerations in Distribution System Evaluation." , University of Saskatchewan, 1998.
- [92] R. Allan, *Reliability Evaluation of Power Systems*. Springer Science & Business Media, 2013.
- [93] P. Wang and R. Billinton, "Reliability benefit analysis of adding WTG to a distribution system," *IEEE Trans. Energy Convers.*, vol. 16, (2), pp. 134-139, 2001.
- [94] S. Conti and S. A. Rizzo, "Monte Carlo simulation by using a systematic approach to assess distribution system reliability considering intentional islanding," *IEEE Trans. Power Del.*, vol. 30, (1), pp. 64-73, 2015.

- [95] S. Conti, R. Nicolosi and S. Rizzo, "Generalized systematic approach to assess distribution system reliability with renewable distributed generators and microgrids," *IEEE Trans. Power Del.*, vol. 27, (1), pp. 261-270, 2012.
- [96] Y. M. Atwa and E. F. El-Saadany, "Reliability evaluation for distribution system with renewable distributed generation during islanded mode of operation," *IEEE Trans. Power Syst.*, vol. 24, (2), pp. 572-581, 2009.
- [97] P. Wang and R. Billinton, "Time-sequential simulation technique for rural distribution system reliability cost/worth evaluation including wind generation as alternative supply," *IEE Proceedings-Generation, Transmission and Distribution*, vol. 148, (4), pp. 355-360, 2001.
- [98] K. Zou *et al*, "An analytical approach for reliability evaluation of distribution systems containing dispatchable and nondispatchable renewable DG units," *IEEE Transactions on Smart Grid*, vol. 5, (6), pp. 2657-2665, 2014.
- [99] G. Celli *et al*, "Reliability assessment in smart distribution networks," *Electr. Power Syst. Res.*, vol. 104, pp. 164-175, 2013.
- [100] S. Conti *et al*, "Effect of islanding and telecontrolled switches on distribution system reliability considering load and green-energy fluctuations," *Applied Sciences*, vol. 6, (5), pp. 138, 2016.
- [101] C. Chen *et al*, "An analytical adequacy evaluation method for distribution networks considering protection strategies and distributed generators," *IEEE Trans. Power Del.*, vol. 30, (3), pp. 1392-1400, 2015.
- [102] M. A. Alotaibi and M. Salama, "An efficient probabilistic-chronological matching modeling for DG planning and reliability assessment in power distribution systems," *Renewable Energy*, vol. 99, pp. 158-169, 2016.
- [103] A. Escalera, B. Hayes and M. Prodanovic, "Reliability assessment of active distribution networks considering distributed energy resources and operational limits," in *CIGRE Workshop 2016*, 2016, pp. 1-4.
- [104] W. Li *et al*, "Reliability evaluation of complex radial distribution systems considering restoration sequence and network constraints," *IEEE Trans. Power Del.*, vol. 19, (2), pp. 753-758, 2004.
- [105] H. Guo, V. Levi and M. Buhari, "Reliability assessment of smart distribution networks," in *Innovative Smart Grid Technologies-Asia (ISGT ASIA), 2015 IEEE*, 2015, pp. 1-6.
- [106] A. C. Neto, M. G. da Silva, A. B. Rodrigues, "Impact of distributed generation on reliability evaluation of radial distribution systems under network constraints," *Int. Conf. Probabilistic Methods Applied to Power Systems (PMAPS)*, pp. 1-6, 2006.
- [107] da Silva, Armando M Leite *et al*, "Distributed energy resources impact on distribution system reliability under load transfer restrictions," *IEEE Transactions on Smart Grid*, vol. 3, (4), pp. 2048-2055, 2012.
- [108] F. J. Massey Jr, "The Kolmogorov-Smirnov test for goodness of fit," *Journal of the American Statistical Association*, vol. 46, (253), pp. 68-78, 1951.

- [109] M. Lavorato *et al*, "Imposing radiality constraints in distribution system optimization problems," *IEEE Trans. Power Syst.*, vol. 27, (1), pp. 172-180, 2012.
- [110] H. Zhang *et al*, "An improved network model for transmission expansion planning considering reactive power and network losses," *IEEE Trans. Power Syst.*, vol. 28, (3), pp. 3471-3479, 2013.
- [111] S. F. Santos *et al*, "New multistage and stochastic mathematical model for maximizing RES hosting capacity—part I: problem formulation," *IEEE Transactions on Sustainable Energy*, vol. 8, (1), pp. 304-319, 2017.
- [112] M. V. Pereira *et al*, "Strategic bidding under uncertainty: a binary expansion approach," *IEEE Trans. Power Syst.*, vol. 20, (1), pp. 180-188, 2005.
- [113] R. Romero *et al*, "A new mathematical model for the restoration problem in balanced radial distribution systems," *IEEE Trans. Power Syst.*, vol. 31, (2), pp. 1259-1268, 2016.
- [114] W. Yao *et al*, "A multi-objective collaborative planning strategy for integrated power distribution and electric vehicle charging systems," *IEEE Trans. Power Syst.*, vol. 29, (4), pp. 1811-1821, 2014.
- [115] W. Yao *et al*, "Scenario-based comprehensive expansion planning for distribution systems considering integration of plug-in electric vehicles," *IEEE Trans. Power Syst.*, vol. 31, (1), pp. 317-328, 2016.
- [116] Independent Electricity System Operator (IESO)., "Data Directory, Independent Electricity System Operator (IESO), Ontario. [Online]. Available:<http://www.ieso.ca/power-data/data-directory>," .
- [117] Environment and natural resources, "Historical Climat Data, Historical data, [Online]. Available:[http://climate.weather.gc.ca/historical\\_data/search\\_historic\\_data\\_e.html](http://climate.weather.gc.ca/historical_data/search_historic_data_e.html)," .
- [118] National Solar Radiation Data Base., "Data Sets, [Online]. Available:[http://rredc.nrel.gov/solar/old\\_data/nsrdb/](http://rredc.nrel.gov/solar/old_data/nsrdb/)," .
- [119] Independent Electricity System Operator (IESO)., "Ontario planning outlook:A technical report on the electricity system prepared by the IESO," Sep. 2016.
- [120] International Renewable Energy Agency (IRENA), "Renewable energy technologies: Cost analysis series (wind power)," 2012.
- [121] P. Jorgensen, J. Christensen and J. Tande, "Probabilistic load flow calculation using monte carlo techniques for distribution network with wind turbines," in *Harmonics and Quality of Power Proceedings, 1998. Proceedings. 8th International Conference On*, 1998, pp. 1146-1151.
- [122] GAMS Development Corporation, "General algebraic modeling system (GAMS)," .
- [123] C. L. Borges and D. M. Falcao, "Optimal distributed generation allocation for reliability, losses, and voltage improvement," *International Journal of Electrical Power & Energy Systems*, vol. 28, (6), pp. 413-420, 2006.

[124] A. Moradi and M. Fotuhi-Firuzabad, "Optimal switch placement in distribution systems using trinary particle swarm optimization algorithm," *IEEE Trans. Power Del.*, vol. 23, (1), pp. 271-279, 2008.

[125] R. N. Allan *et al*, "A reliability test system for educational purposes-basic distribution system data and results," *IEEE Trans. Power Syst.*, vol. 6, (2), pp. 813-820, 1991.